From Denervation to Reinnervation: The Role of Subsynaptic Myonuclei and Lmna in Skeletal Muscle Physiology

by

Lloyd Phillip Ruiz

A dissertation submitted in partial fulfillment
of the requirements for the degree of
Doctor of Philosophy
(Molecular and Integrative Physiology)
in the University of Michigan
2025

Doctoral Committee:

Professor Susan V. Brooks, Chair
Associate Professor Carlos A. Aguilar
Assistant Professor Megan L. Killian
Professor Daniel Michele

Lloyd Phillip Ruiz

llruiz@umich.edu

ORCID iD: 0000-0003-3172-5103

© Lloyd P. Ruiz 2025

Dedication

To my family—for their unwavering love, support, and belief in me, even when the path seemed uncertain. And to my friends—for their constant encouragement, laughter, and grounding presence, reminding me that no matter how hard the journey gets, I am never alone. Thank you all for walking this path with me and allowing me to thrive by any means necessary.

Acknowledgements

I would like to express my sincere gratitude to my thesis advisor, Dr. Sue Brooks, for giving me the opportunity to grow as a scientist and scholar in her lab. Her unwavering support has been instrumental in shaping the outcome of my journey. I am also grateful to everyone I've had the privilege to work with in the Brooks lab.

To Carol, thank you for your exceptional support in managing the lab and for your outstanding skills as an animal surgeon. To Pete, I deeply appreciate your persistence and the challenges you presented, which pushed me to critically evaluate complex questions and materials. Dennis, your ability to provide comedic relief in the lab was invaluable and kept morale high. Sophie, your passion for science and curiosity were truly inspiring, and it was a rewarding experience to mentor and collaborate with you—I'm excited for your bright future ahead. Steve, thank you for your steadfast support throughout this journey and for encouraging me to tackle challenges with determination and optimism.

I would also like to extend my heartfelt thanks to Dr. Dan Michele for his mentorship throughout my PhD. Your insightful advice and guidance helped me approach questions during critical moments. Chelsey Spriggs and Megan Killian, thank you for being a sounding board during my endeavors and for your key input that helped propel my project forward—I appreciate you always making yourself available.

To my friends back home in Los Angeles, thank you for grounding me through our conversations. Your support made me feel connected to home and provided much-needed stability throughout my journey.

Finally, I want to thank my family for their endless love and support in all that I do. I could not have done this without you.

Table of Contents

Dedication ii

Acknowledgements iii

List of Figures vii

Abstract xi

Chapter 1 Introduction 1

1.1 The Dynamic Nature of Skeletal Muscle: Structure and Functions 1

1.2 Developmental Dynamics of the Neuromuscular Junction 2

1.3 The Molecular Mechanisms Regulating Myonuclei Number and Positioning 8

1.4 The Role of the Neuromuscular Junction in Sarcopenia 12

1.5 The Effects of Nerve Injury on the Neuromuscular Junction 16

1.6 Goals of thesis and outline of chapters 19

Chapter 2 Maintenance of Subsynaptic Myonuclei Number is Not Driven by Neural Input 21

2.1 Abstract 21

2.2 Introduction 22

2.3 Materials and Methods 25

2.3.1 Animals 25

2.3.2 Sciatic Nerve Transection 25

2.3.3 Tissue collection 26

2.3.4 Immunohistochemistry 26

2.3.5 Data presentation and statistics 29

2.4 Results 29

2.4.1 Acute nerve injury does not elicit a change in subsynaptic myonuclei number out to 7 days 29

2.4.2 Subsynaptic myonuclei number is not influenced by innervation status 35

2.5 Discussion 37

Chapter 3 Evaluating the Role of Lamin A/C in Muscle Fiber Reinnervation 46

3.1 Abstract 46

3.2 Introduction 48

3.3 Materials and Methods 51

3.3.1 Animals 51

3.3.2 Heterozygous mice 52

3.3.3 Sciatic nerve injuries 52

3.4 Force testing and tissue collection 53

3.5 Whole muscle RNA extraction an RT-qPCR 54

3.6 Western blot for Lamin A/C 55

3.7 Immunohistochemistry 56

3.8 Results 56

3.9 Discussion 69

Chapter 4 Conclusions and Future Development 74

Bibliography 84

List of Figures

Figure 1 Components of the neuromuscular junction (NMJ). Action potentials are propagated down the presynaptic motor neuron that is surrounded and supported by perisynaptic Schwann cells. Depolarization of the motor neuron results in the opening of voltage-sensitive calcium channels leading to an influx of calcium ions, which contributes to synaptic vesicle fusion and the release of the neurotransmitter, acetylcholine (ACh). ACh crosses the synaptic gap and binds to acetylcholine receptors (AChR) on the muscle membrane leading to Na+ ion influx, depolarization, and muscle contraction. Created with BioRender.com. 4

Figure 2 Schematic of structurally intact subsynaptic myonuclei (SSM) maintaining the synaptic domain. 20

Figure 3 *Terminal Schwann cells do not express Nesprin1*. Immunofluorescence of 6-month-old S100-GFP gastrocnemius fibers with terminal Schwann cells labeled in (green), nuclei (blue), acetylcholine receptors (AChR, red), and Nesprin1 (magenta), Solid arrows indicate terminal Schwann cells that do not express Nesprin1, dashed line arrows indicate synaptic nuclei that do not 360 express Nesprin1, and asterisks indicate SSM, those that express Nesprin1 and overlap with AChRs. Images on the left are individual or partially merged channels. Image on right is enlarged merged image of all individual channels. 28

Figure 4 Acute denervation does not alter synaptic nuclei number. Upper panel: representative immunofluorescent images of gastrocnemius muscle fibers for control (CON) muscles and muscles 3 days and 7 days after sciatic nerve transection (3DSNT and 7DSNT) from 6-month-old WT mice stained for DAPI (blue), AChRs (green), NF/SV2 (white), and Nesprin1 (magenta). Lower panel: same images without AChR and NF/SV2 to highlight Nesprin1 nuclear staining. Region of interest (ROIs) highlight the endplate and are indicated by dashed boxes (yellow). Scale bars = 25 μm. **(A)** Quantification average number perisynaptic and **(B)** subsynaptic nuclei number per NMJ. Individual data points represent average values for each muscle sample. Bars represent mean values with error bars ±SEM (n = 3/group, 15 NMJs/sample). There were no significant differences in the average numbers of perisynaptic nuclei/NMJ or in subsynaptic myonuclei number in control, 3DSNT, and 7DSNT. 30

Figure 5 Visualization of synaptic myonuclei in young and old wild type mice. Immunofluorescent images of gastrocnemius muscle fibers from **(A)** 6-month **(B)** 28-month wild type mice and stained for DAPI (blue), AChR (green), NF/SV2 (white), and Nesprin1 (magenta). Scale bars = 25 μm. 32

Figure 6 Number of subsynaptic myonuclei remains unchanged by age. Average number of (A) perisynaptic nuclei and (B) subsynaptic nuclei per NMJ. Individual data points represent Average value or each muscle sample. Bars represent mean values with error bars ±SEM 33

Figure 7 Visualization of synaptic myonuclei in mice deficient in Sod1−/−. Immunofluorescent images of gastrocnemius muscle fibers from (**A**) 6-month and (**B**) 12-month Sod1−/− mice stained for DAPI (blue), AChR (green), NF/SV2 (white), and Nesprin1 (magenta). Scale bars = 25 μm. 34

Figure 8 Number of subsynaptic myonuclei remains unchanged by Sod1 deletion. Average number of **(A)** perisynaptic nuclei and **(B)** subynaptic myonuclei per NMJ. Individual data points represent average value for each muscle sample. Bars represent mean values with error bars ±SEM (n = 5/group, 15 NMJs/sample). **(C)** Data on subsynaptic myonuclear number expressed as a percentage of the NMJ containing 0–2 nuclei (tan bars), 3-4 nuclei (light green bars), 5-6 nuclei (green bars) or 7 or more nuclei (dark green bars). Bars represent mean values with error bars ±SEM..... 35

Figure 9 Synaptic nuclei number is not driven by innervation status. **(A)** Distribution of innervation status of young and aged wildtype and $Sod1^{-/-}$ mouse endplates. Endplates were classified as fully innervated if NF/SV2 signal overlapped with more than 80% of the endplate, partially denervated if overlap was <80–10%, and fully denervated if overlap was less than 10%. **(B)** Average number of perisynaptic nuclei at fully innervated, partially innervated and denervated wildtype and $Sod1^{-/-}$ mice. **(C)** Average number of subsynaptic nuclei at fully innervated, partially innervated and denervated wildtype and $Sod1^{-/-}$ mice. **(D)** Number of perisynaptic nuclei at an NMJ based on innervation status. Each point represents the number of perisynaptic nuclei at an endplate. F, Full; P, Partial; D, Denervated. The total number of NMJs analyzed are as follows 6 m WT F = 88, p = 3, D = 0; 28 m WT F = 25, p = 42, D = 48; 6 m $Sod1^{-/-}$ F = 17, p = 34, D = 42; 12 m $Sod1^{-/-}$ F = 8, p = 33, D = 52. **(E)** Number of subsynaptic nuclei at an NMJ based on innervation status. Each point represents the number of subsynaptic nuclei at an endplate. F, Full; P, Partial; D, Denervated..... 36

Figure 10 LoxP sites flanking exon 10–11 of *Lmna*, which are removed by Cre recombinase. Boxes represent exons, black triangles represent 34-bp loxP sites, and genotyping primers (F1, F2 and R1) are indicated with arrows. 51

Figure 11 Runted phenotype of 2-month-old constitutive knockout mice. A visual comparison of size between flox $Lmna^{+/+}$ mice (Left) and muscle-specific Lmna knockout AC-$Lmna^{+/-}$ (Right). Acta-Cre (AC). 52

Figure 12 Transcript levels in 6-month-old WT mice in uninjured control, 3- and 7-days after sciatic nerve transection (SNT). ***p<.005, ****p<0.0001 by ANOVA, Mean ± SEM. N=3/group. 57

Figure 13 Lamin A/C Protein expression in 6-month old WT mice in uninjured control, 3-, 7-, and 14-days after sciatic nerve transection (SNT). ***p<.005, ****p<0.0001by ANOVA, Mean ± SEM. N=3/group. 58

Figure 14 Lamin A/C is upregulated 7-days post denervation in 6-month-old WT mice. (**A-C**) Uninjured extensor digitorum longus (EDL) muscles and (**D-F**) 7-days after sciatic nerve transection (7DSNT) in WT mice. (**A**) and (**D**) whole muscle cross-sections, Dashed and solid

yellow boxes represent region of interest and are magnified in (**B&E**) and (**C&F**). Acetylcholine receptor (AChR) (green), DAPI (blue), and Lamin A/C (red). 58

Figure 15 Muscle Lmna is increased by both sciatic nerve crush (SNC) and sciatic nerve transection (SNT) injury models in 2-month-old mice. Transcript levels 7-days after nerve injury in WT mice. CON=uninjured, *p<.05, **p<.005. Means ± SEM by ANOVA. n=3..... 59

Figure 16 Lamin A/C is elevated in the tibialis anterior muscle 7-days post nerve crush and is present at the endplate in 2-month old mice. Whole cross-section image (**A,B,D,E**) Scale bar = 300 μm; Solid blue square (**B**) and dashed blue square (**E**) represent regions of interest (ROI) that contain endplates; Magnified ROI images (**C,F**) Scale bar = 50 μm. Red = Lamin A/C, Green = Acetylcholine receptor (AChR), Blue = DAPI 60

Figure 17 Transcriptional changes in LMNA, NET39, YAP, and TAZ with denervation are present at 7 days and return towards baseline by 14 days and maintained at 28 days. The LINC complex components SYNE1, SUN1, SUN2, and Emerin are stable following nerve crush. Temporal expression pattern of LMNA in the gastrocnemius muscle of 2-mo WT mice. ****p<.0001. Mean ± SEM by ANOVA, n=7. 61

Figure 18 Immunohistochemistry of the time course following nerve crush in gastrocnemius (GM) muscles. Immunostaining shows DAPI (blue) for nuclear staining, AChR (red) for acetylcholine receptors, NF/SV2 (green) for neurofilament/synaptic vesicles, and Lamin A/C (white) for nuclear staining, AChR (red) for acetylcholine receptors, NF/SV2 (green) for neurofilament/synaptic vesicles and Lamin A/C (white) for nuclear lamina in (**A)** control muscles and muscles (**B)** 7-days post nerve crush, (**C)** 14-days post nerve crush, and (**D)** 28-days post sciatic nerve crush injury. Scale bar = 25 μm 62

Figure 19 Functional innervation is restored in gastrocnemius muscles within 14 days in our nerve crush injury model. Data are shown for maximum specific force (Spo) elicited by (**A)** Direct muscle stimulation or (**B)** Direct nerve stimulation. Force values are normalized by the physiological cross-sectional area of the muscle and expressed as specific forces (N/cm^2). (**C)** Ratio of the forces generated by nerve and muscle stimulation. Statistical significance indicated by *p < 0.05, **p<0.003 ***p<0.0002, ****p<0.0001, ns=non-significant. SNC = sciatic nerve crush data presented as means ± SEM analyzed by ANOVA. n=5 63

Figure 20 Baseline function of gastrocnemius in 2-month uninjured flox ($Lmna^{+/+}$) and heterozygous (AC-$Lmna^{+/-}$) mice. (**A)** Specific force (Spo) from direct muscle stimulation (**B)** Spo from direct nerve stimulation. Force values are normalized by the physiological cross-sectional area of the muscle and expressed as specific forces (N/cm^2). (**C)** Ratio of the forces generated by nerve and muscle stimulation. Statistical significance indicated by ****p<0.0001, data presented as means ± SEM analyzed by ANOVA. n=5 64

Figure 21 Partial deletion of muscle Lmna does not impact post synaptic NMJ morphology. N=3. 30 NMJs/sample. Data presented as means ± SEM analyzed by ANOVA. FL Con = flox uninjured ($Lmna^{+/+}$), H. Con = heterozygous mice uninjured (AC-$Lmna^{+/-}$). **A)** Acetylcholine receptor (AChR) area. **B)** AChR perimeter. **C)** Nerve terminal area. **D)** Nerve terminal

perimeter. **E)** Overlap. **F)** Endplate Area. **G)** Endplate perimeter. **H)** Endplate diameter. **I)** Unoccupied AChR area. **E)** Compactness. 65

Figure 22 Muscle histology of uninjured Lmna flox and uninjured heterozygous extensor digitorum longus (EDL) muscle (**A, B**) reveals no difference in myofiber number or cross-sectional size between Lmna flox and Lmna heterozygous mice (**C, D**). n=5, scale bar = 200 μm. FL = Flox (Lmna$^{+/+}$), Het. = Heterozygous (AC-Lmna$^{+/-}$)..... 66

Figure 23 Functional innervation is restored in the gastrocnemius muscles of heterozygous mice 14 days post nerve crush. Data are shown for maximum specific force (SPo) elicited by (**A)** Direct muscle stimulation (**B)** Direct nerve stimulation. Force values are normalized by the physiological cross-sectional area of the muscle and expressed as specific forces (N/cm^2). (**C)** Specific force of nerve stimulation indicating the significant interaction effect 14 days post nerve crush. **(D)** Fidelity of NMJ transmission 14 days post injury determined by comparing Spo Nerve:Spo Muscle in uninjured controls and 14 days after nerve crush injury. Statistical significance indicated by ***p<0.005, ***p<0.0005, ****p<0.0001., Flox = Lmna$^{+/+}$, Het.= ActaCre-Lmna$^{+/-}$, 7DSNC= 7-day nerve crush, 14DSNC = 14-day nerve crush. Data presented as means ± SEM analyzed by Two-way ANOVA and Sidak post-hoc analysis. n=5..... 67

Figure 24 Transcripts from heterozygous mice (AC-Lmna$^{+/-}$). Nerve injury induces AChRα, LMNA, and NET39 and YAP transcriptional trends similar to wildtype mice. **P<.005, ***<.00005. SNC= Sciatic nerve crush. WT= Wildtype. H.Con = heterozygous ActaCre-Lmna$^{+/-}$ uninjured..... 68

Figure 25 Lamin A/C localization does not ascertain a defined pattern throughout the soleus 7-days after injury in Lmna floxed (Lmna$^{+/+}$) mouse soleus muscle. Whole section image of uninjured (CON) soleus (**A,B**) and injured (7DSNC (**D,E**), scale bar = 300 μm. Magnified ROIs highlighting increased Lamin A/C signal near endplates and surrounding nuclei **(C,F)**, scale bar = 50 μm. Red = Lamin A/C, Green = Acetylcholine receptor (AChR), Blue = DAPI . 69

Abstract

This dissertation investigates the roles of subsynaptic myonuclei (SSM) and the nuclear envelope protein Lamin A/C in maintaining neuromuscular junction (NMJ) health, particularly during aging and after nerve injury. SSM, a specialized subset of myonuclei located beneath the motor endplate, are thought to support NMJ development and maintenance, yet their relationship to NMJ integrity and response to denervation remains unclear. To begin to address this knowledge gap, SSM counts and NMJ innervation status were analyzed in three mouse models of acute and chronic NMJ disruption: surgical denervation, aging, and chronic oxidative stress ($Sod1^{-/-}$ mice). SSM were identified via Nesprin 1 immunolabeling and anatomical localization. SSM numbers remained stable during aging, chronic oxidative stress, and after 7 days of denervation following a nerve transection injury. Despite significant NMJ degeneration and denervation in aged and $Sod1^{-/-}$ mice, SSM counts showed no relationship to NMJ innervation status, challenging the hypothesis that SSM loss drives NMJ decline. These findings highlight the need to explore other SSM characteristics, such as transcriptional profiles and structural roles, to better understand their contribution to NMJ health. We then shifted focus to explore the critical role of Lamin A/C, a protein encoded by the Lmna gene, in maintaining myonuclear integrity and reinnervation. Lamin A/C, a key intermediate filament protein in the nuclear lamina, is expressed in skeletal muscle and decreases with age, and with muscle-specific deletion reported to accelerate NMJ degradation, resembling age-associated NMJ decline. The role of Lamin A/C was examined in the context of NMJ regeneration following sciatic nerve injury in wildtype (WT) and muscle-

specific heterozygous knockout mice (AC-Lmna$^{+/-}$). Lamin A/C expression, significantly upregulated post-injury at both transcript and protein levels, returned to baseline by 14–28 days. NMJ morphology analysis revealed no structural differences across several features of the NMJ between genotypes. Despite intact NMJ morphology, AC-Lmna$^{+/-}$ mice exhibited delayed recovery of nerve-stimulated force generation and impaired NMJ transmission fidelity post-injury, implicating Lamin A/C in functional recovery rather than or perhaps in addition to structural maintenance. Notably, this response was specific to Lamin A/C and not part of a general nuclear envelope response. These results suggest that while Lamin A/C is non-essential for NMJ reinnervation, its partial loss delays functional recovery, raising questions about nuclear integrity disruptions in age-associated NMJ decline. Together, this work provides new insights into NMJ maintenance and regeneration by decoupling SSM count from NMJ integrity and highlighting Lamin A/C's role in functional recovery. These findings underscore the complexity of NMJ regulation and reinnervation, suggesting Lamin A/C has a marginal role and additional targets influence muscle decline and NMJ deterioration.

Chapter 1 Introduction

1.1 The Dynamic Nature of Skeletal Muscle: Structure and Functions

Skeletal muscle is a highly dynamic and plastic tissue that accounts for approximately 40% of total body weight and contains the majority (50-75%) of the body's proteins by mass. Skeletal muscle performs numerous critical functions in the body, including providing locomotion, contributing to basal energy metabolism, storing energy substrates, and producing heat to maintain core temperature. Muscle fibers can be broadly classified into two types: slow-twitch (type I) and fast-twitch (type II). Slow-twitch fibers are more fatigue-resistant and primarily use aerobic metabolism to produce energy, making them well-suited for activities that require sustained muscle contraction, such as long-distance running (Frontera & Ochala, 2015a). They are rich in mitochondria and myoglobin, which gives them their reddish color (Bourdeau Julien et al., 2018). Fast-twitch fibers, on the other hand, comprise a broad continuum from fibers that display capacities for oxidative metabolism equivalent to or even greater than slow twitch fibers (Blemker, Brooks, Esser & Saul, 2024) to fibers that primarily use anaerobic metabolism to produce energy. These so-called fast fatiguable fibers are well-suited for activities that require quick, powerful muscle contractions, such as sprinting or weightlifting (Frontera & Ochala, 2015b). They are pale in color due to their lower myoglobin content. Other characteristics that differentiate the two types of fibers include their sensitivity to calcium and their sarcoplasmic reticulum calcium handling (fast vs. slow). The makeup of muscle fibers is unique to each muscle and is influenced by factors such as the pattern of neuronal activating

stimuli, the level of physical activity, and the specific demands of the muscle (Bourdeau Julien et al., 2018; Frontera & Ochala, 2015b).

Satellite cells, also known as muscle stem cells (MuSC), are a population of quiescent stem cells located between the sarcolemma and the basal lamina of skeletal muscle fibers. They play a crucial role in muscle growth, repair, and regeneration, differentiating into new muscle cells when needed for recovery from an injury or fusing with existing fibers to increase their size (Sinha-Hikim et al., 2003). These cells are activated in response to various stimuli, such as muscle loading, damage, and aging, and proliferate to maintain their pool and facilitate muscle homeostasis. The activation and differentiation of satellite cells are regulated by numerous signaling pathways and transcription factors that support increased protein synthesis (Sinha-Hikim et al., 2003). As myofibers grow in length and cross-sectional area, additional nuclei from stem cells are required to provide the necessary trophic support for muscle growth. Recent studies have demonstrated that specialized populations of muscle stem cells are localized near neuromuscular junctions (NMJs) and act to support NMJ integrity by developing into synaptic myonuclei (W. Liu et al., 2017; Urzi et al., 2023). Furthermore, depletion of MuSCs impairs NMJ regeneration following injury, and MuSCs have been shown to respond to perturbed NMJs (Larouche et al., 2021; W. Liu et al., 2015). Due to their essential roles, it is not surprising that dysregulation of MuSC function has been implicated in muscle disorders such as atrophy and weakness (Bourdeau Julien et al., 2018).

1.2 Developmental Dynamics of the Neuromuscular Junction

Neuromuscular junctions (NMJs) are the fundamental site where the nervous system transmits signals responsible for voluntary movements such as locomotion to skeletal muscle.

This intricate membranous and cytoskeletal structure forms and develops early in life through a series of steps that involve complex signaling events between the nerve terminal, muscle fiber, and Schwann cells to produce a chemical synapse (Sanes & Lichtman, 1999). Deficits occurring in NMJ formation and development lead to neuromuscular disorders such as myasthenia gravis. This section will encompass neuromuscular junction development from a structural and functional lens and make comparisons between humans and mice.

Initially, myoblasts fuse to form myotubes, and before innervation, acetylcholine receptor (AChRs) genes are transcribed. The AChR genes are then translated and spontaneously cluster uniformly at a density of ~1000/μm^2 throughout the post-synaptic membrane forming aneural clusters during a phenomenon called muscle prepatterning. As motor nerve terminals innervate muscle fibers, the axon terminal, also known as a synaptic bouton, secretes agrin, a potent activator of AChR cluster formation at the synaptic cleft that is approximately 50 nm across (Kummer et al., 2006; L. Li et al., 2018). Synapse development continues over the course of weeks in which AChR clusters mature and structurally organize into a pretzel-like morphology. Once formed, the adult muscle AChR density of the endplate is >10,000 AChRs/μm^2, the stability of the NMJ increases upon maturation, and it is capable of neurotransmission. enabling lifelong motor performance (Sanes, n.d.; Slater, 2020).

The sequence of events responsible for muscle fiber excitation has been well characterized. Action potentials propagate down the motor neuron triggering the release of acetylcholine-carrying vesicles into the synaptic cleft (Fig. 1). Each synaptic vesicle contains on the order of 10,000 acetylcholine (ACh) neurotransmitter molecules, which cross the synapse and bind to post-synaptic AChRs. Upon the binding of two acetylcholine molecules, the AChR

channel will open to allow sodium influx and potassium efflux resulting in a positive net flow of positive charge into the cell leading to depolarization and an excitatory post-synaptic potential (EPSP) or endplate potential (EPP). At a normal healthy neuromuscular synapse, the AChR in response to the neuron action potential causes an EPP that reaches threshold to trigger an action potential in the muscle fiber membrane. The muscle action potential triggers muscle contraction (Aidley, 2012).

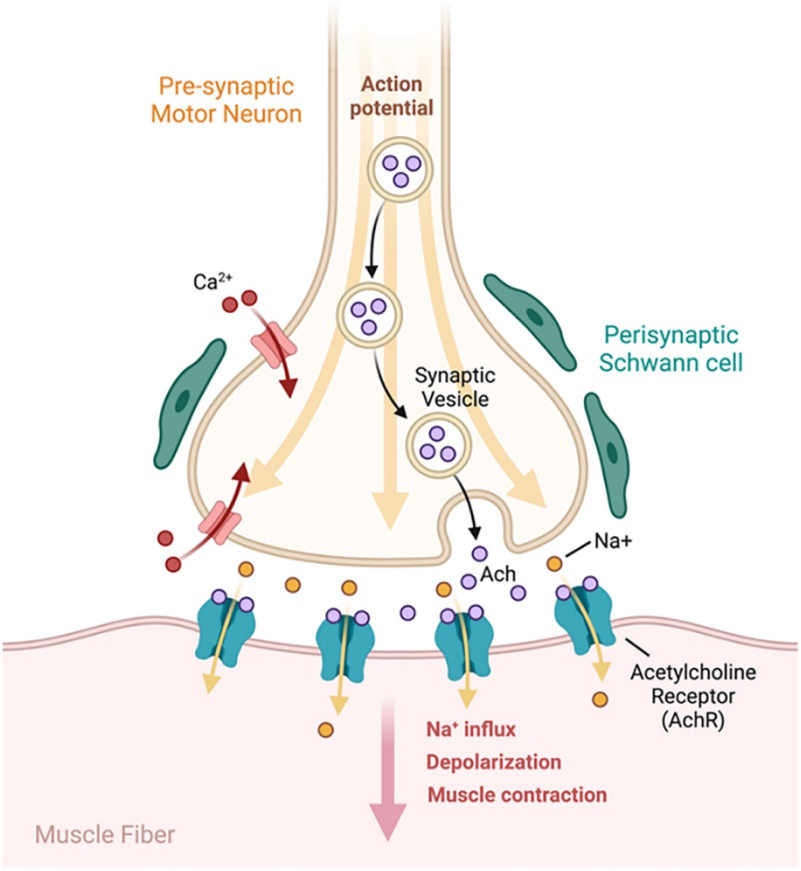


Figure 1 Components of the neuromuscular junction (NMJ). Action potentials are propagated down the presynaptic motor neuron that is surrounded and supported by perisynaptic Schwann cells. Depolarization of the motor neuron results in the opening of voltage-sensitive calcium channels leading to an influx of calcium ions, which contributes to synaptic vesicle fusion and the release of the neurotransmitter, acetylcholine (ACh). ACh crosses the synaptic gap and binds to acetylcholine receptors (AChR) on the muscle membrane leading to Na+ ion influx, depolarization, and muscle contraction. Created with BioRender.com.

Much of what is known about synapse formation and maturation has been established through extensive studies in rodents (Cetin et al., 2020). Therefore, it is likely that not all

aspects directly apply to humans. Comparative analysis suggests a high degree of heterogeneity exists in mammalian NMJ morphology. Interestingly, mice have among the largest NMJs despite have the smallest muscle fiber diameters. The NMJ morphology of sheep closely matches humans and may be the best model for studying human endplates; however, mice are a more practical animal model for laboratory study (Boehm et al., 2020). The ligand-gated nicotinic AChR ion channel in muscle are heteropentamers composed of two-α, one-β, and one fetal-specific subunit that forms a central pore. The ε-subunit replaces the embryonic-specific γ-subunit in AChRs during early development, marking a critical transition in the maturation of the NMJ. In mice, this transition occurs within the first two weeks of the postnatal stage, (Missias et al., 1996; Villarroel & Sakmann, 1996), whereas in humans the transition occurs during the second to the third trimester of fetal development (Hesselmans et al., 1993). The γ-to-ε subunit transition has a major functional impact on the receptor. The embryonic γ-subunit forms receptors with longer channel open times and slower kinetics, which is suited for the less frequent synaptic activity during early muscle development. When the ε-subunit replaces the γ-subunit, the receptor's kinetics become faster, and channel open times shorten, leading to a more rapid response to acetylcholine. This results in more efficient synaptic transmission and is essential for the increased precision and control required for mature muscle function (Villarroel & Sakmann, 1996). Disorders to this developmental milestone are related to the onset of null mutations to the CHRNE gene responsible for the production of the ε-subunit and lead to NMJ disorders such as congenital myasthenic syndrome (Croxen et al., 2001).

Each AChR contains two agonist binding sites in the extracellular domain, where the α-γ site shows the greatest affinity for acetylcholine in mice (Nayak et al., 2014, 2016). Complex molecular pathways certainly regulate the γ-to-ε subunit change; however, motor neuron

innervation seems critical in stimulating subsynaptic nuclei to initiate transcription of the epsilon subunit. The gamma subunit is actively transcribed in all myonuclei in the initial formation of myotubes but becomes restricted to subsynaptic myonuclei upon the nerve arrival of the nerve. mRNA expression of the ε-subunit also seems to be exclusive to the adult subsynaptic nuclei (Missias et al., 1996; Sakmann & Brenner, 1978). One core group of proteins has been shown to be required for beginning the AChR clustering event and synapse formation through the activity of the synaptic organizer agrin, *low-density lipoprotein receptor-related protein 4* (LRP4), *muscle-specific tyrosine kinase* (MuSK), *Docking Protein 7* (Dok7) (Tintignac et al., 2015; Wu et al., 2010) and rapsyn which directly interacts with AChRs (Borges et al., 2008). During postnatal maturation of the NMJ, alterations in AChRs transform clusters into pretzel-like shapes with an expected half-life of receptors being about 14 days at fully functional synapses (Akaaboune et al., 1999). During the lifespan of an animal, AChRs at the NMJ undergo both recycling and degradation processes. Recycled AChRs are those that have been internalized and then reinserted into the postsynaptic membrane, while preexisting AChRs are the original receptors that have been stably embedded in the membrane since their initial synthesis (Bruneau et al., 2005, 2006). It has been reported that recycled AChRs turnover more rapidly than pre-existing AChRs however, the mechanism is still unclear. Several regulatory signaling molecules converge on the metabolic stability of AChRs and are well-reviewed (Martinez-Pena Y Valenzuela & Akaaboune, 2021). As AChRs are remodeled, the post-synaptic membrane specializes by forming invaginations known as junctional folds (JFs). These folds are unique to the NMJ and contain high-density clusters of nicotinic acetylcholine receptors; thus, they are thought to increase the reliability of transmission and enhance depolarization. The mechanism of JFs formation is unknown. A leading theory suggests that JFs develop opposite to the active

zone, the area where vesicles release acetylcholine across the synapse, but this does not explain what physically draws the membrane in to form the invaginations (Hong & Etherington, 2011; S. Zou & Pan, 2022). Nevertheless, defects in JFs are a consistent phenotype in disease states such as amyotrophic lateral sclerosis (ALS), Myasthenia gravis (MG), and muscular dystrophy (MD)(York & Zheng, 2017).

Table 1 Feature comparisons of adult neuromuscular junctions across species

Feature	**Human**	**Mouse**
Pre-synaptic		
Active zone size	153 x 96 nm	80 x 73 nm
Active zone density	2.6/ μm^2	2.3 - 2.7/ μm^2
Quantal content	20 - 30	50 - 100
Nerve terminal area	122.7 μm^2	304.0 μm^2
Post-synaptic		
Endplate area	351.5 μm^2	678.2 μm^2
Number of AChR/NMJ	1.3 - 3.4 x 10^7	3.1 - 8.7 x10^7

The physiology of the neuromuscular junction is dictated by the structure and function of the presynaptic motor neuron and the post-synaptic acetylcholine receptors. The size of the active zone is significantly smaller in mice (80 x 73 nm) (Fukuoka et al., 1987) compared to humans (153 x 96 nm) (Fukunaga et al., 1983) with a similar density seen between species (2.6/ μm^2 vs. 2.3-2.7/μm^2) (J. Chen et al., 2012; Fukunaga et al., 1982; Fukuoka et al., 1987). The mouse NMJ is also estimated to have more than double the quantal content of human NMJs (20 – 30 vs. 50 - 100 in mice) (C. Slater, 2017), and mouse nerve terminal areas are also much

greater (122.7 μm^2 vs. 304.0 μm^2 in mice) (Boehm et al., 2020). Functionally, fetal AChRs differ from adult endplates in several species. The channel open time varies between species and between maturity. The human fetal AChR open time has been reported to be 7.9 ms vs 5.7 ms in mice with a significant reduction compared to adult AChR open times or 4.1 ms vs 1.5 ms in mice (Fucile et al., 2006; Ragozzino et al., 1998). The adult AChR also consistently displays greater Ca^{2+} permeability compared to developing fetal AChRs consistent in both humans and mice, leading to greater cytoplasmic calcium levels (Shen et. al., 2009), and modulation of neurotransmitter release, synaptic plasticity, and cell motility (Fucile et al., 2003, 2006). The post-synaptic endplate also varies across species, likely driving variation in NMJ physiology. Mice display larger (351.5 μm^2 vs 678.2 μm^2) and denser (1.3 - 3.4 x 10^7 vs 3.1 – 8.7 x 10^7 AChR number per NMJ) (Albuquerque, 1974; Bollen et al., 1992; Pestronk et al., 1985) endplates. A summary of this information can be found in table 1.

1.3 The Molecular Mechanisms Regulating Myonuclei Number and Positioning

The proper arrangement of myonuclei within skeletal muscle fibers is important for normal muscle physiology, and an imbalance and improper localization of myonuclei is linked to skeletal muscle pathologies such as centronuclear myopathy and muscular dystrophies. Despite this, our understanding of the mechanisms that control myonuclei number, positioning, and anchorage is incomplete (Cadot et al., 2015; Cisterna & Malatesta, 2024; Folker & Baylies, 2013).

Myofibers are a unique type of cell that are multinucleated and post-mitotic, meaning that the myonuclei do not undergo cell division once they have matured, although this dogma has recently been challenged (Borowik et al., 2022). The myonuclear domain (MND) theory

proposes that each nucleus in a muscle regulates the proteins synthesized in its region in a controlled manner (Teixeira & Duarte, 2011). Myofibers gain nuclei through satellite cell-mediated myonuclear accretion, which involves the incorporation of new myonuclei into muscle fibers through the fusion of satellite cells. This process is thought to be critical for driving hypertrophy, or to compensate for a loss of existing myonuclei that may occur during muscle atrophy (Abou Sawan et al., 2021). Interestingly, studies have found no loss of nuclei with age-related atrophy, but rather an alteration in the spatial organization of myonuclei. This alteration may affect the local quantity of DNA per muscle fiber volume through decreased activity or cooperativity of myonuclei in a gender- and muscle fiber type-specific manner (Cristea et al., 2010). Furthermore, Type-2 fibers seem to hypertrophy without the accretion of myonuclei, in contrast to Type-1 fibers, which show an increase in myonuclear density during exercise-induced hypertrophy. These observations provide just a few examples that highlight the nuanced and complex behaviors and roles of myonuclei in muscle (Conceição et al., 2018; Kadi et al., 2004; Petrella et al., 2006). Further challenges of the myonuclear domain theory are well-reviewed (Murach et al., 2018). Nevertheless, it is well established that the products of a myonucleus associate with the Golgi remain localized near their myonuclear origin (Pavlath et al., 1989), and single-nuclei RNA-seq and fluorescent in-situ hybridization (FISH) reveal unique populations of myonuclei including but not limited to; body myonuclei, myotendinous junction nuclei, and subsynaptic myonuclei. Furthermore, myonuclei display spatial transcriptional heterogeneity and gene expression related to innervation (Dos Santos et al., 2020). Collectively, the data supports regional specialization of myonuclei and neural control of transcription in muscle tissue and the following discussion focuses on mechanisms of regional positioning of myonuclei and resultant regulation of gene expression by myonuclei in muscle fibers, with a specific focus on the NMJ.

The SYNE (synaptic nuclear envelope) genes play a crucial role in the positioning and anchorage of myonuclei within muscle tissue through their encoding of Nuclear Envelope Spectrin Repeat proteins (Nesprins) (Apel et al., 2000). Nesprins, which are highly expressed in both skeletal and cardiac muscle (Duong et al., 2014; Grady et al., 2005), specifically associate with synaptic nuclei in adult muscle fibers and are essential for anchoring myonuclei at the NMJ in mice (Packard et al., 2015). Notably, the deletion of the KASH domain of SYNE1, but not SYNE2, abolishes the formation of the nucleus cluster associated with the NMJ and disrupts the organization of non-synaptic nuclei in skeletal muscle (Zhang et al., 2007). During development, SYNE1 gene networks are believed to facilitate the localization of mRNAs that migrate from the nucleus to the NMJ (Holt et al., 2019). In both humans and rodents, a Nesprin1-α2 (N1-α2) isoform is specifically expressed in skeletal muscle and colocalizes with subsynaptic myonuclei (Packard et al., 2015). Nesprins interact with SUN (Sad1p-UNC-84) proteins, which span the inner nuclear envelope membrane and form the LINC (Linker of Nucleoskeleton to Cytoskeleton) complex (X. I. N. Chen et al., 2019; Crisp et al., 2006). SUN1 and SUN2 proteins function redundantly to anchor myonuclei (Lei et al., 2009). Additionally, a muscle-specific isoform of the cardiac islet-1 interaction protein (CIP), which is critical for connecting the LINC complex with the microtubule system, plays a significant role in myonuclei alignment and positioning (J. Liu et al., 2020). Loss of CIP and SUN genes results in severe positioning defects and muscular dystrophy. Finally, the LINC complex can physically interact with nuclear lamins, linking the nuclear lamina with chromatin factors in the nucleoplasm (Barton et al., 2015) and enabling transcriptional regulation (Tajik et al., 2016).

Lamins are type-V intermediate filament proteins that provide structural support to the nucleus by forming a mesh-like scaffold known as the nuclear lamina. There are two types of

lamins: A-type (lamin A and C) and B-type (lamin B1, B2, and B3). A-type lamins are encoded by the LMNA gene and are mostly located at the periphery of the nucleus, while B-type lamins are encoded by the LMNB1 and LMNB2 genes and are important during development. Lamins, much like the LINC complex, have been shown to play a role in mechanotransduction, a process by which mechanical signals are converted into biological responses to impact various cell functions (Donnaloja et al., 2020). Lamin A/C has been found in the nucleoplasm (Briand & Collas, 2020; Naetar et al., 2017) and participates in chromatin organization, DNA replication, and transcription regulation (Alcorta-Sevillano et al., 2020; De Leeuw et al., 2018; Zhang et al., 2019) through interactions with inner nucleus membrane proteins, transcriptions factors, and DNA. Lamin proteins can undergo molecular rearrangements in response to mechanical stimuli, which can affect the structure of the nuclear lamina.

Mutations in LMNA result in a wide range of diseases known as laminopathies (Worman & Bonne, 2007). Mutations in A-type lamins can cause the accelerated aging disease, Hutchinson-Gilford progeria syndrome (HGPS) (Chang et al., 2019). Emery-Dreifuss muscular dystrophy (AD-EDMD) and limb-girdle muscular dystrophy (LGMD) are two of the most common laminopathies which impact skeletal and cardiac muscles (Broers et al., 2006). Interestingly, in a mouse model of AD-EDMD, endplates were severely disorganized and 86% of synapses had altered morphology with mislocalized synaptic nuclei and increased histone acetylation (Méjat et al., 2009). More recently, muscle-specific deficiency of lamin A/C were found to cause progressive degeneration of NMJs in mice, which also had fewer subsynaptic myonuclei (Gao et al., 2020). These findings suggest that lamins are important for positioning myonuclei at the NMJ, although it is unclear if the decrease in subsynaptic myonuclei is the cause or consequence of NMJ degeneration.

In conclusion, it is clear that the complex interplay between myonuclei, the SYNE gene, and the nuclear lamina plays a crucial role in the proper functioning and organization of skeletal muscle. The myonuclear domain theory suggests that each nucleus within a muscle regulates the proteins synthesized in its region in a controlled manner. However, the specific mechanisms by which changes in myonuclei number and fiber type specificity occur in relation to the myonuclear domain theory are not fully understood. The SYNE gene is thought to play a crucial role in myonuclei positioning and anchorage, while the nuclear lamina is a key structural component that is essential for proper myonuclei organization. Mutations in proteins of the nuclear lamina have been linked to disruptions in the organization of the neuromuscular junction, highlighting the importance of this structure for normal muscle function and as a potential cause for NMJ decline.

1.4 The Role of the Neuromuscular Junction in Sarcopenia

Sarcopenia, the age-related loss of muscle mass and strength, is a significant concern for the elderly population due to its negative impacts on mobility, overall health, and quality of life (Rosenberg, 1989). Aging is the primary risk factor for developing sarcopenia, with individuals over the age of 50 generally experiencing a yearly loss of around 1% of muscle mass (Koster et al., 2011; Lexell et al., 1988.). While physical activity is currently the main treatment option for sarcopenia, it is only moderately successful, and its effectiveness decreases with advanced age. (Yoo et al., 2018). The loss of muscle mass can also lead to frailty and increase the risk of falls and fractures. The major mechanisms behind the age-related loss of muscle mass and function are not fully understood, but inflammation, impaired muscle regeneration due to a loss of satellite cell number and function, the loss of motor neurons, mitochondrial dysfunction, the

accumulation of reactive oxygen species (ROS), and degenerative changes at the neuromuscular junction have all been proposed as potential contributing factors (T. N. Kim & Choi, 2013; McCormick & Vasilaki, 2018).

Reactive oxygen species (ROS) are highly reactive molecules produced during the process of mitochondrial oxidative phosphorylation that can cause oxidative damage and are thought to contribute to aging (Scialò et al., 2017). However, ROS also play a role in normal physiological processes and cell signaling (Ray et al., 2012). The enzyme Cu/ZnSOD, which removes free radical superoxide anions in cells and mitochondria, is a key antioxidant enzyme. Mice lacking Cu-Zn superoxide dismutase 1 ($Sod1^{-/-}$) display markers of oxidative stress and damage in essentially all tissues, including muscle, and exhibit premature muscle atrophy and weakness, similar to what is observed in aged wild-type mice (Muller et al., 2006). In addition, $Sod1^{-/-}$ mice display accelerated AChR fragmentation, a shared phenotype with aged wild-type mice (Deepa et al., 2019; Ivannikov & Van Remmen, 2015). Boosting NAD+ levels to reduce age-related and transgenically elevated oxidative stress appears to be promising in reducing ROS and improving the function of the aged NMJ (Cameron et al., 2019; Ito et al., 2022). Additionally, dietary restriction has also been shown to alleviate sarcopenia by decreasing mitochondrial ROS accumulation and structural changes at the NMJ (Jang et al., 2012). While the exact cause of sarcopenia remains unknown, these data strongly support a link between oxidative stress in vivo with muscle wasting and weakness with fragmentation of the postsynaptic apparatus and functional decline at the NMJ as key contributing factors.

The structure of neuromuscular junctions (NMJs) in mammals changes as they age (Y. Li et al., 2011). These changes often include the formation of new branches of the terminal axon,

which contact muscle at previously non-synaptic sites and acquire features of postsynaptic differentiation, including accumulations of acetylcholinesterase and acetylcholine receptors. Studies using antibodies and genetically expressed fluorescent cellular markers have confirmed that NMJ structure changes with age at the light microscope level, including an increase in the extent and complexity of terminal axon branching and in the total number and area of postsynaptic fragments. Ultrastructural studies of NMJ aging have shown a decrease in the density of synaptic vesicles within the nerve terminal (Cheng et al., 2013; Rosenheimer & Smith, 1985; Valdez et al., 2010). Aging is also associated with decline in the postsynaptic side, including a decrease in the number and regularity of postsynaptic folds and an increase in the width of the synaptic cleft. Changes in the number of synaptic myonuclei also may be a driving factor of degradation of the postsynaptic apparatus (Cossins et al., 2020; Gao et al., 2020; Willadt et al., 2016). Reductions of the NMJ could be mechanistically linked to a variety of factors, including oxidative stress, inflammation, and changes in gene expression, but the finding of fewer myonuclei at NMJs of older animals is not universal, and neither the structural of functional significance of a reduction is not yet fully understood.

Fragmentation, or the breaking up of the neuromuscular junction (NMJ) into smaller, isolated areas of postsynaptic differentiation, has sometimes been thought to be a sign of NMJ degeneration and a decline in function (Willadt et al., 2016). However, there is no evidence to suggest that NMJ fragmentation alone would reduce transmission efficacy at the NMJ (C. R. Slater, 2020). In fact, in certain situations where new synapses are formed on previously non-synaptic regions of mature muscle fibers, such as after blockage of nerve impulses by tetrodotoxin (Ribchester & Taxt, 1984), muscle fiber damage, or recovery from botulinum

intoxication (Duchen & Strich, 1968; Rogozhin et al., 2008), NMJs with many spot-like contacts are still able to function effectively.

Few studies have correlated structural and functional deficits of the NMJ. The lack of the protein desmin has been shown to affect the structure and function of NMJs in mice, as well as the transcription of genes that code for postsynaptic proteins. Desmin knockout mice exhibit fragmentation of NMJs in the soleus muscle, but not in the extensor digitorum longus muscle. In addition, the soleus muscle fibers of these mice have larger NMJs. The transcription levels of acetylcholine receptor (AChR) genes are also increased in the muscles of these mice, particularly in the AChRγ subunit, which is typically associated with muscle fiber regeneration. Electrophysiological recordings in these mice showed a pathological decrement in nerve-dependent endplate potentials and an increased rise time in nerve-independent miniature endplate potentials, which may be linked to the fragmentation of NMJs in these mice (Eiber et al., 2020). A study of Lamin associated protein (LAP) knockout mice revealed that changes in NMJ structure were accompanied by a decline in electrophysiology readings of synaptic transmission. Furthermore, an increase in fragmentation in LAP knockout mice was found to be correlated with an increase in the number of synaptic nuclei, indicating that lamin associate proteins are involved in maintaining the structure of the endplate (Cossins et al., 2020). The deletion of Lamin A/C specifically in muscle led to the degeneration of NMJs, both structurally and functionally, and levels of this protein were found to decrease with age (Gao et al., 2020). These findings suggest that Lamin A/C may have a protective role in preserving the integrity of NMJs.

In summary, the structural changes that occur at the neuromuscular junction (NMJ) during aging may affect the function of the NMJ and transmission of nerve impulses. The

functional impact of these changes is not fully understood, but it is possible that they contribute to a decrease in transmission efficacy at the NMJ. The precise causes of these structural changes in the NMJ remain unclear and warrant further investigation. Studies have produced conflicting results regarding the number of subsynaptic myonuclei at a given endplate and the status of NMJ fragmentation (Ang et al., 2022; Bai et al., 2022, Cossins et al., 2020; Gao et al., 2020, W. Liu et al., 2017), therefore, greater clarity on the number of SSM at a given NMJ is warranted. Additionally, the role of Lamin A/C in NMJ function and aging is also an area of active research. Reports that Lamin A/C levels in muscle decline with aging and deletion of Lamin A/C specifically in muscle lead to degeneration of NMJs suggest that Lamin A/C may represent a target of intervention for preventing the decline of NMJs and alleviate sarcopenia (Gao et al., 2020).

1.5 The Effects of Nerve Injury on the Neuromuscular Junction

To better understand the mechanisms underlying sarcopenia, sciatic nerve transection and sciatic nerve crush are commonly used models to study the effects of nerve injury on the neuromuscular junction (NMJ) and skeletal muscle. Sciatic nerve transection involves the complete severing of the sciatic nerve, while sciatic nerve crush is a mechanical injury that damages the nerve without completely severing it. Both models lead to muscle atrophy, characterized by a decrease in muscle mass, strength, and function. Investigating the processes of nerve injury and regeneration is essential for developing therapies to preserve muscle function and mitigate muscle atrophy.

Sciatic nerve transection is a widely used model to study the effects of denervation on skeletal muscle. This procedure triggers a sequence of events known as Wallerian degeneration,

a process in which the damaged axons and myelin of motor neurons undergo systematic breakdown. Wallerian degeneration involves a coordinated cellular response, including Schwann cells, fibroblasts, endothelial cells, and macrophages, along with signaling molecules that facilitate the phagocytosis of the damaged axon. This process is crucial for initiating nerve repair and has been observed in vivo as early as 30 hours (Kerschensteiner et al., 2005) and as late as 6 weeks post injury (Conforti et al., 2014; Farrar et al., 2012; Zou et al., 2022).

Sciatic nerve crush, another model used to study axonal injury followed by reinnervation, involves applying pressure to the sciatic nerve with a small clamp. Studies using this model have shown that muscle function and mass decrease by approximately 30% following the injury but recover to nearly pre-injury levels by 30 days post-crush (dpc). Although there is no loss of muscle fibers or significant change in the number of nuclei per fiber, a shift in fibers expressing myosins I and II occurs, which reverts to control levels by 30 dpc (Grönholdt-Klein et al., 2019). Recent research has also uncovered gene regulatory network reprogramming associated with denervation-induced muscle atrophy, revealing molecular mechanisms such as metabolic remodeling and myonuclear transition (Lin et al., 2022). **Myonuclear transition** refers to the process by which myonuclei within a muscle fiber adapt or shift their transcriptional programs in response to physiological or pathological conditions. For example, in studies investigating responses to denervation, distinct subgroups of myonuclei in type II myofibers undergo transitions characterized by the emergence of specialized states, such as type IIb2 myonuclei (Lin et al., 2022). This process reflects the dynamic ability of myonuclei to reprogram gene expression, contributing to fiber type-specific adaptations, giving insights into new targets for improving the health of myofibers or the NMJ after injury.

The NMJ is a dynamic structure that continuously remodels throughout an organism's life and in response to injury. Functional recovery after nerve injury is largely dependent on the reinnervation of denervated motor endplates (Rich et al., 2023). Structurally, in 3-month-old mice, nearly all (98%) endplates are denervated one week after nerve injury. However, by 8 weeks, endplates are either partially (28.3%) or fully (71.7%) reinnervated, and by 16 weeks, NMJ reinnervation reaches 87.3%. Functionally, the compound muscle action potential (CMAP) amplitude, which ideally correlates with muscle contraction strength, recovers to 83% of the level seen in uninjured mice at 16 weeks, correlating with the percentage of fully reinnervated NMJs. Researchers also observed morphological differences between injured and non-injured NMJs further highlighting the ability of the NMJ to adapt after nerve injury (Vannucci et al., 2019).

Notably, even though reversible nerve damage led to complete reinnervation after 11 days, studies have shown that more than 30% of NMJs remain poly-innervated and around 65% of postsynaptic domains remain fragmented even 3 months after injury (Bermedo-García et al., 2022). These observations of long-term abnormalities in NMJ morphology following denervation injury suggest that while nerve injury may be reversible and synaptic transmission may be fully recovered two months after injury, postsynaptic stability at the NMJ may be irreversibly compromised after chronic denervation. There are many emerging therapeutic approaches and advanced techniques with promising findings for aiding NMJ recovery after nerve injury. Targets such as DOK7 and AAV-NRIP have shown potential (Chen et al., 2024; Kosco et al., 2023), while single-nuclei sequencing experiments continue to identify novel NMJ-specific targets (Ham et al., 2024). However, further studies are needed to fully understand and validate these approaches, particularly regarding the role of nuclei in proximity to the NMJ.

These developments and gaps in understanding of subsynaptic myonuclei, underscore the critical importance of studying the long-term effects of nerve injury on the NMJ and exploring therapies that can enhance postsynaptic stability in the context of chronic denervation.

1.6 Goals of thesis and outline of chapters

Several unresolved questions in the current landscape of skeletal muscle physiology are highlighted in the forthcoming exploration into the role of subsynaptic myonuclei and their engagement at the NMJ to maintain homeostasis and the facilitate reinnervation post nerve injury. The overall goal is to unravel some of the complexities of aging and reinnervation following injury, employing advanced in vivo and in situ techniques to systematically investigate the factors influencing neuromuscular health and integrity in mouse models.

Chapter 2 critically examines the existing literature, focusing on inconsistencies in methodologies and techniques used to quantify subsynaptic myonuclei. It raises important questions about the physiological impact of minor fluctuations, such as changes in just 1-2 nuclei. The experimental efforts in this chapter aim to demonstrate the stability of subsynaptic myonuclei numbers across three models of NMJ degradation, offering valuable insights into the current understanding of these dynamics and to clarify inconsistencies found within the literature.

Chapter 3 extends from and expands upon a pivotal discovery revealing a notable upregulation of the Lmna gene subsequent to nerve injury. The Lmna gene, renowned for its protein product Lamin A/C, plays a crucial role in constructing the structural framework of myonuclei (**Figure 2**). The experiments outlined in this chapter delve into the interdependence of

skeletal muscle innervation and Lmna expression, investigating the repercussions of its removal and its influence on the reinnervation process.

Chapter 4 summarizes the thesis's contributions to the fields of myonuclei biology and aging, emphasizing the knowledge gaps that have been addressed. Additionally, this chapter outlines potential avenues for future research, building on the findings of this work and identifying remaining gaps in understanding that warrant further investigation.

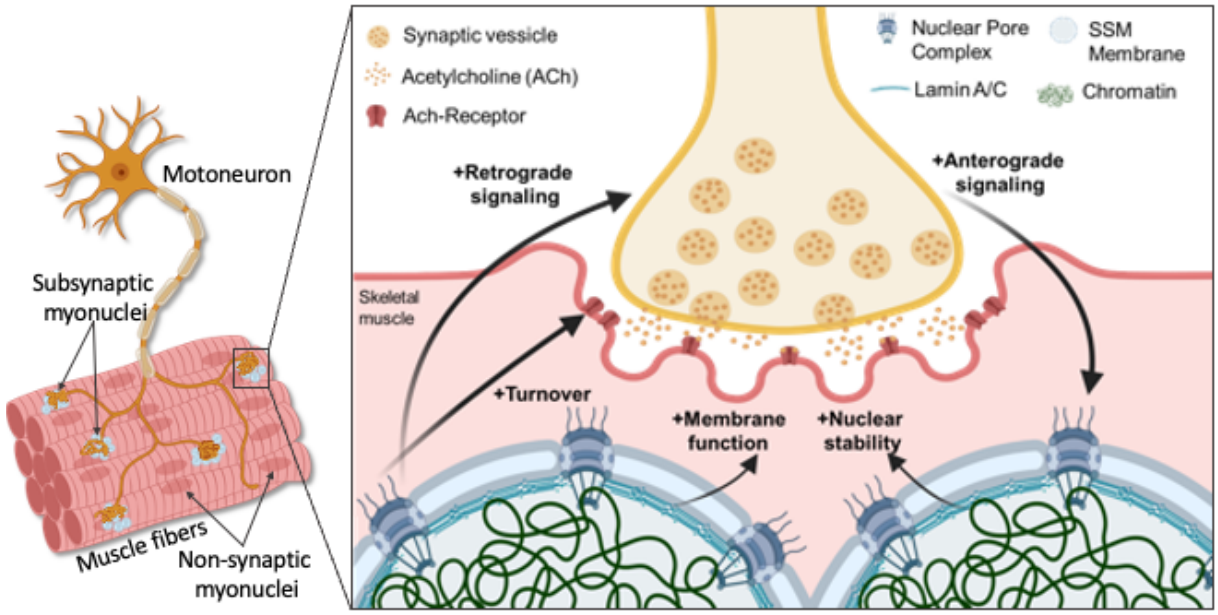


Figure 2 Schematic of structurally intact subsynaptic myonuclei (SSM) maintaining the synaptic domain.

Chapter 2 Maintenance of Subsynaptic Myonuclei Number is Not Driven by Neural Input

2.1 Abstract

The development and maintenance of neuromuscular junctions (NMJ) are supported by a specialized population of myonuclei that are referred to as the subsynaptic myonuclei (SSM). The relationship between the number of SSM and the integrity of the NMJ as well as the impact of a loss of innervation on SSM remain unclear. This study aimed to clarify these associations by simultaneously analyzing SSM counts and NMJ innervation status in three distinct mouse models of acute and chronic NMJ disruption. SSM were identified using fluorescent immunohistochemistry for Nesprin 1 expression, which is highly enriched in SSM, along with anatomical location beneath the muscle fiber motor endplate. Acute denervation, induced by surgical nerve transection, did not affect SSM number after seven days. Additionally, no significant changes in SSM number were observed during normal aging or in mice with chronic oxidative stress ($Sod1^{-/-}$). Both aging WT mice and $Sod1^{-/-}$ mice accumulated degenerating and denervated NMJ in skeletal muscle, but there was no correlation between innervation status of a given NMJ and SSM number in aged or $Sod1^{-/-}$ mice. These findings challenge the notion that a loss of SSM is a primary driver of NMJ degradation and leave open questions of the mechanisms that regulate SSM number as well as the physiological significance of the precise SSM number. Further investigations are required to define other properties of the SSM, such as transcriptional profiles and structural integrity, to better understand their role in NMJ maintenance.

2.2 Introduction

Maintenance of the neuromuscular junction (NMJ), the synapse between a motor neuron and muscle fiber, relies on a specialized population of muscle fiber nuclei referred to as subsynaptic myonuclei (SSM). Positioned beneath the muscle endplate, SSM play a crucial role in locally enriching acetylcholine receptors (AChRs) and other proteins essential for establishing NMJ structure and function(Apel et al., 2000; Bourdeau Julien et al., 2018, 2018; Sanes & Lichtman, 2001; Schaeffer et al., 2001; Shi et al., 2012). The specialization of SSM involves both activity- and load-dependent mechanisms (Haddix et al., 2018; Purves & Sakmann, 1974a, 1974b; Ruegg, 2005) and likely receives trophic support from the associated motor neuron (Saini et al., 2021). Consequently, disruption of NMJ integrity is anticipated to impact anterograde signaling, as well as the structure, function, or number of SSM. Simultaneously, alterations in SSM structure, number, or function may trigger degenerative changes at the NMJs. The impact of acute loss of innervation on SSM remains undefined, and the role of SSM loss in NMJ degeneration has yet to be fully elucidated.

Degeneration of NMJs and loss of innervation are often cited as important contributors to the age-associated loss of muscle referred to as sarcopenia (Delbono et al., 2021; Doherty et al., 1993; Hashizume et al., 1988). The hypothesis of a causative link between decreased integrity of the NMJ and sarcopenia is based largely on reports of an accumulation of NMJs that display morphological abnormalities including partial or complete loss of overlap of pre- and post-synaptic structures and discontinuous staining pattern of postsynaptic AChRs during aging

(Deschenes et al., 2022; Jang & Van Remmen, 2011; Y. Li et al., 2011; Valdez et al., 2010; Verma et al., 2022; Willadt et al., 2016).

Recent studies of the relationship between NMJ degeneration and SSM number have produced conflicting results. While Liu et al. (2017) found a reduction in SSM number in old animals compared to adults, a recent report by Ang et al. (2022) concluded that age-associated differences in SSM number are modest and may be secondary to NMJ structural modifications. Furthermore, Larouche et al. (2021) found no differences in baseline SSM numbers between young and old mice; however, an increase in perisynaptic nuclei 28-days after sciatic nerve transection appeared in young mice only. In contrast to the findings of Larouche et al. (2021), Bai et al. (2022) reported a decrease in synaptic nuclei number 16 days after denervation, with the decreased number remaining stable out to 30 days. Finally, Bai et al. (2022) also found that the number of SSM in the mouse model of amyotrophic lateral sclerosis (SOD1G93A) was less than that of its wildtype counterpart 90-days after birth, suggesting a relationship between innervation and SSM number. These collective findings indicate that questions of whether the loss of innervation triggers loss of SSM or whether the loss of SSM triggers degenerative changes at NMJs are in need of further investigation.

The goal of the present study was to further clarify the association between SSM number and NMJ integrity. We addressed this goal through simultaneous analysis of counts of total perisynaptic myonuclei and specific SSM along with assessments of NMJ innervation status using identical methods across models of both acute and chronic NMJ disruption. SSM were identified using an antibody specific to Nesprin1. Nuclear envelope spectrin repeat proteins (Nesprins) are highly expressed in skeletal muscle (Duong et al., 2014; Grady et al., 2005) and

act to anchor myonuclei at the NMJ (Grady et al., 2005; Holt et al., 2019; Packard et al., 2015). The nesprin-1-alpha-2 isoform is specifically expressed in the synaptic nuclei in adult muscle fibers (Holt et al., 2019). A novel aspect of the present study was the use of Nesprin1 staining in conjunction with markers for pre- and post-synaptic structures to establish associations of SSM with innervation status.

Based on the known importance of the motor neuron in SSM specialization (Ruegg, 2005; Saini et al., 2021) along with reports of fewer SSM at NMJs in muscle fibers of old compared with adult animals (W. Liu et al., 2017) and links between SSM number and NMJ structural modifications (Ang et al., 2022; Bai et al., 2022), our overall hypothesis was that a relationship exists between the loss of innervation and a loss of SSM or vice versa, i.e., a loss of SSM drives disruption of NMJ structure. To address this hypothesis, we determined SSM number in three models of NMJ degeneration in mice. First, we asked whether acute denervation induced by surgical nerve transection triggered a loss of SSM. We next examined muscles from adult and old wild type mice to establish whether SSM number changed during normal aging. Lastly, we studied muscles from mice deficient in the antioxidant enzyme superoxide dismutase 1 ($Sod1^{-/-}$ mice). $Sod1^{-/-}$ mice develop degenerative changes at NMJs during adulthood, including fragmentation of the endplates and frank muscle fiber denervation (Deepa et al., 2019; Ivannikov & Van Remmen, 2015). We tested the specific hypotheses that the number of Nesprin1 positive nuclei sub-adjacent to muscle fiber endplates would be lower 1) in muscles following nerve transection compared with innervated controls, 2) for muscles of old compared with adult wild type mice, and 3) for muscles of $Sod1^{-/-}$ compared with wild type mice. We further hypothesized that in all cases, the loss of nesprin positive myonuclei would be correlated with the extent of NMJ disruption, from fully innervated through to fully denervated.

2.3 Materials and Methods

2.3.1 Animals

Male and female mice of the C57BL/6 background and male and female Sod1$^{-/-}$ mice and wild type (WT) littermates were used in this study. All mice were housed in specific-pathogen-free conditions, with ad-libitum access to standard laboratory food and water and were subjected to a 12-hour light/dark cycle. The animal experiments described here were reviewed and approved by the University of Michigan Institutional Animal Care and Use Committee (IACUC).

2.3.2 Sciatic Nerve Transection

C57BL/6 mice approximately 6-months of age were subjected to sciatic nerve transection (SNT) and randomly assigned to either a 3-day or 7-day recovery group. The procedure was as follows. First, mice were anesthetized with 5% isoflurane as required to ensure no response to tactile stimuli, followed by continuous administration of 2% isoflurane for maintenance. Next, carprofen (5 mg/kg) was administered as a preoperative analgesic. The hindlimbs were carefully shaved and the skin was cleaned with chlorhexidine and 70% alcohol. A small skin incision (<10 mm) was made 1 mm posterior and parallel to the femur, and the superficial biceps femoris was split to expose the sciatic nerve. The sciatic nerve was then transected, and a 5 mm segment was removed. The incision was closed with wound clips (Autoclip, BD Clay Adams, Franklin Lakes, NJ). The same procedure was performed on the contralateral leg. After surgery, the mice were placed on a heating pad and closely observed until they recovered from the anesthetic. Mice recovered for three or 7 days before being sacrificed.

2.3.3 Tissue collection

For tissue collection, mice were anesthetized with intraperitoneal injection of avertin (0.5 mg/g). The bilateral gastrocnemius (GTN) muscles were carefully dissected from mice exposed to SNT (N = 3/time-point, 2 males and 1 female at each timepoint), as well as from 6-month-old young WT mice, 28-month-old aged WT mice, 6-month-old $Sod1^{-/-}$ mice, and 12-month-old adult $Sod1^{-/-}$ mice (N = 5/group, 3 males and 2 females). Muscles were briefly fixed for 10 min in 4% paraformaldehyde for immunohistochemical analysis. Tissue was then cryoprotected in a 20% sucrose solution, then snap-frozen in embedding medium O.C.T compound (Fisher Scientific) with liquid nitrogen cooled isopentane to maintain the integrity of the membranes. The tissue samples were stored at −80°C until thawed and used for analysis. Following removal of the tissues, deeply anesthetized mice are euthanized by an overdose of anesthetic followed be the creation of a pneumothorax.

2.3.4 Immunohistochemistry

Myofiber bundles were mechanically teased from GTN muscles under a dissecting microscope and processed for immunohistochemistry. The myofiber bundles were first blocked for 1 h at room temperature with a solution of 5% goat serum (Gibco), 1% bovine serum albumin (Fisher Scientific), 0.5% Triton X-100 (Sigma-Aldrich), and 0.01% sodium-azide (Sigma-Aldrich), then blocked for 30 min with 10% Mouse IgG, Fab fragment (Jackson ImmunoResearch). The myofiber bundles were then incubated overnight at 4°C with primary

antibodies (Nesprin1 rabbit-polyclonal antibody (Invitrogen) at 1:500 dilution and Neurofilament (2H3)/Synaptic vesicle glycoprotein 2A mouse-monoclonal antibody (NF/SV2) (2H3 1:50 and SV2 1:25 dilutions). 2H3 was deposited to the DSHB by Jessell, T.M./Dodd, J and SV2 was deposited by Buckley, K.M. (DSHB Hybridoma Products 2H3 and SV2). The following morning, bundles were washed with phosphate-buffered saline (PBS), treated with secondary antibodies (goat-anti-rabbit 594 at 1:500 dilution and goat-anti-mouse 647 at 1:1000 dilution) (Invitrogen), and co-stained with alpha-bungarotoxin (α- BTX) conjugates 488 (Invitrogen) at 1:1000 dilution and DAPI (4′,6-diamidino-2-phenylindole, dihydrochloride) (Invitrogen) at 1:1000 dilution for 1 h at room temperature. The myofiber bundles were then washed with PBS, mounted onto slides with DAKO fluorescence mounting media, and imaged using oil immersion and Nikon A1 High-sensitivity confocal microscopy.

To analyze and quantify perisynaptic nuclei and subsynaptic myonuclei (SSM) and assess innervation status, Z-stack confocal images were processed and projected as 3-D images in ImageJ as described (Schneider et al., 2001). For the purposes of the present manuscript all images are presented as 2-D maximum intensity projections. We performed a preliminary analysis to confirm that the expression of Nesprin1, a protein involved in the organization and anchoring of the nucleus to the cytoskeleton, would differentiate between SSM and terminal Schwann cell nuclei associated with the NMJ. This analysis of Nesprin1 expression was performed in adult S100-GFP mice. In the S100-GFP animal model, terminal Schwann cells are labeled with GFP under the control of the S100 promoter, whereas myonuclei do not express GFP (Figure 3). Nesprin1, labeled in magenta, was entirely absent from terminal Schwann cell nuclei, as indicated by the solid arrows, highlighting that Nesprin1 expression represents a feature of SSM that allows for its use to distinguish SSM from perisynaptic terminal Schwann

cell nuclei at the neuromuscular junction (Figure 3). Furthermore, Nesprin-1+/GFP- nuclei that didnot overlap with the endplate were also observed. These nuclei were not counted as SSM and therefore not included in our analysis but represent an interesting population of nuclei for future study. Finally, our analysis also revealed synaptic nuclei, indicated by dashed line arrows, that do not express GFP or Nesprin1. These observations emphasize the importance of rigorous scrutiny when examining SSM and underscores the relevance of using both anatomical location and Nesprin1 expression as our identifying criteria for SSM based on the high likelihood of miscounting SSM when relying entirely on proximity to the endplate.

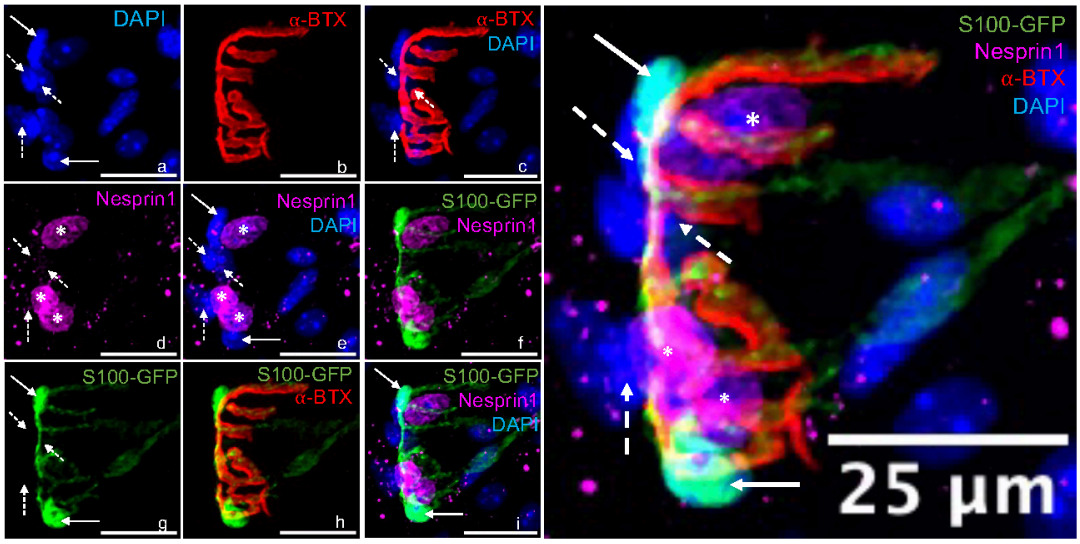


Figure 3 *Terminal Schwann cells do not express Nesprin1*. Immunofluorescence of 6-month-old S100-GFP gastrocnemius fibers with terminal Schwann cells labeled in (green), nuclei (blue), acetylcholine receptors (AChR, red), and Nesprin1 (magenta), Solid arrows indicate terminal Schwann cells that do not express Nesprin1, dashed line arrows indicate synaptic nuclei that do not 360 express Nesprin1, and asterisks indicate SSM, those that express Nesprin1 and overlap with AChRs. Images on the left are individual or partially merged channels. Image on right is enlarged merged image of all individual channels.

In the analysis of all images to quantify SSM and innervation status, the nerve and presynaptic terminal were labeled by NF/SV2 and postsynaptic acetylcholine receptors were stained with α-BTX. Endplates were classified as fully innervated when more than 80% of the

NF/SV2 signal overlapped with the α-BTX signal, partially denervated when the overlap was between 10% and 80%, and denervated when the overlap was less than 10%. Perisynaptic myonuclei were defined as nuclei showing overlap with the α-BTX signal, while Nesprin1 protein expression served as a marker for SSM. A nucleus was classified as a SSM by expression of Nesprin1 along with at least 25% overlap of the DAPI signal with α-BTX.

2.3.5 Data presentation and statistics

A minimum of 15 NMJs were analyzed per individual muscle in each mouse. The data are presented as means ± standard error of the mean with data points for individual muscles included on each figure. Statistical analysis was performed by two-tailed unpaired Student's t-test, and one-way ANOVA where applicable. Significance was set a priori at $p < 0.05$. Only a p value of less than 0.05 is labeled in the figure.

2.4 Results

2.4.1 Acute nerve injury does not elicit a change in subsynaptic myonuclei number out to 7 days

The effect of acute denervation on SSM was quantified in myofiber bundles from GTN muscles 3 (3DSNT) and 7 days (7DSNT) following SNT by immunohistochemistry as described above. Uninjured control mice displayed fully innervated endplates with pretzel-like morphology, with perisynaptic and subsynaptic nuclei labeled by DAPI and Nesprin1 (Fig. 4 upper panel images). Three days after injury, the nerve began to clear and a loss of innervation was evidenced by the remains of only a faint NF/SV2 signal, and by 7 days after injury, NF/SV2 staining is completely absent (Fig. 4 upper panel images). When assessed by 3-D image analysis,

we identified no differences in the average number of perisynaptic nuclei per endplate between control (x = 7.2 ± 0.2 nuclei), 3DSNT (x = 7.5 ± 0.2 nuclei), and 7DSNT (x = 7.5 nuclei ±0.2). We also found no change from control levels (x = 6.0 ± 0.2 nuclei) (Figure 4A) in subsynaptic myonuclei (SSM) number 3 days or 7 days post-SNT (3DSNT: x = 5.0 ± 0.2 nuclei; 7DSNT: x = 5.5 nuclei ±0.197) (Figure 4B). Our results indicate that acute denervation does not significantly impact the number of SSM at the NMJ.

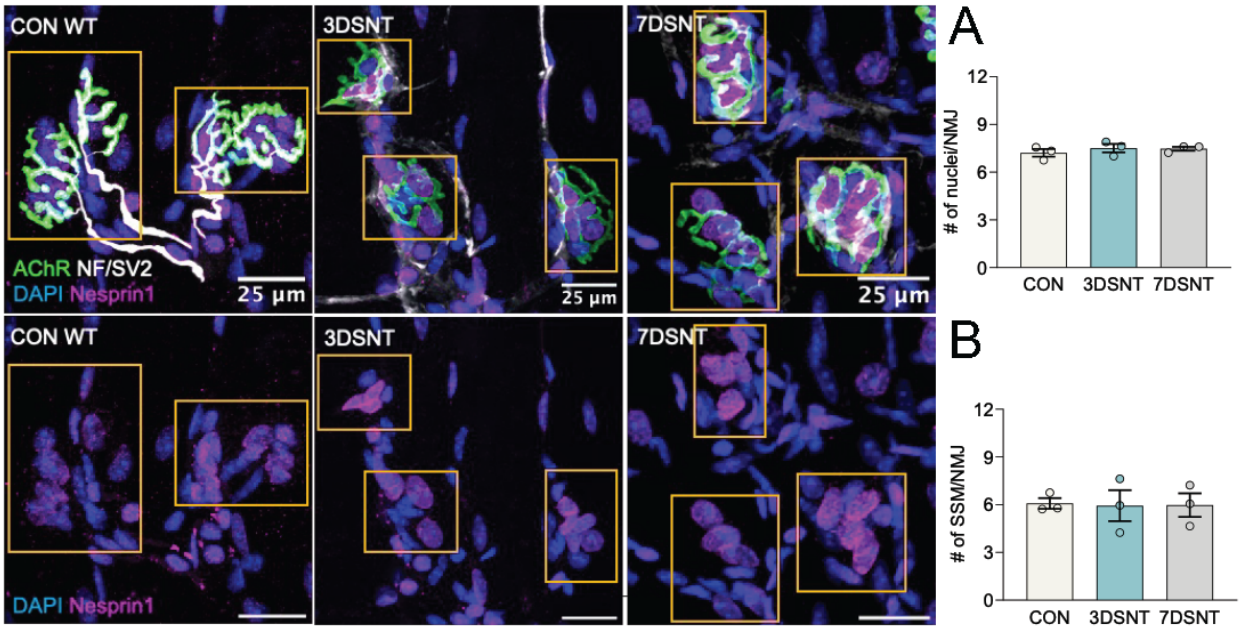


Figure 4 Acute denervation does not alter synaptic nuclei number. Upper panel: representative immunofluorescent images of gastrocnemius muscle fibers for control (CON) muscles and muscles 3 days and 7 days after sciatic nerve transection (3DSNT and 7DSNT) from 6-month-old WT mice stained for DAPI (blue), AChRs (green), NF/SV2 (white), and Nesprin1 (magenta). Lower panel: same images without AChR and NF/SV2 to highlight Nesprin1 nuclear staining. Region of interest (ROIs) highlight the endplate and are indicated by dashed boxes (yellow). Scale bars = 25 µm. **(A)** Quantification average number perisynaptic and **(B)** subsynaptic nuclei number per NMJ. Individual data points represent average values for each muscle sample. Bars represent mean values with error bars ±SEM (n = 3/group, 15 NMJs/sample). There were no significant differences in the average numbers of perisynaptic nuclei/NMJ or in subsynaptic myonuclei number in control, 3DSNT, and 7DSNT.

2.4.2 Subsynaptic myonuclei number is not influenced by NMJ degeneration associated with normal aging or chronic oxidative stress

To investigate the effect of chronic NMJ disruption on SSM number and the relationship of innervation status at the NMJ to SSM, we analyzed isolated myofiber bundles from GTN muscles of 6- and 28-month-old WT mice (Fig. 5) and 6- and 12-month-old $Sod1^{-/-}$ mice (Figure 2.5). In WT mice, we identified an approximately 20% increase in the number of perisynaptic nuclei per endplate for muscles of 28-month compared with 6-month mice (Fig. 6A) ($p < .01$), but when SSM specifically were compared we found no differences in SSM number between 6-month and 28-month mouse endplates (Fig. 6B). We then reanalyzed and further scrutinized the data by generating histograms as similarly presented in (Liu et al., 2017) with the number of NMJs containing specific numbers of SSM counted. Bin sizes for the histograms were 0–2, 3–4, 5-6 or 7+ SSM per NMJ (Fig. 6C). While this analysis revealed a greater representation in muscles of 28-month-old compared with 6-month-old mice of NMJs with 0–2 nuclei (7% vs 1%), there was simultaneously a greater proportion at 28 months of NMJs with 7 or more SSM, 45% and 29% for 28-month and 6-month mice, respectively. There were no differences between the age groups for the percentage of endplates containing 3-4 SSM or 5-6 SSM (Fig. 6C).

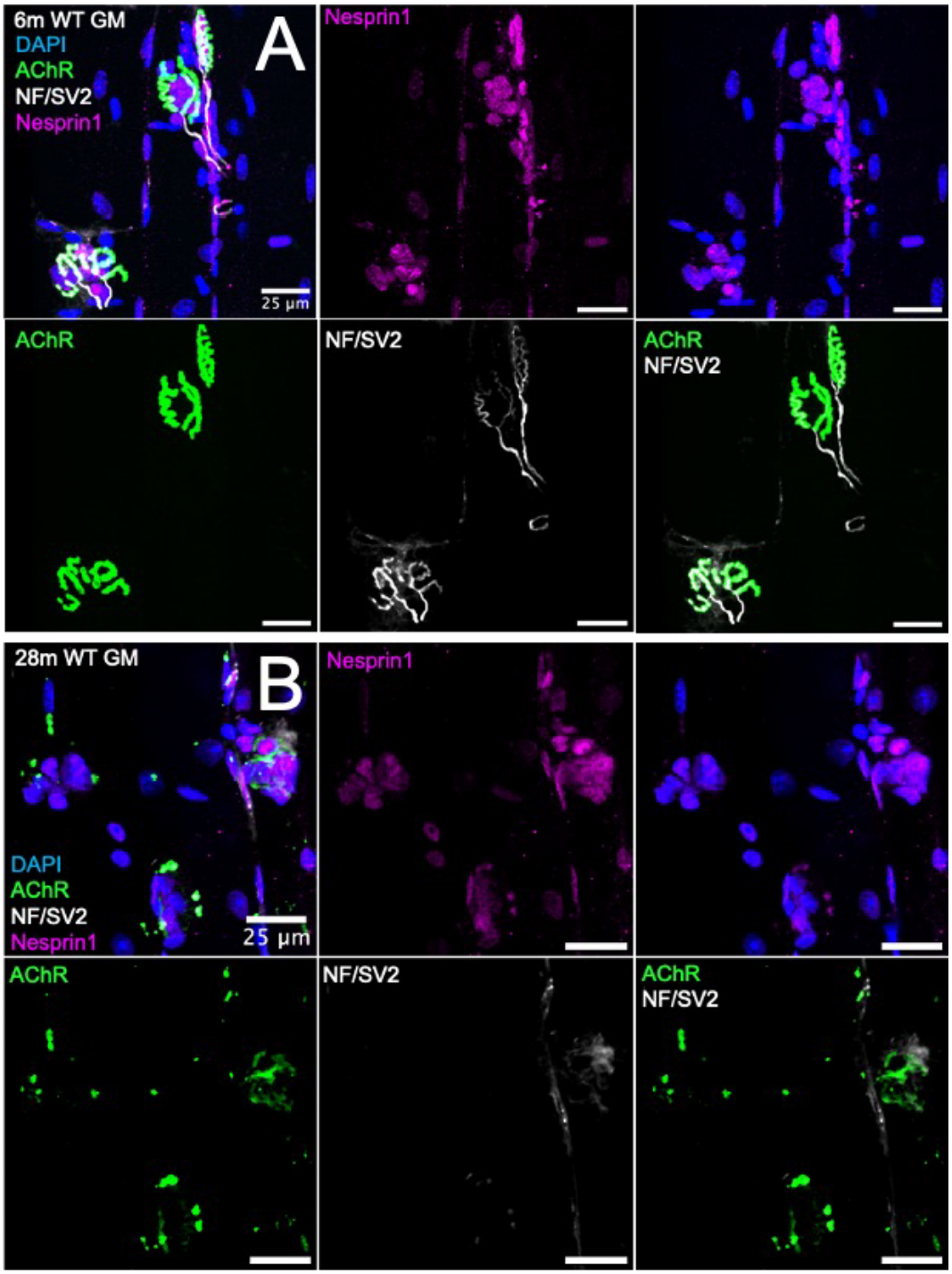


Figure 5 Visualization of synaptic myonuclei in young and old wild type mice. Immunofluorescent images of gastrocnemius muscle fibers from **(A)** 6-month **(B)** 28-month wild type mice and stained for DAPI (blue), AChR (green), NF/SV2 (white), and Nesprin1 (magenta). Scale bars = 25 µm.

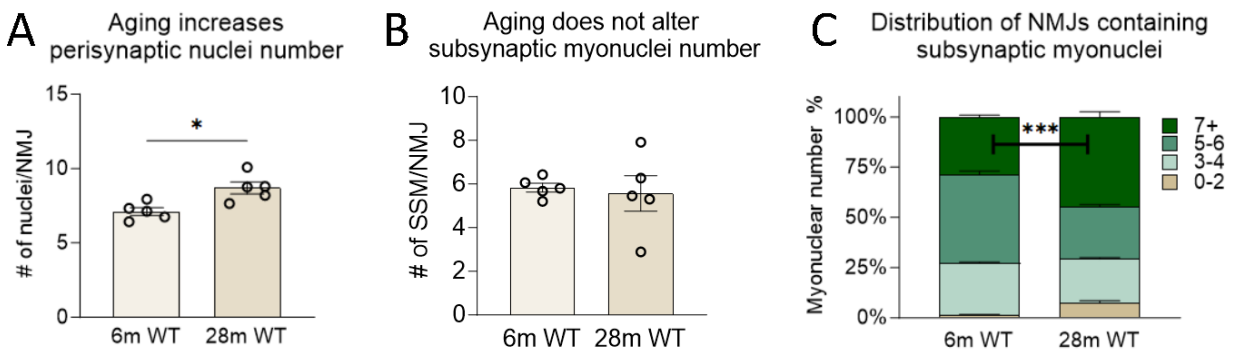


Figure 6 Number of subsynaptic myonuclei remains unchanged by age. Average number of (A) perisynaptic nuclei and (B) subsynaptic nuclei per NMJ. Individual data points represent Average value or each muscle sample. Bars represent mean values with error bars ±SEM

Similar analyses were performed on NMJs from muscle fiber bundles of 6- and 12-month Sod1$^{-/-}$ mice. The average number of SSM were similar between 6-month Sod1$^{-/-}$ mice and age-matched WT mice (Fig. 8B; Fig. 6B). There was also no change between 6 and 12 months in Sod1$^{-/-}$ mice in the average number of perisynaptic or SSM per NMJ (Fig. 8A,B); however, in the case of Sod1 deletion and contrary to the findings in aging WT mice, we observed a trend ($p = 0.08$) toward fewer NMJs with high numbers (7+) of SSM at the older age (Fig. 8C) (6-month Sod1$^{-/-}$: 49% and 12-month Sod1$^{-/-}$: 35%). This decrease in the percentage NMJs with 7+ SSM was accompanied by similarly higher numbers of NMJs with either 3-4 or 5-6 SSM, but neither increased reached statistical significance.

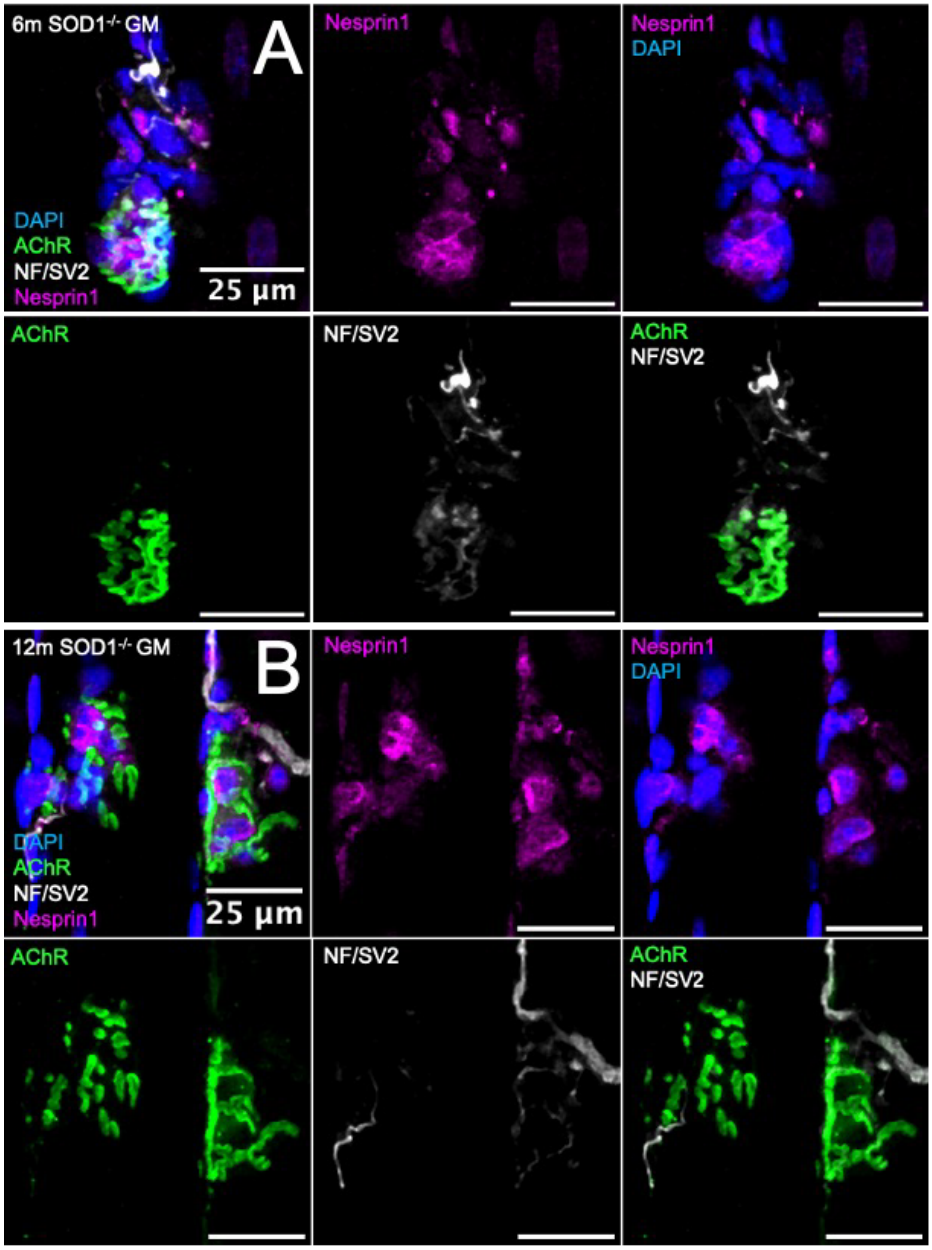


Figure 7 Visualization of synaptic myonuclei in mice deficient in Sod1−/−. Immunofluorescent images of gastrocnemius muscle fibers from (**A**) 6-month and (**B**) 12-month Sod1−/− mice stained for DAPI (blue), AChR (green), NF/SV2 (white), and Nesprin1 (magenta). Scale bars = 25 µm.

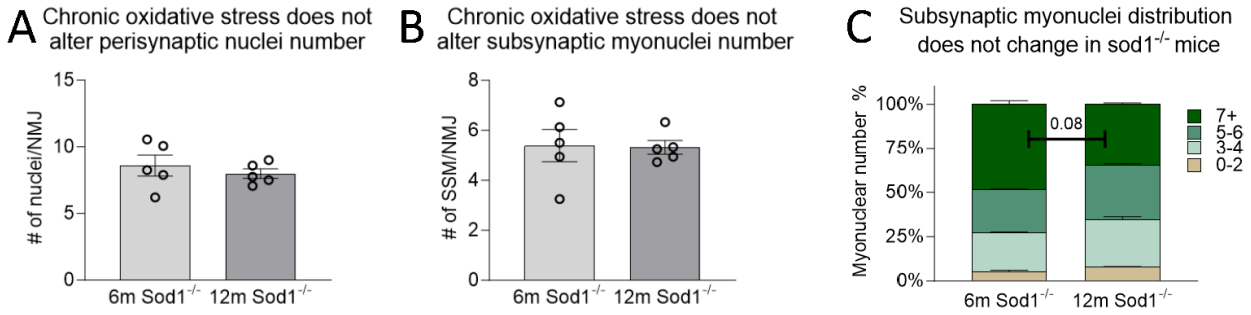


Figure 8 Number of subsynaptic myonuclei remains unchanged by Sod1 deletion. Average number of **(A)** perisynaptic nuclei and **(B)** subynaptic myonuclei per NMJ. Individual data points represent average value for each muscle sample. Bars represent mean values with error bars ±SEM (n = 5/group, 15 NMJs/sample). **(C)** Data on subsynaptic myonuclear number expressed as a percentage of the NMJ containing 0–2 nuclei (tan bars), 3-4 nuclei (light green bars), 5-6 nuclei (green bars) or 7 or more nuclei (dark green bars). Bars represent mean values with error bars ±SEM.

2.4.2 Subsynaptic myonuclei number is not influenced by innervation status

Whether the number of SSM is influenced by the innervation state of a given NMJ during aging or with exposure to chronic oxidative stress, we grouped SSM numbers based on NMJ innervation status (Fig. 9). Consistent with previous reports (Deepa et al., 2019) we found the majority of endplates in GTN muscles of 6-month WT mice to be fully innervated, with a very small percentage being partially denervated. In contrast, in 28- month WT mice, only 22% of endplates are fully innervated, 39% partially denervated and 38% were identified as denervated. In GTN muscles of 6-month Sod1$^{-/-}$ mice, more than 84% of the endplates were denervated or partially denervated, and by 12 months of age, there were essentially no fully innervated endplates remaining in Sod1$^{-/-}$ mice (Fig. 9A). Despite these dramatic shifts in innervation status between genotypes and across age, we observed no differences in the number of SSM at a given NMJ (Fig. 9B; Fig. 9C). We also analyzed the number of nuclei present at every individual NMJ imaged and in 6-month WT mice, we did not observe any denervated endplates (Fig. 9D,E). While we observed increased variability in nuclei counts under conditions of significant NMJ denervation, in aged WT mice and with deletion of Sod1, the cause of this variability remains

unknown. Our results demonstrate that SSM number is not affected by the innervation status in aging WT or Sod1$^{-/-}$ mice.

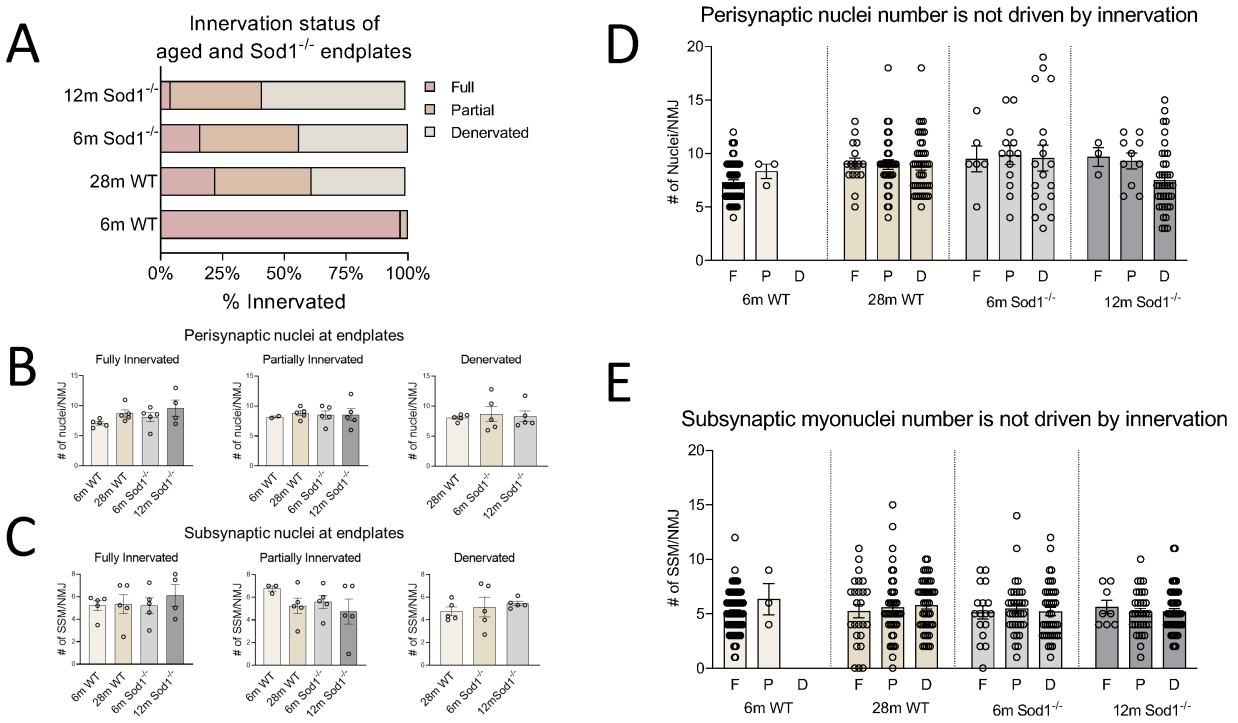


Figure 9 Synaptic nuclei number is not driven by innervation status. **(A)** Distribution of innervation status of young and aged wildtype and Sod1$^{-/-}$ mouse endplates. Endplates were classified as fully innervated if NF/SV2 signal overlapped with more than 80% of the endplate, partially denervated if overlap was <80–10%, and fully denervated if overlap was less than 10%. **(B)** Average number of perisynaptic nuclei at fully innervated, partially innervated and denervated wildtype and Sod1$^{-/-}$ mice. **(C)** Average number of subsynaptic nuclei at fully innervated, partially innervated and denervated wildtype and Sod1$^{-/-}$ mice. **(D)** Number of perisynaptic nuclei at an NMJ based on innervation status. Each point represents the number of perisynaptic nuclei at an endplate. F, Full; P, Partial; D, Denervated. The total number of NMJs analyzed are as follows 6 m WT F = 88, p = 3, D = 0; 28 m WT F = 25, p = 42, D = 48; 6 m Sod1$^{-/-}$ F = 17, p = 34, D = 42; 12 m Sod1$^{-/-}$ F = 8, p = 33, D = 52. **(E)** Number of subsynaptic nuclei at an NMJ based on innervation status. Each point represents the number of subsynaptic nuclei at an endplate. F, Full; P, Partial; D, Denervated.

2.5 Discussion

Based on the knowledge that neural activity is an important regulator of the specialization of SSM (Cisterna et al., 2020; Haddix et al., 2018; Purves & Sakmannt, 1974b) we hypothesized that a strong relationship would exist between NMJ innervation and the distribution of myonuclei at and around the synapse. Contrary to our hypotheses, we observed no effect of acute denervation on the number of SSM nor any differences in SSM number between fully innervated, partially innervated, and fully denervated endplates in two different models of progressive NMJ degeneration. In addition to the rigor in these data provided by our simultaneous analysis of multiple muscle fiber denervating conditions, we have also, for the first time, used both anatomical position of nuclei as well as a marker reported to be specific for SSM (Holt et al., 2019; Grady et al., 2005) in our identification of different populations of myonuclei and demonstrated that location is not sufficient to discriminate SSM from other nuclei proximal to the NMJ. These findings are significant based on disparate reports in the literature that have evaluated individual models separately using purely anatomical definitions of SSM.

Our studies of sciatic nerve transections allowed us to directly test for the impact of both electrical activity at the endplate and anterograde signaling from the motor neuron on SSM number. Our observation of no significant changes from innervated controls in the number of perisynaptic nuclei or Nesprin1+ SSM at 3 days or 7 days post-injury is contrary to reports of a decrease in SSM number 5 days after sciatic nerve axotomy (Picchiarelli et al., 2019). Although these data reported 5 days after denervation are inconsistent with our findings at 3 and 7 days, we cannot rule out the possibility of transient changes in the localization of nuclei occurring due to migration following denervation. In contrast to the report of Picchiarelli et al. (2019) of a decrease in SSM following denervation, Larouche et al. (2021) attributed an increase in

perisynaptic nuclei 28 days following nerve transection to muscle stem cell engraftment at the NMJ as a mechanism to restore the population of SSM following denervation. Again, while inconsistent with our findings, we may very well have observed a similar increase in synaptic nuclei at this later time point. Physiological injury to the muscle fiber membrane triggers a response in which nuclei migrate towards the injury site within 24 h, initiating a repair process that is independent of satellite cells (Roman et al., 2021). The number of nuclei is reported to subsequently show a significant reduction back toward the pre-injury state by 48 h (Roman et al., 2021). These findings suggest that muscle nuclei, perhaps due at least in part to their association with muscle membranes, are highly responsive to muscle and nerve injury and can initiate rapid migratory behavior.

The possibility that nuclear positioning is dynamic and responsive to neural input and/or muscle injury is interesting when considered with our observation of an apparent upregulation of Nesprin1 in muscle nuclei after injury. In Drosophila, Nesprin1 has been shown to serve as a track upon which RNA is transported to regulate synaptic growth and functionality during development (Packard et al., 2015). Following nerve injury, tracks may be formed to transport trophic factors towards the synapse and promote stability of the endplate. Alternatively, it is possible that nerve injury may cause temporary migration of SSM to initiate a degradation process of the NMJ. Following nerve injury, deep bulk RNA sequencing of sciatic nerve samples reveals the activation of an acute immune response which remains active for up to 14 days (Yi et al., 2015). Additionally, single-nuclei RNA sequencing showcased substantial changes in transcription profiles in myonuclei classified as type IIb, further divided into subpopulations of type IIb1 and type IIb2 due to the dynamic nature of myonuclei transcription and the significant impact of denervation after nerve injury (Lin et al., 2022). Collectively, the characterization of

numerous properties of myonuclei strongly supports the notion that, even if they are not lost, the emergence of local domains within myofibers likely has a major impact on the responses to denervation (Bruusgaard & Gundersen, 2008).

Our findings of no changes in the number of SSM in GTN muscles of aged (28-months) compared with young (6-months) WT mice are contrary to those of previous studies that reported fewer SSM in the tibialis anterior and diaphragm muscles of 24-month-old compared to 6-month old mice (Liu et al., 2017). Moreover, Ang et al. (2022) recently reported a modest reduction in the number of perisynaptic myonuclei in both male and female mice between 6- and 28-months of age, but the specific identity of the nuclei counted remains unknown due to the presence of alternative cells such as terminal Schwann cells and immune cells at the synapse (Alhindi et al., 2021; Rios et al., 2021).

Histograms meant to help visualize the likelihood of specific numbers of SSMs present at a given NMJ have been previously used to establish the optimal number of nuclei required to maintain the synaptic domain and to provide insight into the functional impact of a loss of several nuclei (Liu et al., 2017). Even upon analysis of our data in the manner used by (Liu et al., 2017), our observation of an increase in the number of NMJs presenting with high numbers of SSM in muscles of old mice is contrary to their findings. Further, nearly 50% of the NMJs in muscles of 6-month $Sod1^{-/-}$ mice, which are phenotypically similar to aged WT mice (Deepa et al., 2019), displayed 7 or more SSM.

Finally, our observation of a simultaneous increases in muscles of 28- compared with 6-month-old mice in the proportion NMJs with 0–2 nuclei and NMJs with 7+ SSM precluded any general conclusion about an overall increase or decrease with aging in the number of SSM at the

NMJ. The numbers of SSM reported in the literature have shown a high degree of variability, likely based largely on the different criteria used among studies for identification of SSM (Ang et al., 2022; Bai et al., 2022; Liu et al., 2017; Picchiarelli et al., 2019). While some studies classify SMM as those with >25% DAPI signal covered by alpha-bungarotoxin, others use a more stringent definition requiring >70% of the nuclear volume to be overlapping with alpha-bungarotoxin.

In the present study, we utilized Nesprin1 as a marker of SSM (Holt et al., 2019; Mark Grady et al., 2005; Packard et al., 2015), in addition to overlap with the endplate to identify SSM and avoid the possibility of misidentification of terminal Schwann cells that are integrated into the NMJ as SSM. Our findings of a significant increase in the number of perisynaptic nuclei defined anatomically in muscles of 28- month compared with 6-month WT mice but no difference between the groups when Nesprin1 staining was included as a criterion for classification of SSM strongly supports the possibility that using physical location of myonuclei and their proximity to alpha-bungarotoxin staining is insufficient to identify SSM in immunofluorescent images, even when confocal microscopy is used to generate 3D reconstructions. The results of the present study, using the rigorous criteria of both overlap with acetylcholine receptors and Nesprin1 staining to identify SSM, support the conclusion that the number of SSM remains stable across the lifespan under normal physiological conditions and with the presence of chronic oxidative stress.

Our findings of no changes in the number of SSM in GTN muscles of aged (28-months) compared with young (6-months) WT mice are contrary to those of previous studies that reported fewer SSM in the tibialis anterior and diaphragm muscles of 24-month-old compared to 6-month

old mice (Liu et al., 2017). Moreover, Ang et al. (2022) recently reported a modest reduction in the number of perisynaptic myonuclei in both male and female mice between 6- and 28-months of age, but the specific identity of the nuclei counted remains unknown due to the presence of alternative cells such as terminal Schwann cells and immune cells at the synapse (Alhindi et al., 2021; Rios et al., 2021).

Histograms meant to help visualize the likelihood of specific numbers of SSMs present at a given NMJ have been previously used to establish the optimal number of nuclei required to maintain the synaptic domain and to provide insight into the functional impact of a loss of several nuclei (Liu et al., 2017). Even upon analysis of our data in the manner used by (Liu et al., 2017), our observation of an increase in the number of NMJs presenting with high numbers of SSM in muscles of old mice is contrary to their findings. Further, nearly 50% of the NMJs in muscles of 6-month Sod1−/− mice, which are phenotypically similar to aged WT mice (Deepa et al., 2019), displayed 7 or more SSM.

Finally, our observation of a simultaneous increases in muscles of 28- compared with 6-month-old mice in the proportion NMJs with 0–2 nuclei and NMJs with 7+ SSM precluded any general conclusion about an overall increase or decrease with aging in the number of SSM at the NMJ. The numbers of SSM reported in the literature have shown a high degree of variability, likely based largely on the different criteria used among studies for identification of SSM (Liu et al., 2017; Picchiarelli et al., 2019; Ang et al., 2022; Bai et al., 2022). While some studies classify SMM as those with >25% DAPI signal covered by alpha-bungarotoxin, others use a more stringent definition requiring >70% of the nuclear volume to be overlapping with alpha-bungarotoxin.

In the present study, we utilized Nesprin1 as a marker of SSM (Grady et al., 2005; Packard et al., 2015; Holt et al., 2019), in addition to overlap with the endplate to identify SSM and avoid the possibility of misidentification of terminal Schwann cells that are integrated into the NMJ as SSM. Our findings of a significant increase in the number of perisynaptic nuclei defined anatomically in muscles of 28- month compared with 6-month WT mice but no difference between the groups when Nesprin1 staining was included as a criterion for classification of SSM strongly supports the possibility that using physical location of myonuclei and their proximity to alpha-bungarotoxin staining is insufficient to identify SSM in immunofluorescent images, even when confocal microscopy is used to generate 3D reconstructions. The results of the present study, using the rigorous criteria of both overlap with acetylcholine receptors and Nesprin1 staining to identify SSM, support the conclusion that the number of SSM remains stable across the lifespan under normal physiological conditions and with the presence of chronic oxidative stress.

The etiology of sarcopenia, a progressive age-associated loss of skeletal muscle mass and function, remains incompletely understood. Evidence suggests that alterations during aging in the structure of the synaptic apparatus and a decrease in the degree of muscle fiber innervation may contribute to sarcopenia (Deschenes et al., 2022; Jang & Van Remmen, 2011; Y. Li et al., 2011; Valdez et al., 2010; Willadt et al., 2016)

Although recent studies postulate that SSM, which provide support to the synaptic apparatus, may be linked to the integrity of the NMJ (Dos Santos et al., 2020; Saini et al., 2021), our findings of no change with aging in either WT mice or $Sod1^{-/-}$ mice, a model of accelerated neuromuscular aging (Deepa et al., 2019), in SSM indicates that any contribution of alterations

in SSM to breakdown of the NMJ and loss of innervation is not related to SSM number. This conclusion is further supported by our analysis of the relationship between the state of innervation of a given endplate and the associated number of SSM.

Although our data on the extent of denervation during normal aging and with Sod1 deficiency aligned well with previous literature, in which muscles of Sod1$^{-/-}$ mice showed a similar distribution of innervated endplates at 12 months of age as observed in WT mice at 28 months (Deepa et al., 2019; Pollock et al., 2023), we observed no substantial differences based on innervation status in the number of SSM nuclei present. These observations showing a lack of any relationship between innervation status and SSM number were contrary to the recent report of Ang et al. (2022), who concluded that any changes with aging in SSM number were likely secondary to NMJ structural modifications.

Interestingly, we observed a higher degree of variability in SSM number in the muscles of mice subjected to sciatic nerve transection and in Sod1$^{-/-}$ mice compared with muscles of young WT mice. The degree of variability was comparable to the variance in synaptic nuclei number previously reported in Sod1$^{-/-}$ mice(Bai et al., 2022) and in 4EBP1-transgenic mice(Ang et al., 2022). An increase in variability is perhaps not surprising based on the heterogeneity of the state and duration of denervation or reinnervation across NMJs. Together these findings suggest that the position of nuclei may not necessarily be static, rather that migration of myonuclei and other cell types is ongoing in response to changes in innervation status or other signals that may trigger changes in both position and function of nuclei as well as NMJ disruption.

A dynamic population of nuclei may explain some of the disparate findings in the literature. It is important to note that our study has limitations, such as examining only two time

points for each genotype, which are unlikely to capture transient changes in myonuclei number that may occur throughout the mouse lifespan, particularly in response to injury as observed by Bai and colleagues. In addition, although using Nesprin1 as one of the identifying features of SSM is a strength of the study, the mechanisms regulating Nesprin1 expression are not known. The hypothesis that neural input is at least in part responsible for maintaining Nesprin1 expression is not unreasonable. In fact, since many of the NMJs in the muscles of 12-month $Sod1^{-/-}$ mice have likely been chronically denervated, our observation of a decrease in the percentage of NMJs with high numbers (7+) of SSM in this group is consistent with a loss of Nesprin1 expression with "long" term loss of neural input. Future studies defining the regulation of Nesprin1 expression are warranted.

In addition, in this study, we did not control for variations in muscle fiber type, which introduces intriguing complexities related to the NMJ. Specifically, within the extensor digitorum longus (EDL) muscle of the rat, a notable difference exists between NMJs associated with Type 1 fibers, which have been documented to be morphologically larger, compared to those linked to Type 2 fibers. In contrast, in the soleus muscles, the observation is reversed, with Type 2 fibers exhibiting larger NMJ morphologies (Deschenes et al., 2013). More recent studies in mice suggest a correlation wherein fast-twitch fibers are more prone to innervation by smaller endplates, while slow-twitch fibers exhibit larger post-synaptic structures, as documented by Mech et al. (2020). However, when considering the context of aging, recent findings support the prevailing notion that aging primarily affects fast-twitch fibers. Instead, the latest evidence suggests that the impact of aging is more likely to be muscle-specific rather than solely determined by fiber type, as indicated by Skinner et al. (2021).

Nonetheless, it is worth noting that the gastrocnemius muscle of mice contains only 5% Type 1 fibers (Augusto et al., 2017), indicating that we have evaluated NMJs from almost exclusively Type 2 Fibers. Further investigation is warranted to delve into the quantity and properties of subsynaptic myonuclei in various contexts. Finally, we have not characterized other properties of the nuclei, such as shape (Battey et al., 2023; Kalukula et al., 2022; Rader & Baker, 2022), expression of nuclear proteins, chromatin structure, or transcriptional differences.

Despite these weaknesses, our findings clearly challenge the notion that a loss of SSM is a primary driver of NMJ degradation and suggest that changes in the number of SSM may not imbue significant physiological repercussions to the endplate.

Based on our findings and existing literature, we conclude that maintaining the NMJ is not solely dependent on the number of SSM present, but also on other factors including the transcriptional profile of pre and postsynaptic nuclei (Kim et al., 2020; Perez et al., 2021). Age-related alterations to nuclei and their products may also contribute to the degradation of the NMJ (Yousefzadeh et al., 2021). While our study does not show acute changes in SSM number following nerve injury, future studies should investigate transient and chronic changes in myonuclei number after nerve insult. Additionally, identifying DNA damage in SSM and isolating Nesprin1 positive nuclei for single nuclei sequencing could provide insights into age-related changes to the transcriptional landscape of these nuclei and how motor neuron innervation defines their transcriptional profile (Bai et al., 2022; Roman et al., 2021).

Chapter 3 Evaluating the Role of Lamin A/C in Muscle Fiber Reinnervation

3.1 Abstract

Sarcopenia, the age-related decline in skeletal muscle mass and force, is partly attributed to denervation-induced muscle fiber loss, yet the mechanisms driving this loss of innervation are not well understood. A diminished ability for neuromuscular junctions (NMJ) to regenerate following a disruption of the synapse has been proposed as a contributing factor in age-associated muscle fiber denervation. Lamin A/C, a key intermediate filament protein in the nuclear lamina, is expressed in skeletal muscle and decreases with age, and with muscle-specific deletion reported to accelerate NMJ degradation, resembling age-associated NMJ decline. Thus, this study investigates the role of lamin A/C in NMJ regeneration as a potential contributor to the accumulation of denervated NMJs with aging. We conducted sciatic nerve injuries in wildtype (WT) and muscle-specific Lmna heterozygous knockout mice (AC-Lmna$^{+/-}$), assessing transcript and protein expression, lamin A/C localization, specific force (SPo) from nerve and muscle stimulation, innervation status, and endplate morphology. Our results revealed a significant induction of Lmna concomitant with AChRα by 7 days post-injury, with recovery by day 14 and maintenance at day 28. Western blot confirmed lamin A/C induction at 14 days post-injury. Immunohistochemistry confirmed lamin A/C upregulation throughout the length of the muscle without a specific injury-induced localization pattern. Functional analysis revealed an innate specific force deficit in muscles of AC-Lmna$^{+/-}$ mice but no differences compared with WT mice in SPo at 7 days post-injury. By 14 days, however, AC-Lmna$^{+/-}$ mice exhibited delayed recovery

of nerve-stimulated SPo and impaired neurotransmission fidelity, despite intact NMJ morphology across multiple structural features. These results suggest that partial Lmna deletion delays functional NMJ recovery without affecting structural maintenance. Importantly, the transcriptional response to denervation was specific to Lamin A/C rather than a general nuclear envelope response. These findings highlight Lamin A/C as a potential target for therapeutic intervention for denervating conditions such as aging.

3.2 Introduction

Aging significantly impacts skeletal muscle, leading to a gradual decline in both muscle mass and strength. This phenomenon, known as sarcopenia, affects even healthy, active individuals, with muscle loss estimated between 1% and 8% annually from ages 60-80 (Ang et al., 2022; Bai et al., 2022; Balice-Gordon, 1997). Sarcopenia is linked to reduced functional performance, an increased risk of falls, compromised motor function, and various metabolic and physiological deficits (Battey et al., 2023a, 2023b; Carboni et al., 2013; Crisp et al., 2006; Cutler et al., 2017). Understanding the mechanisms underlying age-related muscle wasting is crucial for facilitating development of effective therapeutic strategies against frailty, loss of independence, physical disability, and premature death in the elderly. A well-established contributor to sarcopenia is age-associated muscle fiber loss that is driven at least in part by breakdown of the synaptic apparatus at the neuromuscular junction (NMJ) and resultant loss of innervation (Dobrowolny et al., 2021; Iyer et al., 2021; Wilkinson et al., 2018). This conclusion is based largely on numerous observations of an accumulation during aging of NMJs that display morphological abnormalities including partial or complete loss of overlap of pre- and post-synaptic structures and loss of the continuous staining of postsynaptic acetylcholine receptors (AChR), referred to as endplate fragmentation (Jang & Van Remmen, 2011). The factors that trigger the degenerative changes at NMJs are not known, but a diminished ability for NMJs to regenerate in older individuals has been proposed (Doherty et al., 1993; Sonjak et al., 2019). The cellular processes and molecular pathways that are critical for muscle fiber reinnervation are not clear. Thus, there is much room for investigating potential targets to enhance reinnervation to protect against age-associated fiber loss.

As introduced in Chapter 2 of this dissertation, there is a growing interest in exploring the role of changes in the number and function of subsynaptic myonuclei (SSM) as contributors to the maintenance of innervation and the relevance in sarcopenia. The SSM are a distinct population of myonuclei that reside directly beneath the postsynaptic assembly. Findings presented in Chapter 2 show that the number of SSM remains stable with age and it is not affected by innervation status of the NMJs during aging (Ruiz et al., 2023). These findings indicate that maintenance of the NMJ is not solely dependent on the number of SSM present, but perhaps influenced by the transcriptional profile of the nuclei in proximity to the endplate (Kim et al., 2020; Perez et al., 2022). Age-related alterations in myonuclear gene expression (Yousefzadeh et al., 2021) rather than simply changes in the number of nuclei (Ruiz et al., 2023) likely contribute to the degradation of the NMJ.

The nucleus is responsible for housing DNA and maintaining its spatial organization, facilitating gene access for transcription. Nuclei harbor a dense protein network of nuclear lamins, which form a scaffold on the inner surface of the nuclear envelope in eukaryotic cells. The nuclear lamina contributes to the size, shape, and rigidity (Battey et al., 2023b) of nuclei and also interacts with chromatin and nuclear membrane proteins to regulate gene expression. Nuclear architecture and membrane function appear to be critical controllers of aging, as evidenced by mutations in Lamin A leading to the premature aging syndrome Hutchinson-Gilford progeria (HGPS), and age-related deterioration of the nuclear pore complexes (D'Angelo et al., 2009; López-Otín et al., 2013; Pathak et al., 2021; Scaffidi & Misteli, 2006). In addition to these effects, the disruption of nuclear-cytoplasmic transport due to alterations in the nuclear envelope and pore complexes has been shown to contribute to age-associated declines in cellular homeostasis (D'Angelo, 2018). Moreover, defects in nuclear lamina organization can impair

DNA repair mechanisms, accelerating the accumulation of DNA damage, which further promotes cellular senescence and organismal aging (Gonzalez-Suarez et al., 2009; Maynard et al., 2019). Lamin A/C is the primary intermediate filament protein of the nuclear lamina and mutations in its gene (*Lmna*) lead to progeroid syndromes (Carboni et al., 2013). Further, Lamin A/C has long been recognized as important for muscle stem cell differentiation, maintenance of nuclear mechanics, and mechanotransduction (Donnaloja et al., 2020; Frock et al., 2006; Lammerding et al., 2004; Méjat et al., 2009), and neuronal knockdown of Lamin impaired motor function and decreased lifespan in flies (Oyston et al., 2018).

Recently, Lamin A/C levels have been reported to decrease during aging in muscles of mice, and muscle-specific deletion of Lmna accelerate the degradation of NMJs, similar to features seen in aging (Gao et al., 2020). These findings led us to question whether an age-associated decline in muscle Lmna, perhaps specific to the SSM, contributes to the impaired NMJ regeneration during aging, or conversely, if muscle Lmna expression is an important regulator of muscle fiber reinnervation in denervating conditions. Thus, the goal of this study was to examine Lmna expression during reinnervation and to test the hypothesis that muscle Lmna is required for effective NMJ regeneration. We approached this goal by examining Lmna gene expression and Lamin A/C levels and localization following surgical nerve injuries in wild type (WT) mice. We then compared the reinnervation response following a recoverable nerve crush injury in WT mice and in mice with a muscle-specific deficiency of Lmna with the expectation that deficiency of Lmna would impair or delay reinnervation following nerve crush.

3.3 Materials and Methods

3.3.1 Animals

Male and female wildtype (WT) C57BL/6 mice and muscle-specific Lmna deficient mice were used in this study. A floxed Lmna mouse line on the C57BL/6 background ($Lmna^{+/+}$), with exons 10 and 11 of the Lmna gene flanked by loxP sites, was generously provided by Ormand MacDougald (University of Michigan) (Fig. 10) (Corsa C. et al., 2021; Wang A.S. et al., 2015). To investigate the role of lamin A/C in skeletal muscle, we developed a muscle-specific Lmna knockout model (AC-$Lmna^{-/-}$), and a muscle-specific Lmna heterozygous (AC-$Lmna^{+/-}$) knockout by breeding Lmna flox ($Lmna^{+/+}$) mice with Acta1-Cre (AC) (#006149, Jackson Laboratory) transgenic mice, kindly provided by Holly Van Remmen (Oklahoma Medical Research Foundation). This breeding strategy facilitated the deletion of Lmna in skeletal muscle through Cre-lox recombination. All mice were housed in specific-pathogen-free conditions, with ad-libitum access to standard laboratory food and water and were subjected to a 12-hour light/dark cycle. The animal experiments described here were reviewed and approved by the University of Michigan Institutional Animal Care and Use Committee (IACUC).

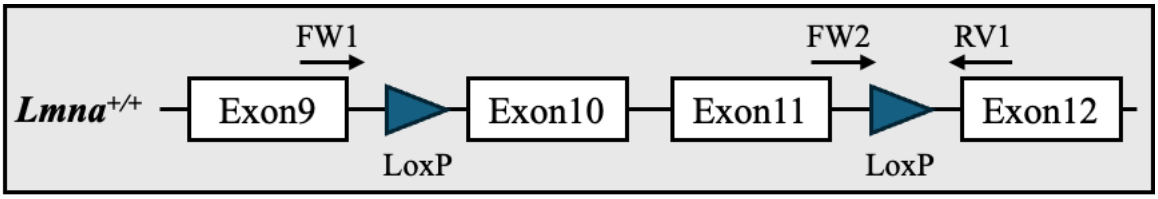


Figure 10 LoxP sites flanking exon 10–11 of *Lmna*, which are removed by Cre recombinase. Boxes represent exons, black triangles represent 34-bp loxP sites, and genotyping primers (F1, F2 and R1) are indicated with arrows.

3.3.2 Heterozygous mice

While breeding Lmna knockout mice, we observed that mice with muscle-specific homozygous deficiency exhibited a runted phenotype (Fig. 11). Additionally, these runted knockouts had an extremely high mortality rate near 90% before 8 weeks of age. Consequently, we determined that embryonic deletion of Lmna was not a suitable model for studying the effects of nerve injury and reinnervation. In contrast, heterozygous mice (AC-Lmna$^{+/-}$) were fully viable and did not display any runting compared to floxed control mice.

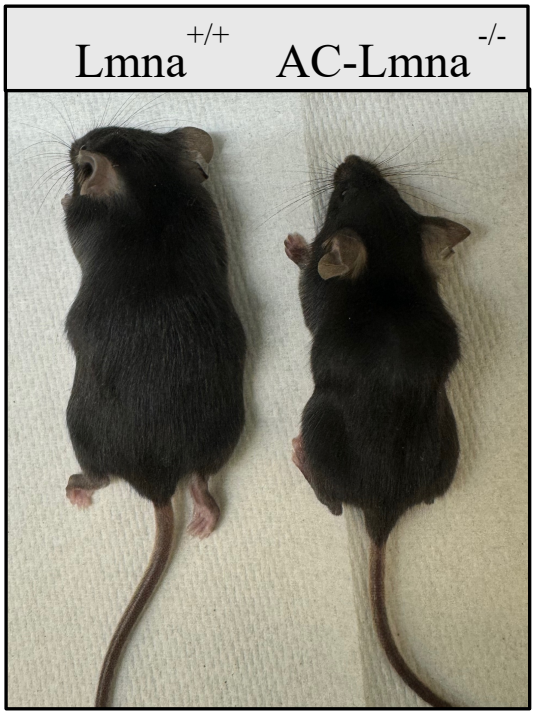


Figure 11 Runted phenotype of 2-month-old constitutive knockout mice. A visual comparison of size between flox Lmna$^{+/+}$ mice (Left) and muscle-specific Lmna knockout AC-Lmna$^{+/-}$ (Right). Acta-Cre (AC).

3.3.3 Sciatic nerve injuries

To assess the response of Lmna to denervation, we first studied WT mice, which were randomly assigned to either a 3-,7-,14-, or 28-day recovery group then subjected to either a sciatic nerve transection (SNT) or a sciatic nerve crush (SNC). The procedure was as follows.

First, mice were anesthetized with 5% isoflurane as required to ensure no response to tactile stimuli, followed by continuous administration of 2% isoflurane for maintenance. Next, carprofen (5 mg/kg) was administered as a preoperative analgesic. The hindlimbs were carefully shaved and the skin was cleaned with chlorhexidine and 70% alcohol. A small skin incision (<10 mm) was made 1 mm posterior and parallel to the femur, and the superficial biceps femoris was split to expose the sciatic nerve. The sciatic nerve was then transected, and a 5 mm segment was removed. If the mouse was assigned to an SNC group, the nerve was crushed with #5 forceps for 30 seconds at the mid-femur level. The incision was closed with wound clips (Autoclip, BD Clay Adams, Franklin Lakes, NJ). The same procedure was performed on the contralateral leg. After surgery, the mice were placed on a heating pad and closely observed until they recovered from the anesthetic.

3.4 Force testing and tissue collection

Mice were anesthetized with an initial induction of 5% isoflurane and maintained with 2% isoflurane. Gastrocnemius (GTN) muscle contractile properties were measured in situ, as described by Larkin et al. (2011). In anesthetized mice, the whole GTN muscle was isolated from surrounding muscle and connective tissue using great care not to damage the nerve and/or blood vessels during the dissection. A 4-0 silk suture was tied around the distal tendon and the tendon was severed. The mouse was then placed on a temperature-controlled platform warmed to maintain optimal body temperature throughout the procedure. The hindlimb was securely tied to a fixed post with 4-0 monofilament nylon suture at the knee and the foot was clamped to the platform. The distal tendon of the GTN muscle was then tied to the lever arm of a servomotor (model 6650LR, Cambridge Technology). A continual drip of saline warmed to 37°C was administered to the GTN muscle to prevent it from drying. The muscle was activated by

stimulation of the sciatic nerve using a bipolar platinum wire electrode. The optimal voltage and optimal length (Lo) were determined based on the length that elicited maximal isometric twitch force (Po). Lo was measured using calipers based on established landmarks for the proximal end and visual inspection of the distal end of the muscle. The same procedure was then repeated, but rather than activating the muscle via the sciatic nerve, a cuff electrode was placed around the proximal and distal ends of the muscle for direct muscle stimulation. After force measurements, the GTN was removed trimmed of tendons, blotted and weighed. GTN muscle fiber length (Lf) was calculated by multiplying Lo by 0.45. CSA and sPo were calculated as described above. The GTN muscles were also removed, trimmed, and weighed and all muscles were either snap-frozen for molecular analyses or coated in tissue-freezing medium (Electron Microscopy Sciences) and rapidly frozen in isopentane cooled with liquid nitrogen for histologic analysis.

3.5 Whole muscle RNA extraction an RT-qPCR

To assess the denervation response in muscle, we analyzed whole muscles by RT-qPCR using the gastrocnemius muscles from two-month or six-month old WT uninjured control mice and mice with either 7-day, 14-day, or 28-day sciatic nerve injuries. GTN muscles were homogenized in TRIzol reagen (Invitrogen, Thermo Fisher Scientific) using a bead mill. RNA isolation was performed by phenol/chloroform extraction and RNA yield was determined using a NanoDrop spectrophotometer (NanoDrop 2000C, Thermo Fisher Scientific). Contaminating genomic DNA was removed by incubation with DNase I (Ambion, Thermo Fisher Scientific, AM2222) followed by heat inactivation. Total RNA (1 μg) was reverse-transciber to cDNA using SuperScript III Master Mix, Random Hexamers, and dNTPs (Invitrogen, Thermo Fisher Scientific) and RT-qPCR was conducted using a CFX96 Real-Time PCR Detection System (Bio-Rad, 1855195) in triplicate 20 μl reactions of iTaq universal SYBER Green Supermix (Bio-Rad,

1725124) with 1 μM forward and reverse primer. Relative mRNA expression was determined using the $2^{-\Delta\Delta CT}$ method with GAPDH serving as a control for the samples.

3.6 Western blot for Lamin A/C

A lysis cocktail using RIPA buffer (Thermo Fisher Scientific #89900), protease inhibitor (Thermo Fisher Scientific #78425), and phosphatase inhibitor (Thermo Fisher Scientific #78428) at a 1:100 dilution. Tissue homogenization was performed using a bead homogenizer. Approximately 30 mg of frozen gastrocnemius muscle was weighed, followed by the addition of 10x tissue weight of lysis buffer. The lysate was centrifuged at 15,000 RPM for 20 minutes at 4°C, and the supernatant containing protein was collected, avoiding the pellet and DNA layer. Protein concentrations were determined using the Pierce BCA Protein Assay Kit (Thermo Fisher Scientific #23225) following the manufacturer's instructions. Standards and samples were prepared, incubated with working reagent at 37°C for 30 minutes, and absorbance was measured at 562 nm using a plate reader. Gels were cast using the Bio-Rad TGX Stain-Free Acrylamide Kit (Bio-Rad #1610180) following the manufacturer's protocol. Proteins were denatured using Laemmli buffer (Bio-Rad #1610737), resolved by SDS-PAGE, and transferred to a PVDF membrane using the Trans-blot Turbo system. Membranes were blocked in 5% milk/TBS-Tween 0.1% for 1 hour and incubated with primary antibodies (Cell Signaling, Lamin A/C #2032) overnight. Membranes subsequently washed with TBS-Tween 0.1% then followed by secondary antibody incubation. Signals were detected using chemiluminescent substrate and imaged using a ChemiDoc system band intensity was measured using Image Lab (Bio-Rad).

3.7 Immunohistochemistry

Myofiber bundles were mechanically teased from tibialis anterior muscles under a dissecting microscope and processed for immunohistochemistry. The myofiber bundles were first blocked for 1 h at room temperature with a solution of 5% goat serum (Gibco), 1% bovine serum albumin (Fisher Scientific), 0.5% Triton X-100 (Sigma-Aldrich), and 0.01% sodium-azide (Sigma-Aldrich), then blocked for 30 min with 10% Mouse IgG, Fab fragment (Jackson ImmunoResearch). The myofiber bundles were then incubated overnight at 4°C with primary antibodies Lamin A/C (1:200) (Cell Signaling Technology) and Neurofilament (2H3)/Synaptic vesicle glycoprotein 2A (NF/SV2) (1:50/1:25) mouse-monoclonal antibody (Developmental Studies Hybridoma Bank). Following overnight incubation, bundles were washed with phosphate-buffered saline (PBS), treated with secondary antibodies goat-anti-rabbit 594 (1:200) and goat-anti-mouse 647 (1:1000) (Invitrogen), and co-stained with alpha-bungarotoxin (α-BTX) conjugates 488 (1:500) (Invitrogen) and DAPI (4′,6-diamidino-2-phenylindole, dihydrochloride) (1:1000) (Invitrogen) for 1 h at room temperature. The myofiber bundles were then washed with PBS, mounted onto slides with DAKO fluorescence mounting media for imaging via confocal microscopy.

3.8 Results

Our first set of experiments examined Lmna mRNA and Lamin A/C protein induction after injury. We identified a marked increase in Lmna mRNA in gastrocnemius (GM) muscles 3 and 7 days (12- and 14-fold, respectively) after sciatic nerve transection (SNT) (Fig. 12). This robust induction of Lmna was mirrored by the dramatic upregulation of AChRα known to be a reliable marker of muscle fiber denervation (Aare et al., 2016). Induction of the protein product Lamin

A/C was confirmed at 14-days after injury via western blot (Fig.13). Immunohistochemistry (IHC) of extensor digitorum longus (EDL) muscles also showed increased levels of the protein product of Lmna, Lamin A/C, following SNT (Fig. 14).

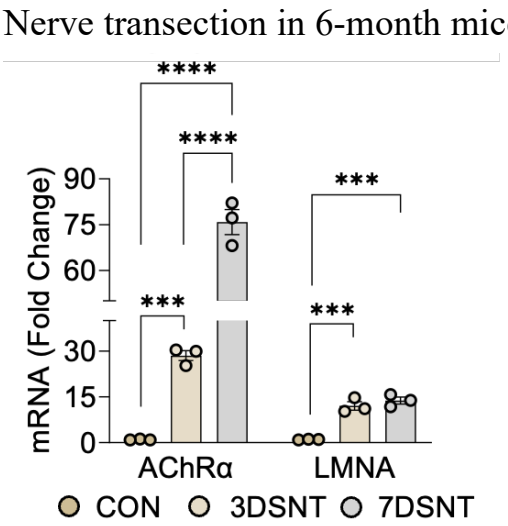


Figure 12 Transcript levels in 6-month-old WT mice in uninjured control, 3- and 7-days after sciatic nerve transection (SNT). ***p<.005, ****p<0.0001 by ANOVA, Mean ± SEM. N=3/group.

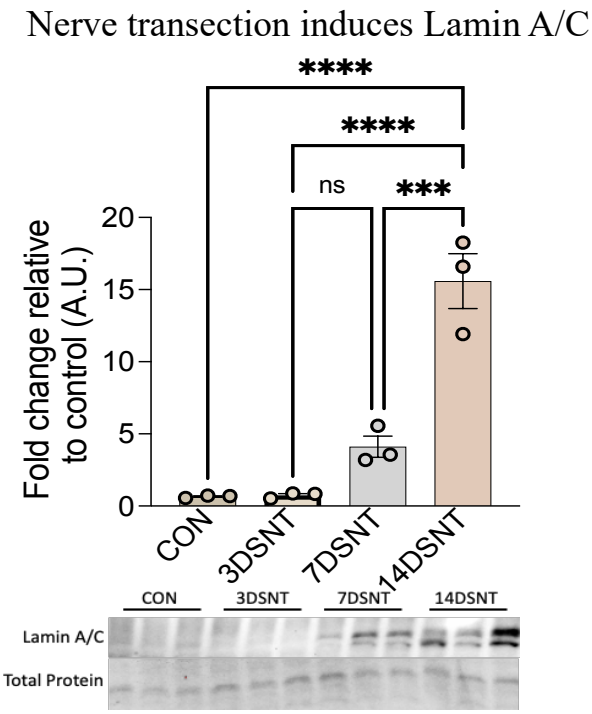


Figure 13 Lamin A/C Protein expression in 6-month old WT mice in uninjured control, 3-, 7-, and 14-days after sciatic nerve transection (SNT). ***p<.005, ****p<0.0001by ANOVA, Mean ± SEM. N=3/group.

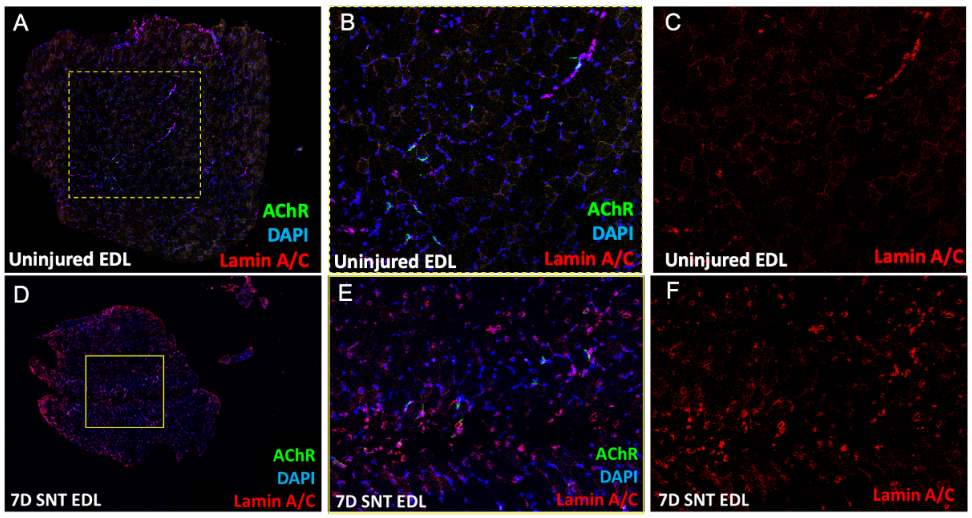


Figure 14 Lamin A/C is upregulated 7-days post denervation in 6-month-old WT mice. (**A-C**) Uninjured extensor digitorum longus (EDL) muscles and (**D-F**) 7-days after sciatic nerve transection (7DSNT) in WT mice. (**A**) and (**D**) whole muscle cross-sections, Dashed and solid yellow boxes represent region of interest and are magnified in (**B&E**) and (**C&F**). Acetylcholine receptor (AChR) (green), DAPI (blue), and Lamin A/C (red).

Prior to pursuing studies of whether Lamin A/C expression may be important for reinnervation following a recoverable nerve injury, we confirmed that expression levels following a sciatic

nerve crush (SNC) injury. Unlike SNT, in which there is no reinnervation, SNC preserves neuronal regeneration, allowing for evaluation of functional recovery coincident with Lmna expression. We found a similar induction of Lmna with SNC to that observed following SNT (Fig. 15). Lamin A/C protein levels were also found elevated following nerve crush injuries (Fig. 16).

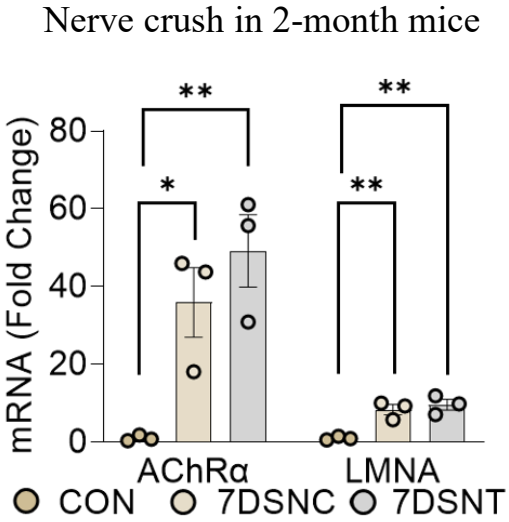


Figure 15 Muscle Lmna is increased by both sciatic nerve crush (SNC) and sciatic nerve transection (SNT) injury models in 2-month-old mice. Transcript levels 7-days after nerve injury in WT mice. CON=uninjured, *p<.05, **p<.005. Means ± SEM by ANOVA. n=3

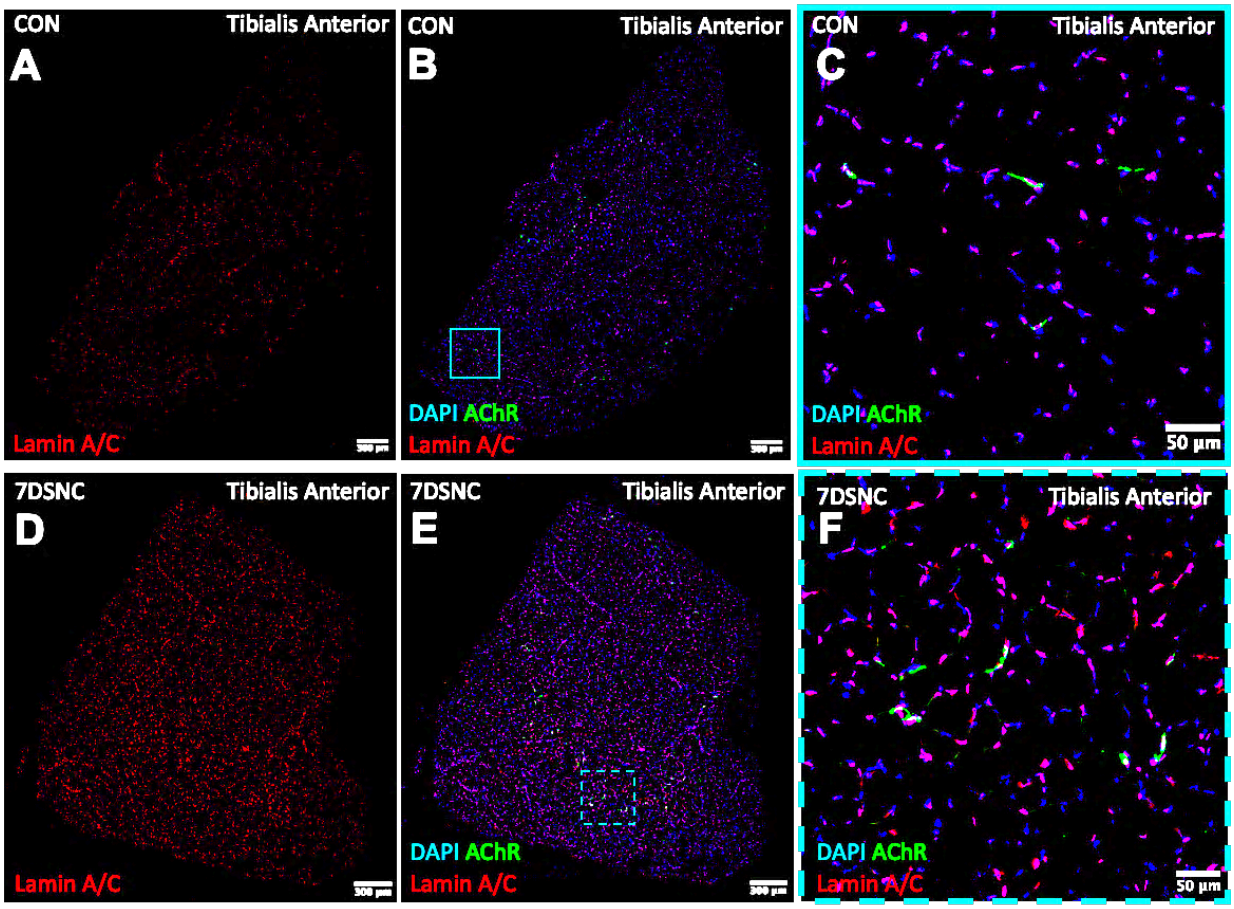


Figure 16 Lamin A/C is elevated in the tibialis anterior muscle 7-days post nerve crush and is present at the endplate in 2-month old mice. Whole cross-section image (**A,B,D,E**) Scale bar = 300 µm; Solid blue square (**B**) and dashed blue square (**E**) represent regions of interest (ROI) that contain endplates; Magnified ROI images (**C,F**) Scale bar = 50 µm. Red = Lamin A/C, Green = Acetylcholine receptor (AChR), Blue = DAPI

To investigate the functional role of Lmna following denervation and to address the question of whether other nuclear envelope proteins displayed the same pattern of induction and resolution as Lmna following denervation, we simultaneously analyzed the expression of Lmna, NET39, SYNE1, SUN1, SUN2, and Emerin at multiple time points following SNC. As previously observed (Fig. 15), Lmna expression increased 10-fold in gastrocnemius muscles at 7 days post-injury but returned to baseline levels by 14 days. NET39 transcript levels were significantly downregulated ($p < .00005$) by day 7, recovered by day 14, and remained stable through day 28 (Fig. 17). In contrast, LINC complex components, including SYNE1, SUN1, SUN2, and Emerin, were unresponsive to nerve injury (Fig. 17), suggesting that these nuclear

envelope proteins are not directly involved in the early stages of reinnervation, and the induction of Lmna is a specific response to denervation and not part of a general upregulation of the nuclear envelope proteins. YAP and TAZ transcripts also showed upregulation by 7 days post-injury, returned to baseline by day 14, and were sustained at day 28. These molecules were assessed due to their established roles as transcriptional coactivators in regulating synaptic gene expression, as well as their involvement in the formation and morphology of NMJs (Gessler et al., 2024), and to investigate whether their expression was influenced by the process of reinnervation.

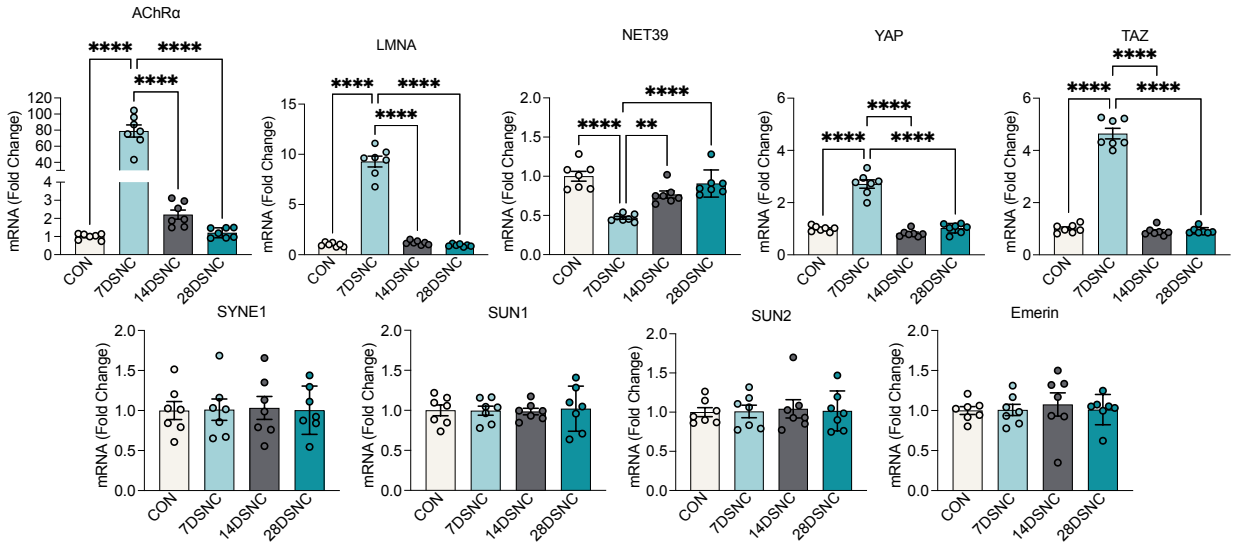


Figure 17 Transcriptional changes in LMNA, NET39, YAP, and TAZ with denervation are present at 7 days and return towards baseline by 14 days and maintained at 28 days. The LINC complex components SYNE1, SUN1, SUN2, and Emerin are stable following nerve crush. Temporal expression pattern of LMNA in the gastrocnemius muscle of 2-mo WT mice. ****p<.0001. Mean ± SEM by ANOVA, n=7.

Immunohistochemistry of fiber bundles from wildtype gastrocnemius muscles was conducted to confirm NMJ denervation and to provide direct evidence of nerve regeneration at endplates following injury. In uninjured muscles, endplates were fully innervated (Fig. 18A), whereas complete loss of innervation was observed at 7 days post-injury (Fig. 18B), along with the presence of Lamin A/C-positive nuclei near the endplates (Fig. 18A, B). By 14 days post-

sciatic nerve crush, reinnervation at the endplates was evident (Fig. 18C) and remained stable through 28 days post-injury (Fig. 18D).

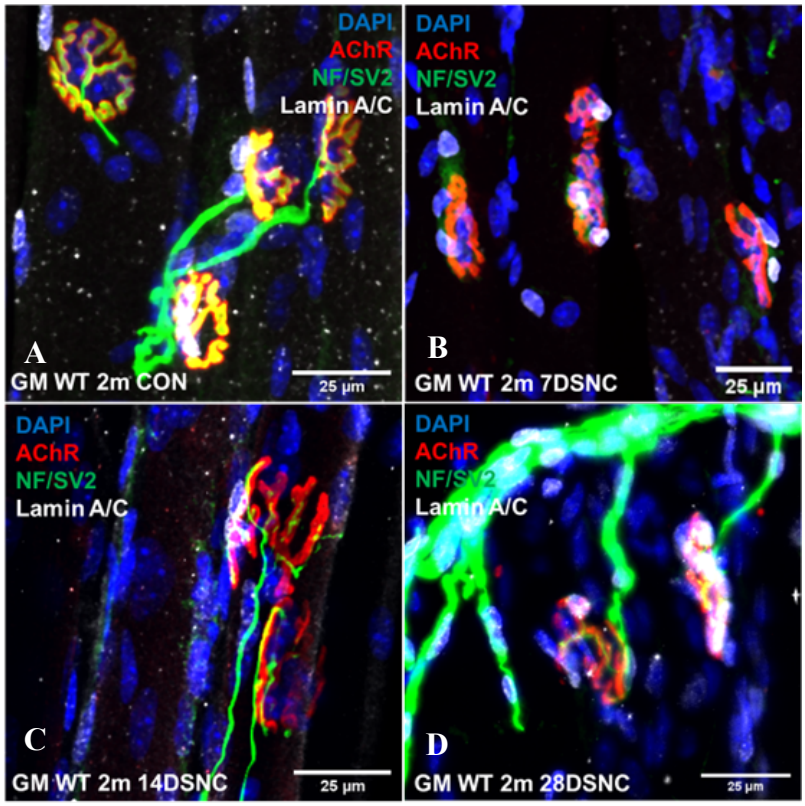


Figure 18 Immunohistochemistry of the time course following nerve crush in gastrocnemius (GM) muscles. Immunostaining shows DAPI (blue) for nuclear staining, AChR (red) for acetylcholine receptors, NF/SV2 (green) for neurofilament/synaptic vesicles, and Lamin A/C (white) for nuclear staining, AChR (red) for acetylcholine receptors, NF/SV2 (green) for neurofilament/synaptic vesicles and Lamin A/C (white) for nuclear lamina in (**A)** control muscles and muscles (**B)** 7-days post nerve crush, (**C)** 14-days post nerve crush, and (**D)** 28-days post sciatic nerve crush injury. Scale bar = 25 µm

We also assessed reinnervation following SNC by measuring GM muscle contractile properties *in-situ* (Fig. 19). Maximum isometric force was measured using both nerve and direct muscle stimulation. In fully innervated muscle with robust neurotransmission, the forces elicited by nerve and muscle stimulation will not be different, i.e. the ratio of the values is close to 1.0. Under circumstances of impaired neurotransmission, there will be muscle fibers present that cannot be activated with nerve stimulation but will respond to direct muscle stimulation. Thus, the force generated in response to nerve stimulation will be less than that achieved with direct

muscle stimulation, and the ratio of the values will be less than 1.0. Our functional analysis corroborates the IHC data, demonstrating essentially no response to nerve stimulation 7 days after nerve crush, consistent with full denervation (Figs. 18B, 19A). By 14 days, the forces generated by nerve and muscle stimulation were not different as indicated by the ratio of ~1.0 between the two values (Fig. 19C), indicating a near complete recovery of innervation. Despite recovery of innervation at 14 days, maximum force elicited by either nerve or muscle stimulation remained 21% lower than the uninjured control values, indicating that muscles had not yet fully recovered from the injury. Muscles appeared to be essentially fully regenerated by 28 days as evidenced by no difference in force generation with nerve stimulation compared to control values and only a small 12% deficit remaining in force elicited by direct muscle stimulation (Fig 19A).

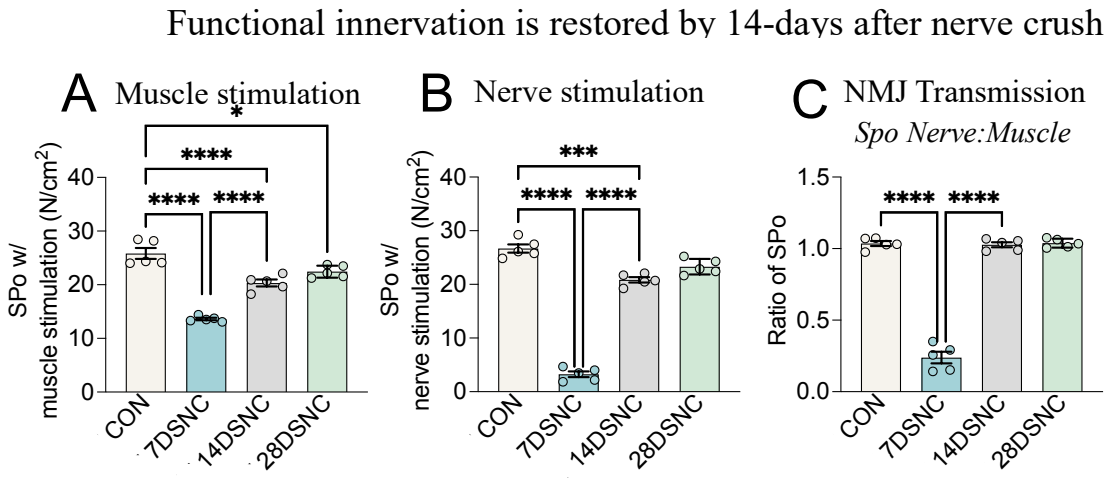


Figure 19 Functional innervation is restored in gastrocnemius muscles within 14 days in our nerve crush injury model. Data are shown for maximum specific force (Spo) elicited by (**A)** Direct muscle stimulation or (**B)** Direct nerve stimulation. Force values are normalized by the physiological cross-sectional area of the muscle and expressed as specific forces (N/cm^2). (**C)** Ratio of the forces generated by nerve and muscle stimulation. Statistical significance indicated by *p < 0.05, **p<0.003 ***p<0.0002, ****p<0.0001, ns=non-significant. SNC = sciatic nerve crush data presented as means ± SEM analyzed by ANOVA. n=5

The rapid and specific induction of Lmna following denervation and the return to baseline associated with reestablishment of functional neurotransmission, suggests a potential

role for increased Lmna as mechanistically important in facilitating reinnervation. Thus, we next aimed to test whether blunting the induction of Lmna following denervation would negatively impact the ability of the muscle to reestablish its neural connection by examining mice partially deficit in Lmna, i.e. the heterozygous muscle specific Lmna deficient mice (AC-Lmna$^{+/-}$ mice). Upon initial examination of these mice, we observed an intrinsic deficit of in specific force of approximately 23% for uninjured AC-Lmna$^{+/-}$ mice, irrespective of direct muscle stimulation ($p<.0001$) (Fig. 20A) or direct nerve stimulation ($p<.0001$) (Fig. 20B).

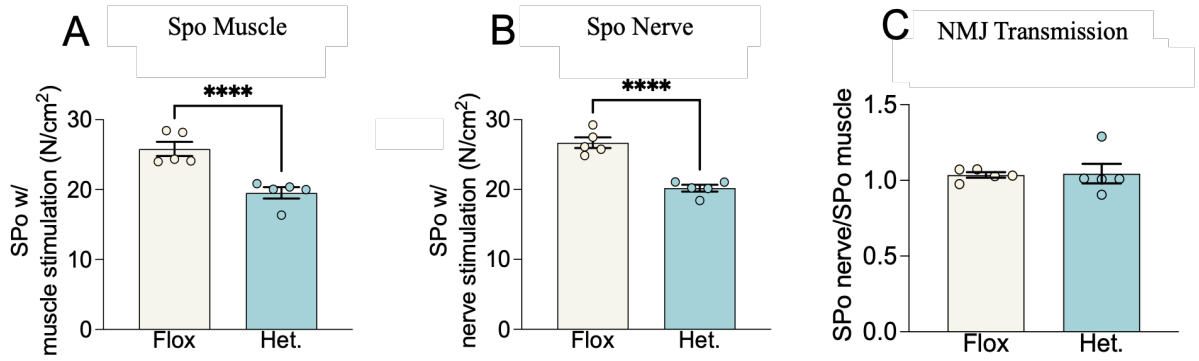


Figure 20 Baseline function of gastrocnemius in 2-month uninjured flox (Lmna$^{+/+}$) and heterozygous (AC-Lmna$^{+/-}$) mice. (**A)** Specific force (Spo) from direct muscle stimulation (**B)** Spo from direct nerve stimulation. Force values are normalized by the physiological cross-sectional area of the muscle and expressed as specific forces (N/cm^2). (**C)** Ratio of the forces generated by nerve and muscle stimulation. Statistical significance indicated by ****$p<0.0001$, data presented as means ± SEM analyzed by ANOVA. n=5

To further understand the impact of Lmna deletion at the NMJ and address whether abnormalities in NMJ structure might explain the baseline force deficit in the AC-Lmna$^{+/-}$ mice, NMJ morphology was evaluated to better define the structural characteristics of the endplate. The data uncovered contradictory findings to prior work showing NMJ degeneration in mice with muscle-specific Lmna deficiency (Gao et al., 2020), as we found no significant difference in ten different morphological features of the NMJ including, AChR area, AChR perimeter, nerve terminal area, nerve terminal perimeter, overlap, endplate area, endplate perimeter, endplate

diameter, unoccupied AChR area, compactness of the NMJ between Lmna$^{+/+}$ and AC-Lmna$^{+/-}$ mice (Fig. 21 A-J). Consistent with the lack of morphological defects observed at the endplates of muscles of AC-Lmna$^{+/-}$ mice, the innate muscle and nerve force deficit in these mice was also not associated with any impairment in NMJ transmission (Fig. 20C).

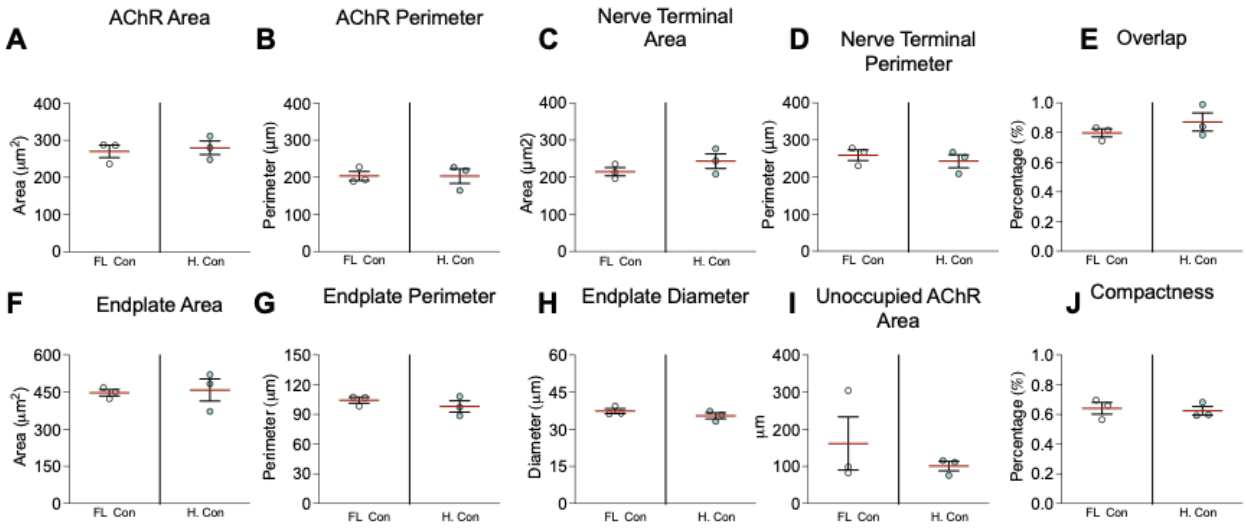


Figure 21 Partial deletion of muscle Lmna does not impact post synaptic NMJ morphology. N=3. 30 NMJs/sample. Data presented as means ± SEM analyzed by ANOVA. FL Con = flox uninjured (Lmna$^{+/+}$), H. Con = heterozygous mice uninjured (AC-Lmna$^{+/-}$). **A)** Acetylcholine receptor (AChR) area. **B)** AChR perimeter. **C)** Nerve terminal area. **D)** Nerve terminal perimeter. **E)** Overlap. **F)** Endplate Area. **G)** Endplate perimeter. **H)** Endplate diameter. **I)** Unoccupied AChR area. **E)** Compactness.

We next assessed potential innate differences between muscles of AC-Lmna$^{+/-}$ and Lmna$^{+/+}$ mice in muscle myofiber number or size. We performed immunohistochemistry with Laminin staining to visualize muscle fiber borders. Our analysis revealed no significant differences in myofiber number or cross-sectional area between groups (Fig. 22). Thus, although the AC-Lmna$^{+/-}$ mice showed a baseline deficit of just over 20% in contractile function (i.e maximum specific force), both NMJ morphology, muscle fiber number and size, and neurotransmission were not different from muscles of Lmna$^{+/+}$ mice. Thus, we felt that

proceeding with the investigation in these mice of reinnervation following SNC injury was justified.

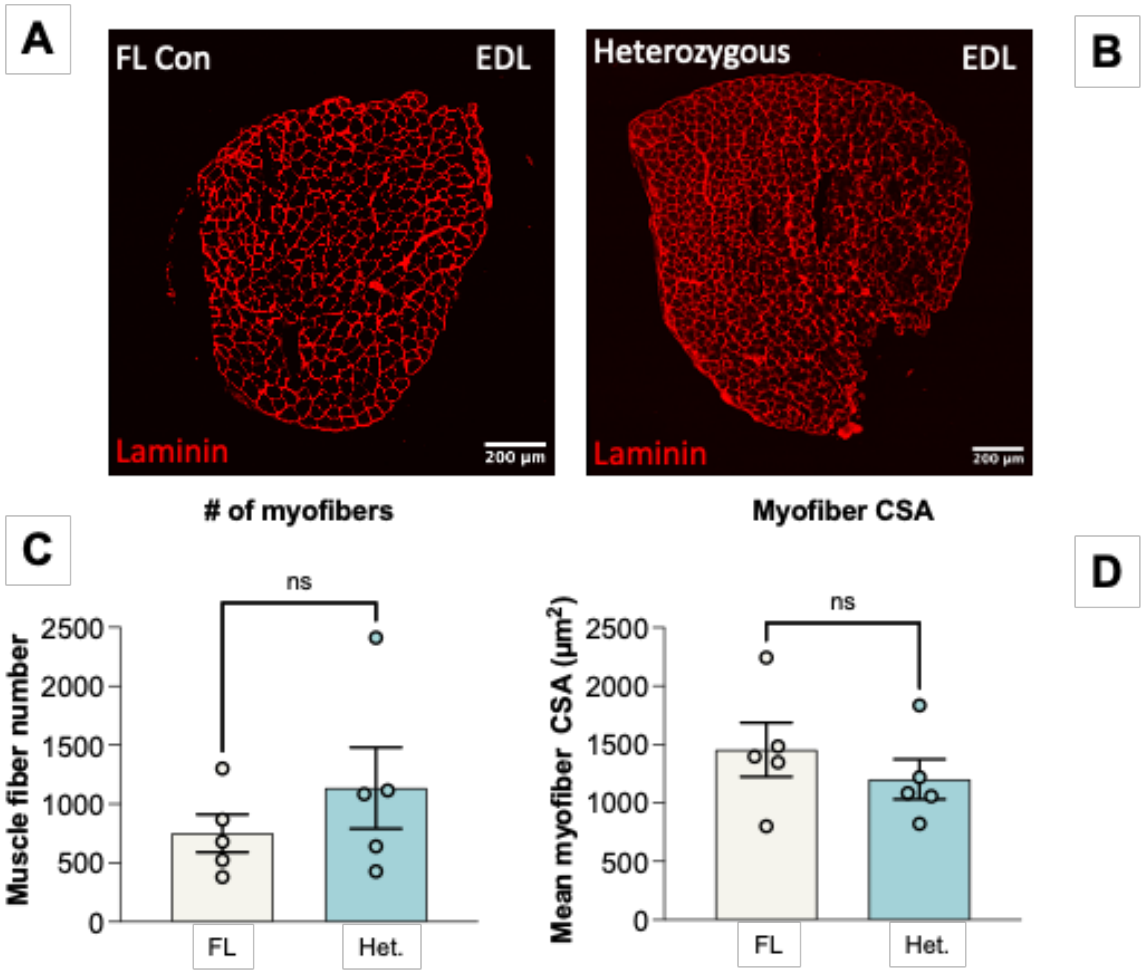


Figure 22 Muscle histology of uninjured Lmna flox and uninjured heterozygous extensor digitorum longus (EDL) muscle (**A, B**) reveals no difference in myofiber number or cross-sectional size between Lmna flox and Lmna heterozygous mice (**C, D**). n=5, scale bar = 200 µm. FL = Flox (Lmna$^{+/+}$), Het. = Heterozygous (AC-Lmna$^{+/-}$)

To assess effects of reduced Lmna on reinnervation, we performed nerve crush injury experiments, evaluating NMJ function 7-days post injury and 14-days post-injury where substantial recovery occurs (Fig. 23). Similar to WT mice (Fig. 19), muscles of AC-Lmna$^{+/-}$ mice displayed near-complete denervation at 7 days as evidenced by the absence of significant force generation with nerve stimulation (Fig 23B) and a significant decrease in specific force elicited by muscle stimulation (Fig. 23A). This severe nerve injury was followed by significant recovery

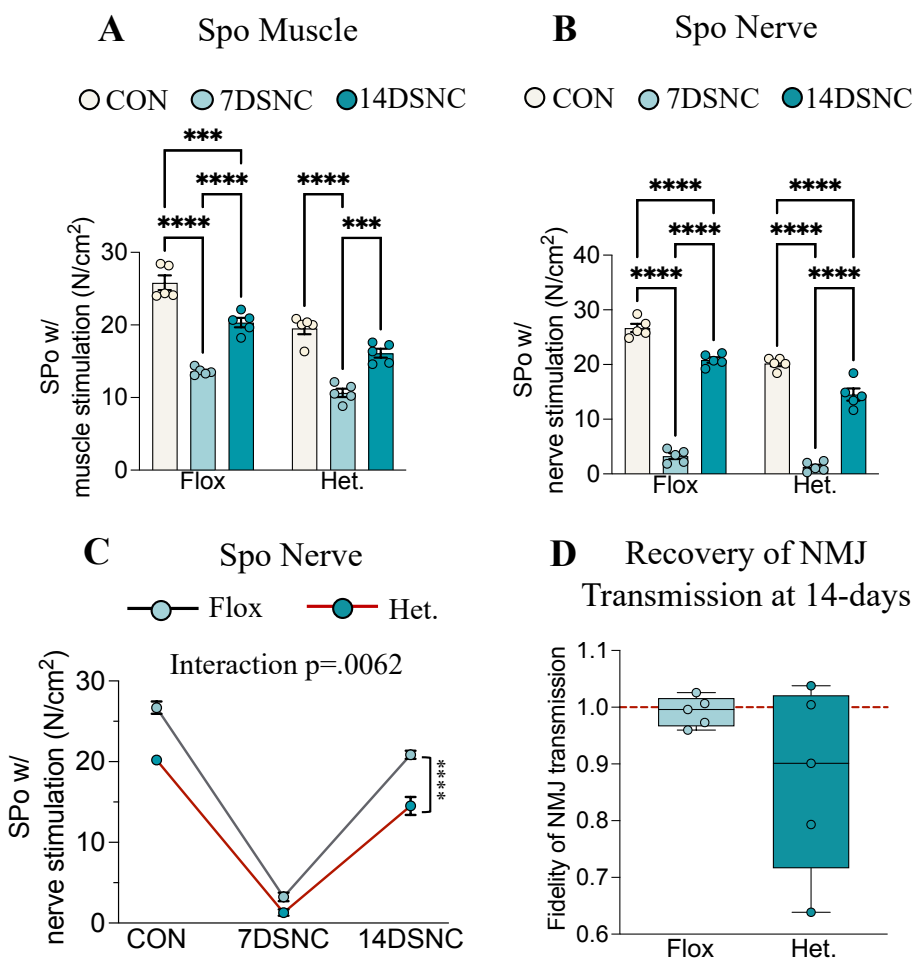


Figure 23 Functional innervation is restored in the gastrocnemius muscles of heterozygous mice 14 days post nerve crush. Data are shown for maximum specific force (SPo) elicited by **(A)** Direct muscle stimulation **(B)** Direct nerve stimulation. Force values are normalized by the physiological cross-sectional area of the muscle and expressed as specific forces (N/cm^2). **(C)** Specific force of nerve stimulation indicating the significant interaction effect 14 days post nerve crush. **(D)** Fidelity of NMJ transmission 14 days post injury determined by comparing Spo Nerve:Spo Muscle in uninjured controls and 14 days after nerve crush injury. Statistical significance indicated by ***p<0.005, ***p<0.0005, ****p<0.0001., Flox = Lmna$^{+/+}$, Het.= ActaCre-Lmna$^{+/-}$, 7DSNC= 7-day nerve crush, 14DSNC = 14-day nerve crush. Data presented as means ± SEM analyzed by Two-way ANOVA and Sidak post-hoc analysis. n=5

by 14 days post-injury (Fig. 23A-B). However, a two-way ANOVA of specific force recovery from nerve stimulation revealed a significant interaction effect between genotype and time, indicating a differential response to injury in AC-Lmna$^{+/-}$ mice compared with Lmna$^{+/+}$ controls. Specifically, the recovery of nerve-elicited force between 7- and 14-days post-injury was impaired in heterozygous AC-Lmna$^{+/-}$ mice (Fig. 23C). The impairment appears to be due at least in part to the persistence at 14 days of a moderate neurotransmission defect (Fig. 23D) as

indicated by the ratio of nerve-stimulated to muscle-stimulated force generation. For Lmna$^{+/+}$ controls, the value in Fig. 23D of 1. 0 indicates a return by 14 days to 100% fidelity in neurotransmission, while the AC-Lmna$^{+/-}$ mice showed significant variation in recovery with some mice still displaying substantially impaired neurotransmission.

To confirm that Lmna upregulation in response to denervation was maintained in the AC-Lmna$^{+/-}$ mice heterozygous mice, we performed qPCR analysis. As anticipated, Lmna was induced following nerve crush injury and showed a trend toward returning to baseline by 14-days (Fig. 24). A similar expression pattern was observed for NET39 and YAP, although the response was substantially blunted compared with controls and none of the changes were statistically significant (Fig. 24). Interestingly, a notable upregulation of AChR-alpha was detected at 14 days in the AC-Lmna$^{+/-}$ mice in contrast to the Lmna$^{+/+}$ controls, in which AChR-alpha had returned to control levels (Fig. 24).

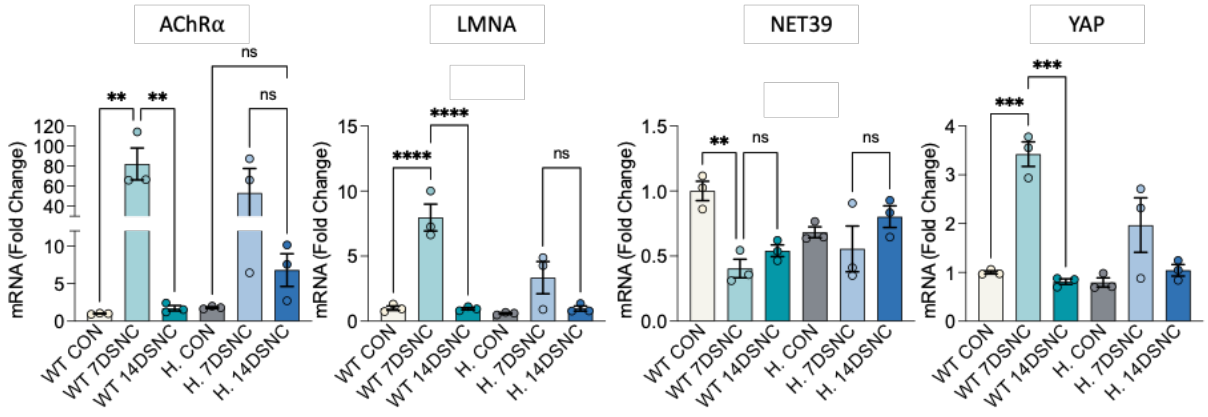


Figure 24 Transcripts from heterozygous mice (AC-Lmna$^{+/-}$). Nerve injury induces AChRα, LMNA, and NET39 and YAP transcriptional trends similar to wildtype mice. **P<.005, ***<.00005. SNC= Sciatic nerve crush. WT= Wildtype. H.Con = heterozygous ActaCre-Lmna$^{+/-}$ uninjured.

Finally, to determine if Lamin A/C upregulation was localized to a distinct pattern after nerve injury to facilitate reinnervation, immunohistochemistry of whole muscle longitudinal

sections was conducted (Fig. 25). Upregulation of Lamin A/C in nuclei appeared uniform throughout the myofibers and challenged our initial assumption of unique localization aiding in reinnervation 7-days after injury.

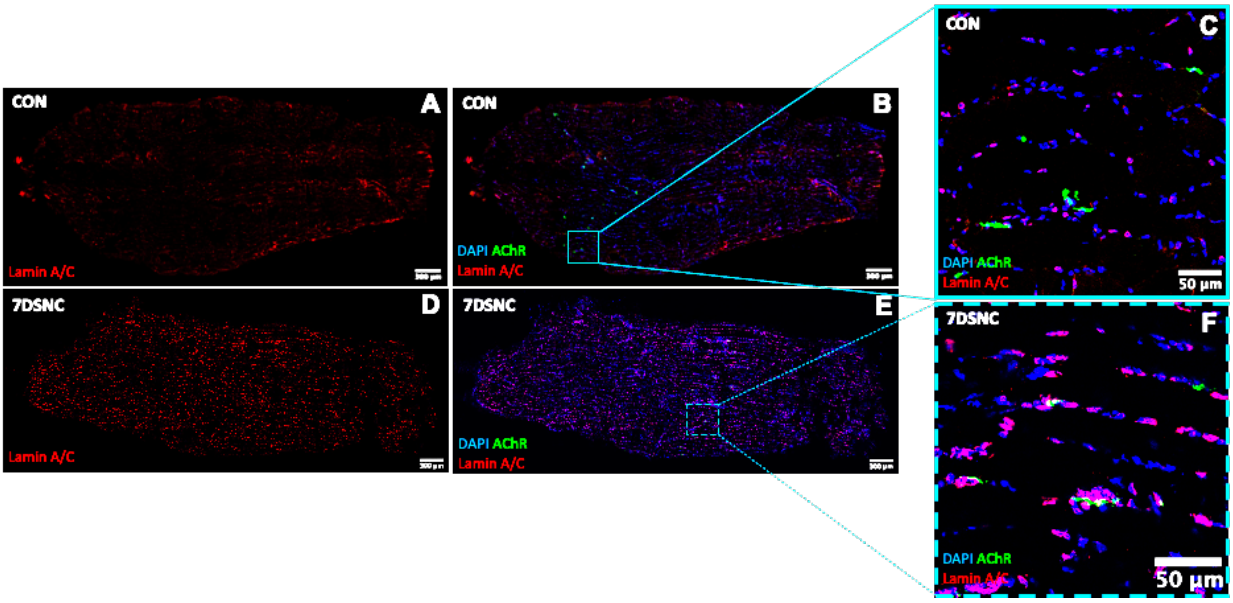


Figure 25 Lamin A/C localization does not ascertain a defined pattern throughout the soleus 7-days after injury in Lmna floxed ($Lmna^{+/+}$) mouse soleus muscle. Whole section image of uninjured (CON) soleus (**A,B**) and injured (7DSNC (**D,E**), scale bar = 300 µm. Magnified ROIs highlighting increased Lamin A/C signal near endplates and surrounding nuclei **(C,F)**, scale bar = 50 µm. Red = Lamin A/C, Green = Acetylcholine receptor (AChR), Blue = DAPI

3.9 Discussion

This study investigated the role of Lmna in neuromuscular junction (NMJ) regeneration following nerve injury, focusing on its potential function in supporting the reinnervation process in skeletal muscle. We observed a significant upregulation of Lmna and its protein product Lamin A/C, in response to two types of denervation injuries: sciatic nerve transection (SNT) and sciatic nerve crush (SNC). Notably, we identified Lmna expression levels returned to baseline

levels concurrently with a recovery of muscle force, suggesting a supportive role of Lmna in the reinnervation process. However, our findings challenge the notion that Lmna is essential for NMJ maintenance in mice as proposed by Gao et al. (2020), and particularly during reinnervation post injury. In our study, muscle-specific heterozygous deletion of Lmna did not substantially hinder the functional or structural recovery of NMJs following SNC.

The rapid upregulation of Lmna mRNA and Lamin A/C protein levels following SNT and SNC suggests a key role for Lmna during the muscle's response to denervation. Within just three days, Lmna mRNA levels increased 12-fold, continuing to rise by 14-fold at seven days post-injury. This dynamic response, which parallels the upregulation of AChRα, a well-established marker of muscle fiber denervation, suggested that Lmna is part of an acute process to potentially facilitate reinnervation. Our immunohistochemistry revealed that Lamin A/C indeed increased near the NMJ and the axon, however, a similar increase was observed uniformly throughout the myofiber, suggesting that the response is not specific to reinnervating axons and reinforcing the idea that Lmna could be critical for muscle fiber integrity in the absence of innervation. Given the well-established role of Lamin A/C maintaining nuclear mechanics, chromatin organization, transcriptional regulation and maintaining overall nuclear and cellular integrity (Carollo & Barra, 2023; Dechat et al., 2008; Donnaloja et al., 2020; Lammerding et al., 2004, 2006), it is plausible that the transient spike in Lmna expression is necessary to stabilize the nuclear architecture during the stress of denervation, to aid in maintenance of the myonuclear domain. This finding points to the need for further research into the specific functions of Lamin A/C in muscle adaptation to injury.

Our functional analysis through in situ force testing provides compelling evidence that partial loss of Lmna does not prevent NMJ reinnervation following nerve injury but may moderately impair the process as evidenced by our observation of a differential recovery in NMJ transmission following nerve crush injury between heterozygous Lmna-deficient (AC-Lmna$^{+/-}$**)** mice and wildtype (Lmna$^{+/+}$) controls. This delayed return to baseline and marked variability suggests that AC-Lmna$^{+/-}$ mice experience marginal but meaningful impairments in the restoration of NMJ transmission fidelity, potentially contributing to slower force recovery. Muscle-specific heterozygosity of Lmna appears sufficient to maintain nuclear-cytoskeletal integrity during the critical window of denervation, allowing other key signaling pathways to orchestrate the reinnervation process. Together, these findings underscore the role of Lmna in modulating the recovery of NMJ function after injury, which may reflect broader disruptions in neuromuscular resilience and repair mechanisms.

Our analysis of NMJ morphology in AC-Lmna$^{+/-}$ and control mice provided additional insight into the non-essential role of Lmna in NMJ maintenance. Despite the reduced levels of Lamin A/C in AC-Lmna$^{+/-}$ mice, we observed no significant differences in key morphological features of the NMJ, including AChR area, nerve terminal area, and postsynaptic overlap. These results were unexpected, as we hypothesized that reduced Lamin A/C would lead to abnormalities in NMJ structure, as a progressive denervation and acetylcholine receptor cluster fragmentation of the endplate with neuromuscular dysfunction as soon as two and up to six months of age was reported by Gao et. al (2020). The lack of observable changes in NMJ morphology, despite partial Lmna deletion, further supports the idea that Lmna upregulation is not strictly necessary for NMJ maintenance. One possible explanation is that Lamin A/C plays a more indirect role in maintaining NMJ stability, such as through the regulation of gene

expression or chromatin structure (Ferraioli et al., 2024; Nava et al., 2020; Stephens et al., 2017, 2019), rather than directly influencing synaptic architecture. It is also possible that unknown alternative compensatory mechanisms are invoked with the embryonic Lmna deletion. This could explain why the loss of one allele of Lmna does not translate into functional deficits at the NMJ level, as other regulatory mechanisms may compensate for the reduced protein levels.

The results of this study raise important questions about the precise role of Lmna in NMJ decline and maintenance. While Lmna is clearly upregulated throughout the muscle fiber in response to denervation in wild-type mice, the minimal structural or functional deficits in AC-Lmna$^{+/-}$ mice raises questions surrounding the mechanisms enabling lamin A/C to regulate NMJ maintenance and the physiological impact of previously reported NMJ morphological fragmentation and NMJ transmission deficits (Gao et al., 2020). This report highlights the complexity of the molecular networks involved in skeletal muscle and suggests that Lmna may be just one component of a larger compensatory system facilitating reinnervation.

Future research should prioritize identifying compensatory pathways that may mitigate the effects of Lmna deficiency during reinnervation. Investigating the roles of nuclear envelope associated proteins, such as emerin, SUN1/2, and nesprins, in maintaining NMJ stability and function could provide new insights into the redundancy and adaptability of the nuclear proteins to preserve nuclear envelope integrity during reinnervation. Lamin A/C deficiency is widely reported to compromise nuclear envelope integrity, leading to DNA damage, changes in nuclear shape and morphology including nuclear bleb formation, impairments in cell mechanics, and nuclear envelope rupture, resulting in double-stranded DNA leak from the nucleus to the cytosol (Kovacs et al., 2023; Lammerding et al., 2004, 2006; Lee et al., 2007; Pho et al., n.d.; Sullivan et

al., 1999). The formation of nuclear blebs and rupture of the nuclear envelope indicate compromised mechanical support of the nucleoskeleton making the nuclei and cell susceptible to damage by mechanical stress. Further, the nuclear pore complex (NPC), nestled in the nuclear envelope and tightly associated with the nucleoskeleton, is a key regulator of molecular traffic between the cytoplasm and the nucleus contributing a critical role in gene expression (Strambio-De-Castillia et al., 2010). Growing evidence in human brain and model animal studies suggest that disturbances in NPC structure and function from neuronal oxidative stress, mirror typical characteristics of degenerating neurons, suggesting that impaired NPCs may contribute to neurodegeneration (Hachiya et al., 2021). In addition, investigating the transcriptional changes linked to Lmna upregulation during denervation and reinnervation may uncover novel regulatory mechanisms essential for nuclear integrity, with potential applications in other injuries where similar upregulation occurs.

In conclusion, this study demonstrates Lmna is upregulated in skeletal muscle during muscle response to denervation, its muscle-specific partial deletion does not impede NMJ recovery, suggesting it is not essential for reinnervation, but does marginally impair recovery of NMJ transmission following injury. Future studies aimed at uncovering the compensatory mechanisms that support NMJ stability in Lmna-deficient muscle will be crucial to understanding the broader regulatory networks involved in NMJ maintenance and sarcopenia.

Chapter 4 Conclusions and Future Development

This dissertation addresses key gaps in the understanding of mechanisms regulating the maintenance and regeneration of neuromuscular junctions (NMJ) under conditions involving disrupted muscle fiber innervation, such as elevated oxidative stress, nerve injury, and natural aging. Through a combination of in-vivo models and in-situ techniques, we investigated the role of subsynaptic myonuclei number and the gene *Lmna* during muscle fiber denervation and reinnervation. Our findings challenge existing assumptions regarding the importance of subsynaptic myonuclei (SSM) and *Lmna* in NMJ maintenance and suggest new avenues for research into the molecular mechanisms driving NMJ degradation in aging and injury.

Chapter 1 provides an overview of skeletal muscle biology, focusing on the neuromuscular junction, subsynaptic myonuclei, and the broader role of the NMJ in sarcopenia. This foundational chapter lays the groundwork for the experimental work described in the subsequent chapters, emphasizing the importance of the NMJ in muscle function and how disruptions in innervation can lead to degenerative changes.

In Chapter 2, a comprehensive study critically examining existing literature is described and essential questions are raised regarding the physiological impact of variability in 1-2 nuclei at a neuromuscular synapse. The study demonstrates the stability of SSM across three different models of muscle fiber innervation disruption. Contrary to our initial hypothesis, we found no significant changes in SSM number following acute denervation, nor differences in SSM number

among fully innervated, partially innervated, and fully denervated endplates in various models of progressive NMJ degeneration. Our findings challenge the notion that the presence of SSM is a major driver or a significant consequence of NMJ degeneration and denervation. This study also highlighted contradictory results in published reports on postsynaptic myonuclei numbers and suggests that results need to be interpreted with greater caution, as the methods for identifying SSM vary widely across studies (Ruiz et al., 2023; Von Saucken et al., 2024). Moving forward, standard markers and morphological features should be used to identify subsynaptic myonuclei.

The substantial variability observed in SSM numbers across nerve injury models underscores the dynamic nature of these nuclei in response to electrical activity and innervation status. Electrical activity from innervation is a known trigger for spatial myonuclear rearrangements (Bai et al., 2022; Grady et al., 2005) and is believed to drive the progressive segregation of gene expression between synaptic and extra-synaptic myonuclei, but the exact molecular pathways remain unclear (Belotti & Schaeffer, 2020; Ferraro et al., 2012). Our findings in Chapter 2 suggest that maintaining NMJ integrity in the context of sarcopenia is influenced by a complex interplay of factors beyond SSM numbers, including the transcriptional profiles of pre- and postsynaptic nuclei, the transient migratory behavior of nuclei following injury, and overall myonuclear integrity. Single-nuclei RNA sequencing (snRNA-seq) offers exciting new opportunities to elucidate these transcriptional changes. Current snRNA-seq studies have generated insights into the transcriptional profile of SSMs (Chemello et al., 2020; Dos Santos et al., 2020; M. Kim et al., 2020; Petrany et al., 2020) and have identified novel markers NMJ nuclei such as Ablim2, Ano4, Etv4, Gramd1b, Lrfn5, Prkar1a, and Ufsp1. Ets transcription factors, such as Etv4, are known to regulate the expression of synapse-specific genes and coordinate the formation of the postsynaptic apparatus, indicating their potential role in

orchestrating gene expression at the NMJ (Ham et. al., 2024; Ruegg & Briguet, 2000). These factors likely influence gene expression in response to electrical activity and innervation, shaping the dynamic molecular landscape of synaptic and extra-synaptic myonuclei. However, it remains unclear whether all the newly identified markers are regulated by Ets transcription factors, their specific roles in vivo, and how their expression changes based on the degree of innervation.

Chapter 3 describes studies carefully evaluating the role of muscle Lmna expression during reinnervation. In Chapter 2, we identified that the number of SSM was not a critical factor in maintenance of the NMJ and highlighted the need to further investigate the relationships between SSM and age-associated degenerative changes at the NMJ. A key structure maintaining the integrity of myonuclei is the nuclear lamina, which forms a scaffold on the inner surface of the nuclear envelope in eukaryotic cells. The nuclear lamina interacts with chromatin and nuclear membrane proteins to regulate gene expression, and nuclear architecture and membrane function appear to be critical controllers of aging (López-Otín et al., 2013). Lamin A/C is the primary intermediate filament protein of the nuclear lamina and mutations in its gene (Lmna) lead to progeroid syndromes (Carboni et al., 2013). Further, Lamin A/C has long been recognized as important for muscle stem cell differentiation, maintenance of nuclear mechanics, and mechanotransduction (Donnaloja et al., 2020; Frock et al., 2006; Lammerding et al., 2004; Méjat et al., 2009), and neuronal knockdown of Lamin impaired motor function and decreased lifespan in flies (Oyston et al., 2018). Finally, Lamin A/C levels are reported to decrease during aging in muscles of mice and muscle-specific deletion of Lmna accelerates the degradation of NMJs, similar to features seen in aging (Gao et al., 2020)

To further evaluate Lamin A/C in muscle during aging, single-nuclei sequencing, ChIP-seq, and novel technologies may need to be leveraged. This combined approach will offer a more comprehensive understanding of NMJ maintenance and the progression of sarcopenia at varying states of NMJ innervation. ChIP-seq, specifically, would allow for the mapping of Lamin A/C binding sites across the genome, revealing how these nuclear proteins interact with active and inactive chromatin regions during reinnervation. Recent studies, like those by Ferraioli et al. (2023), have shown that pS22-Lamin A/C binds near highly transcribed genes, suggesting a critical role in regulating gene expression during muscle differentiation (Ferraioli et al., 2024). Similarly, ChIP-seq could be used to explore how Lamin A/C binding patterns shift in response to changes in NMJ innervation and sarcopenia progression, potentially identifying genomic regions where these nuclear components regulate muscle-specific genes. Additionally, insights from progeria studies indicate that dysregulation of Lamin A/C at enhancers leads to aberrant gene expression, which could further inform research into how altered nuclear structure contributes to NMJ degradation. Unraveling these transcriptional and epigenetic changes could reveal key networks involved in reinnervation and potentially identify novel targets to enhance reinnervation or delay NMJ degradation. Through our studies we demonstrated that Lmna and the protein product Lamin A/C are robustly upregulated in muscle after nerve injury; however, reduced Lmna in the muscle does not prevent reinnervation, although the extent or at least the rate of reinnervation following nerve injury appears to be modestly impaired.

Future studies on innervation and the role of Lmna in myonuclei could focus on nuclear shape and mechanotransduction. Two models of Lmna mutations have already shown altered innervation patterns and abnormal NMJ morphology, characterized by mislocalized synaptic nuclei and altered expression of nuclear envelope genes (Méjat et al., 2009). Furthermore,

muscle-specific deletion of Lmna resulted in progressive NMJ degeneration during adulthood (Gao et al., 2020), and age-related declines in Lamin A have been linked to increased myonuclear deformability (Battey et al., 2022). Our findings indicate that Lamin A/C is highly prominent in SSM and significantly induced upon denervation. However, whether the deformation of SSM in aged muscle or the impact of denervation on SSM shape correlates with the structural integrity of SSM and Lamin A/C levels has yet to be investigated.

A rigorous assessment of SSM structural integrity during aging and after denervation is necessary to fully understand the interplay between these factors and their implications for NMJ function. SSM shape and integrity has previously been quantified in 2D with measurements of nuclear area and aspect ratio, and sphericity in 3D along with 3D aspect ratio (Battey, Furrer, et al., 2022; Schindelin et al., 2012). We predict that aged mice will show an increased number of severely deformed SSMs, accompanied by elevated levels of DNA damage (Earle et al., 2020). Recent findings suggest that Lamin A/C plays a critical role in orchestrating DNA damage repair (DDR) by facilitating the interaction between key proteins such as ATM (ataxia telangiectasia mutated) and the MRE11-RAD50-NBS1 (MRN) complex, which are essential for detecting and repairing DNA breaks (Kume et al., 2019). Lamin A/C depletion disrupts the recruitment of DDR proteins to damaged DNA, leading to impaired DNA repair efficiency and decreased homologous recombination (HR) (S. Kim et al., 2024). Thus, SSMs in aged or denervated muscle may exhibit compromised Lamin A/C function, which could exacerbate DNA damage accumulation and hinder efficient repair (Belotti et al., 2024). Such impairments in the DDR could contribute to a greater prevalence of denervated endplates following recovery from sciatic nerve crush (SNC) in older mice compared to young or adult wild-type mice (Deepa et al., 2019).

To further support the potential biological relevance of primary SSM shape and structural integrity outcomes addressed above, an evaluation of nuclear pore complex (NPC) proteins could also be conducted, as NPCs are essential for transporting macromolecules between the nucleus and cytoplasm. Mice deficient in NPC components exhibit progressive muscle deterioration, highlighting the role of NPCs in maintaining muscle structure and function (Megat et al., 2023). In particular, the depletion of nucleoporin 210 has been associated with age-related muscle integrity alterations and an increased prevalence of centrally nucleated fibers, a marker of muscle damage and regeneration (Sakuma et al., 2022). Despite the established role of NPCs in muscle health, no study has specifically examined the quality of NPCs in subsynaptic myonuclei or their potential interactions with the neuromuscular junction (NMJ). Exploring this relationship could provide new insights into how NPC dysfunction contributes to NMJ degeneration and age-related muscle decline.

While Lamin A/C is recognized as a critical component of nuclear structure, with its sensitivity to innervation status being evident, other nuclear envelope proteins warrant investigation. These include Lamin B1 (Lukášová et al., 2018; Matias et al., 2022; Wesley & Levy, 2023), components of the LINC complex (Nesprin1/2, SUN1/2, Emerin, BAF) (Crisp et al., 2006; Stroud et al., 2017; Wong et al., 2021), and nuclear pore complexes (D'Angelo et al., 2009; Sakuma et al., 2022). Additionally, proteins like Lem2 (Kume et al., 2019) and nuclear envelope transmembrane protein 39 (Net39) (Ramirez-Martinez et al., 2021; Y. Zhang et al., 2023) should also be considered. Lem2, plays a critical role in regulating nuclear size and membrane flow, acting as a barrier to membrane dynamics within the nuclear envelope (Kume et al., 2019). Its deletion has been shown to augment nuclear size enlargement in fission yeast, highlighting its importance in maintaining nuclear integrity during cellular stress (Kume et al.,

2019). Lem2 may have a similar function in muscle cells, where maintaining nuclear size and structure is vital for myonuclear stability and function. Alternatively, recent studies have shown that Net39 is essential for maintaining myonuclear integrity, with its conditional knockout leading to increased DNA damage. However, the impact of these impairments on neuromuscular junction (NMJ) function has yet to be explored (Zhang et al., 2023). Investigating the role of Lem2 and Net39 in relation to NMJ health and function could provide valuable insights into the broader mechanisms governing neuromuscular integrity. Considering these additional players will inform future research directions.

The network of lamin intermediate filament proteins is fundamental for establishing nuclear rigidity and ensuring the integrity of nuclei, particularly in mechanically demanding environments such as muscle tissue (Stephens et al., 2017; Swift et al., 2013). Mechanotransduction studies indicate that changes in cellular stiffness can be transmitted to the nucleus, leading to alterations in the structure of the nuclear lamina and chromatin, which in turn influence gene expression (Nava et al., 2020; Stephens et al., 2017, 2019). The nuclear lamina is critical for both sensing and responding to mechanical signals (Osmanagic-Myers et al., 2015). Specifically, the mechanical properties of the nucleus—such as stiffness and viscosity—are heavily influenced by A-type lamins, while B-type lamins contribute to nuclear deformability and elasticity. Notably, lamin A expression increases in response to heightened tissue stiffness (Swift et al., 2013), underscoring its role in adapting to mechanical cues. Moreover, mechanical loading can suppress lamin A/C phosphorylation, and since lamin A/C degradation typically follows phosphorylation, this suppression highlights the pivotal role of the nuclear lamina in mechanotransduction and the maintenance of muscle homeostasis (Buxboim et al., 2014). Recent findings further elucidate that mechanical forces generated in the cell microenvironment can alter

the epigenetic landscape by propagating through the nuclear lamina and chromatin, affecting gene regulatory mechanisms (e.g., activation of histone modifications and changes in chromatin accessibility) (Mishra et al., 2023). The interplay between the mechanical load on the nucleus and lamin A/C dynamics exemplifies how the nuclear lamina facilitates the transmission of mechanical forces to the nuclear interior, ultimately orchestrating cellular responses to mechanical stimuli and influencing gene regulation in mechanically active muscle tissue.

Proteins like YAP and MLK1 serve as markers of nuclear mechanotransduction, with their nuclear signaling increasing in response to mechanical load. Interestingly, when lamin A is depleted, nuclear levels of both YAP and MLK1 rise (Wiggan et al., 2020). Under normal conditions, cyclic strain enhances the nuclear accumulation of YAP due to increased mechanical load; however, mutations in the LMNA gene reverse this effect, leading to reduced YAP accumulation under cyclic strain (Bertrand et al., 2014). This suggests that LMNA-mutated human myoblasts have defective mechanosensing due to dysregulated YAP signaling, indicating a critical role for lamin A/C in mediating mechanotransduction (Bertrand et al., 2014). Furthermore, the accumulation of YAP in the nucleus is often accompanied by alterations in actomyosin networks, suggesting that the integrity of lamin intermediate filaments is essential for proper nucleo-cytoskeletal signaling (Wiggan et al., 2020; Bertrand et al., 2023). These findings emphasize the intricate relationship between lamin A/C, mechanotransduction, and cellular signaling networks in maintaining muscle homeostasis. Recent studies have also shown increased nuclear YAP accumulation and signaling in aging skeletal muscles, which coincide with a reduction in lamin-B1; however, the link between these observations remains to be clarified (Iyer et al., 2021; Yoshida et al., 2019). At the NMJ, YAP1/TAZ function as transcriptional coactivators that regulate synaptic gene expression, as well as the formation and

morphology of NMJs. Single knockout mice exhibit functional deficits, while double knockouts display extreme lethality and a near-complete absence of NMJs. Additionally, denervated gastrocnemius muscles show a shift towards YAP1/TAZ-dependent transcriptional activity, underscoring the significance of this pathway (Gessler et al., 2024). In our nerve injury time course, we observed an upregulation of YAP and TAZ transcripts that followed a pattern similar to Lmna. This suggests potential crosstalk between YAP/TAZ and Lmna in processes such as reinnervation, synaptic gene regulation, and NMJ maintenance, although the precise mechanisms remain to be fully elucidated.

To further investigate a mechanotransducive role of Lmna, YAP, and TAZ in skeletal muscle, we propose studies utilizing models such as compressive force loading or mechanical stretch is application to primary myocytes, as well as in vivo hindlimb unloading via hindlimb suspension. Hindlimb unloading is a well-established model for inducing mechanical unloading and muscle atrophy, mimicking conditions such as prolonged bed rest, microgravity, or immobilization, and providing insights into the molecular pathways affected by reduced mechanical stimuli without neural damage. Notably, Gene Ontology analysis has identified lamin binding genes as enriched during muscle atrophy induced by hindlimb unloading (Sun et al., 2021). These models could be complemented small interfering RNA oligonucleotides (siRNAs) to modulate Lmna expression. Downstream experiments should incorporate a range of established techniques, including qRT-PCR and RNA-Seq for gene expression and pathway analysis, Western blotting for protein detection, and immunocytochemistry for visualizing cellular components. These approaches will allow for a comprehensive evaluation of the effects of mechanical forces on **Lmna** function and its downstream impact on skeletal muscle cell.

In conclusion, this dissertation provides new insights into the complex relationship between SSM numbers, Lmna expression, and NMJ integrity during aging and after nerve injury. While the initial hypotheses regarding the role of SSM in NMJ degeneration were not supported, our findings point to the importance of transcriptional and mechanotransductive mechanisms in maintaining NMJ integrity. By focusing on the molecular underpinnings of NMJ maintenance, particularly the role of nuclear envelope proteins, this research opens new avenues for developing interventions that may delay or prevent sarcopenia and other muscle-related disorders.

Bibliography

Aare, S., Spendiff, S., Vuda, M., Elkrief, D., Perez, A., Wu, Q., Mayaki, D., Hussain, S. N., Hettwer, S., & Hepple, R. T. (2016). Failed reinnervation in aging skeletal muscle. *Skeletal muscle*, *6*(1), 29. https://doi.org/10.1186/s13395-016-0101-y

Abou Sawan, S., Hodson, N., Babits, P., Malowany, J. M., Kumbhare, D., & Moore, D. R. (2021). Satellite cell and myonuclear accretion is related to training-induced skeletal muscle fiber hypertrophy in young males and females. *Journal of Applied Physiology*, *131*(3), 871–880. https://doi.org/10.1152/japplphysiol.00424.2021

Aidley, D. J. (2012). *The Physiology of Excitable Cells* (4th ed.). Cambridge University Press.

Akaaboune, M., Culican, S. M., Turney, S. G., & Lichtman, J. W. (1999). Rapid and Reversible Effects of Activity on Acetylcholine Receptor Density at the Neuromuscular Junction in Vivo. *Science*, *286*(5439), 503–507. https://doi.org/10.1126/science.286.5439.503

Albuquerque, E. X. (1974). The Density of Acetylcholine Receptors and Their Sensitivity in the Postsynaptic Membrane of Muscle Endplates. *Proc. Nat. Acad. Sci. USA*.

Alcorta-Sevillano, N., Macías, I., Rodríguez, C. I., & Infante, A. (2020). Crucial Role of Lamin A/C in the Migration and Differentiation of MSCs in Bone. *Cells*, *9*(6), 1330. https://doi.org/10.3390/cells9061330

Ang, S.-T. J., Crombie, E. M., Dong, H., Tan, K.-T., Hernando, A., Yu, D., Adamson, S., Kim, S., Withers, D. J., Huang, H., & Tsai, S.-Y. (2022). Muscle 4EBP1 activation modifies the structure and function of the neuromuscular junction in mice. *Nature Communications*, *13*(1), 7792. https://doi.org/10.1038/s41467-022-35547-0

Apel, E. D., Lewis, R. M., Grady, R. M., & Sanes, J. R. (2000). Syne-1, A Dystrophin- and Klarsicht-related Protein Associated with Synaptic Nuclei at the Neuromuscular Junction. *Journal of Biological Chemistry*, *275*(41), 31986–31995. https://doi.org/10.1074/jbc.M004775200

Bai, L., Tu, W.-Y., Xiao, Y., Zhang, K., & Shen, C. (2022). Motoneurons innervation determines the distinct gene expressions in multinucleated myofibers. *Cell & Bioscience*, *12*(1), 140. https://doi.org/10.1186/s13578-022-00876-6

Barton, L. J., Soshnev, A. A., & Geyer, P. K. (2015). Networking in the nucleus: A spotlight on LEM-domain proteins. *Current Opinion in Cell Biology*, *34*, 1–8. https://doi.org/10.1016/j.ceb.2015.03.005

Battey, E., Ross, J. A., Hoang, A., Wilson, D. G. S., Han, Y., Levy, Y., Pollock, R. D., Kalakoutis, M., Pugh, J. N., Close, G. L., Ellison-Hughes, G. M., Lazarus, N. R., Iskratsch, T., Harridge, S. D. R., Ochala, J., & Stroud, M. J. (2022). *Myonuclear alterations associated with exercise are independent of age in humans*. https://doi.org/10.1101/2022.09.20.506578

Belotti, E., Lacoste, N., Iftikhar, A., Simonet, T., Papin, C., Osseni, A., Streichenberger, N., Mari, P.-O., Girard, E., Graies, M., Giglia-Mari, G., Dimitrov, S., Hamiche, A., & Schaeffer, L. (2024). H2A.Z is involved in premature aging and DSB repair initiation in muscle fibers. *Nucleic Acids Research*, *52*(6), 3031–3049. https://doi.org/10.1093/nar/gkae020

Belotti, E., & Schaeffer, L. (2020). Regulation of Gene expression at the neuromuscular Junction. *Neuroscience Letters*, *735*, 135163. https://doi.org/10.1016/j.neulet.2020.135163

Bermedo-García, F., Zelada, D., Martínez, E., Tabares, L., & Henríquez, J. P. (2022). Functional regeneration of the murine neuromuscular synapse relies on long-lasting morphological adaptations. *BMC Biology*, *20*(1), 158. https://doi.org/10.1186/s12915-022-01358-4

Blemker, S. S., Brooks, S. V., Esser, K. A., & Saul, K. R. (2024). Fiber-type traps: revisiting common misconceptions about skeletal muscle fiber types with application to motor control, biomechanics, physiology, and biology. Journal of Applied Physiology, 136(1), 109-121. https://doi.org/10.1152/japplphysiol.00337.2023

Boehm, I., Alhindi, A., Leite, A. S., Logie, C., Gibbs, A., Murray, O., Farrukh, R., Pirie, R., Proudfoot, C., Clutton, R., Wishart, T. M., Jones, R. A., & Gillingwater, T. H. (2020). Comparative anatomy of the mammalian neuromuscular junction. *Journal of Anatomy*, *237*(5), 827–836. https://doi.org/10.1111/joa.13260

Bollen, E., Den Heyer, J. C., Tolsma, M. H. J., Bellar, S., Bos, J. E., & Wintzn, A. R. (1992). STRUCTURE AND FUNCTION OF NEUROMUSCULAR JUNCTIONS IN THE VASTUS LATERALIS OF MAN. *Brain*, *115*(2), 451–478. https://doi.org/10.1093/brain/115.2.451

Borges, L. S., Yechikhov, S., Lee, Y. I., Rudell, J. B., Friese, M. B., Burden, S. J., & Ferns, M. J. (2008). Identification of a Motif in the Acetylcholine Receptor β Subunit Whose Phosphorylation Regulates Rapsyn Association and Postsynaptic Receptor Localization. *The Journal of Neuroscience*, *28*(45), 11468–11476. https://doi.org/10.1523/JNEUROSCI.2508-08.2008

Borowik, A. K., Davidyan, A., Peelor, F. F., 3rd, Voloviceva, E., Doidge, S. M., Bubak, M. P., Mobley, C. B., McCarthy, J. J., Dupont-Versteegden, E. E., & Miller, B. F. (2022). Skeletal Muscle Nuclei in Mice are not Post-mitotic. *Function (Oxford, England)*, *4*(1), zqac059. https://doi.org/10.1093/function/zqac059

Bourdeau Julien, I., Sephton, C. F., & Dutchak, P. A. (2018). Metabolic Networks Influencing Skeletal Muscle Fiber Composition. *Frontiers in Cell and Developmental Biology*, *6*, 125. https://doi.org/10.3389/fcell.2018.00125

Briand, N., & Collas, P. (2020). Lamina-associated domains: Peripheral matters and internal affairs. *Genome Biology*, *21*(1), 85. https://doi.org/10.1186/s13059-020-02003-5

Briguet, A., & Ruegg, M. A. (2000). The Ets transcription factor GABP is required for postsynaptic differentiation in vivo. *The Journal of neuroscience : the official journal of the Society for Neuroscience*, *20*(16), 5989–5996. https://doi.org/10.1523/JNEUROSCI.20-16-05989.2000

Broers, J. L. V., Ramaekers, F. C. S., Bonne, G., Yaou, R. B., & Hutchison, C. J. (2006). Nuclear Lamins: Laminopathies and Their Role in Premature Ageing. *Physiological Reviews*, *86*(3), 967–1008. https://doi.org/10.1152/physrev.00047.2005

Bruneau E, Sutter D, Hume RI, Akaaboune M. Identification of nicotinic acetylcholine receptor recycling and its role in maintaining receptor density at the neuromuscular junction in vivo. J Neurosci. 2005 Oct 26;25(43):9949-59. doi: 10.1523/JNEUROSCI.3169-05.2005. PMID: 16251443; PMCID: PMC6725561.

Bruneau EG, Akaaboune M. The dynamics of recycled acetylcholine receptors at the neuromuscular junction in vivo. Development. 2006 Nov;133(22):4485-93. doi: 10.1242/dev.02619. Epub 2006 Oct 18. PMID: 17050625.

Cadot, B., Gache, V., & Gomes, E. R. (2015). Moving and positioning the nucleus in skeletal muscle – one step at a time. *Nucleus*, *6*(5), 373–381. https://doi.org/10.1080/19491034.2015.1090073

Corsa C, Walsh C, Bagchi D, McDougald O., Adipocyte-specific deletion of lamin A/C largely models human familial partial lipodystrophy type 2. *Diabetes*. 2021;db201001. 10.2337/db20-1001

Cameron, A. M., Castoldi, A., Sanin, D. E., Flachsmann, L. J., Field, C. S., Puleston, Daniel. J., Kyle, R. L., Patterson, A. E., Hässler, F., Buescher, J. M., Kelly, B., Pearce, E. L., & Pearce, E. J. (2019). Inflammatory macrophage dependence on NAD+ salvage is a consequence of reactive oxygen species–mediated DNA damage. *Nature Immunology*, *20*(4), 420–432. https://doi.org/10.1038/s41590-019-0336-y

Carboni, N., Mateddu, A., Marrosu, G., Cocco, E., & Marrosu, M. G. (2013). Genetic and clinical characteristics of skeletal and cardiac muscle in patients with lamin A/C gene mutations: LMNA and Muscle Disease. *Muscle & Nerve*, *48*(2), 161–170. https://doi.org/10.1002/mus.23827

Carollo, P. S., & Barra, V. (2023). Chromatin epigenetics and nuclear lamina keep the nucleus in shape: Examples from natural and accelerated aging. *Biology of the Cell*, *115*(1),

2200023. https://doi.org/10.1111/boc.202200023

Cetin, H., Beeson, D., Vincent, A., & Webster, R. (2020). The Structure, Function, and Physiology of the Fetal and Adult Acetylcholine Receptor in Muscle. *Frontiers in Molecular Neuroscience*, *13*, 581097. https://doi.org/10.3389/fnmol.2020.581097

Chang, W., Wang, Y., Luxton, G. W. G., Östlund, C., Worman, H. J., & Gundersen, G. G. (2019). Imbalanced nucleocytoskeletal connections create common polarity defects in progeria and physiological aging. *Proceedings of the National Academy of Sciences*, *116*(9), 3578–3583. https://doi.org/10.1073/pnas.1809683116

Chemello, F., Wang, Z., Li, H., McAnally, J. R., Liu, N., Bassel-Duby, R., & Olson, E. N. (2020). Degenerative and regenerative pathways underlying Duchenne muscular dystrophy revealed by single-nucleus RNA sequencing. *Proceedings of the National Academy of Sciences*, *117*(47), 29691–29701. https://doi.org/10.1073/pnas.2018391117

Chen, H.-H., Yeo, H.-T., Huang, Y.-H., Tsai, L.-K., Lai, H.-J., Tsao, Y.-P., & Chen, S.-L. (2024). AAV-NRIP gene therapy ameliorates motor neuron degeneration and muscle atrophy in ALS model mice. *Skeletal Muscle*, *14*(1), 17. https://doi.org/10.1186/s13395-024-00349-z

Cheng, A., Morsch, M., Murata, Y., Ghazanfari, N., Reddel, S. W., & Phillips, W. D. (2013). Sequence of Age-Associated Changes to the Mouse Neuromuscular Junction and the Protective Effects of Voluntary Exercise. *PLoS ONE*, *8*(7), e67970. https://doi.org/10.1371/journal.pone.0067970

Cisterna, B., & Malatesta, M. (2024). Molecular and Structural Alterations of Skeletal Muscle Tissue Nuclei during Aging. *International Journal of Molecular Sciences*, *25*(3), 1833. https://doi.org/10.3390/ijms25031833

Conceição, M. S., Vechin, F. C., Lixandrão, M., Damas, F., Libardi, C. A., Tricoli, V., Roschel, H., Camera, D., & Ugrinowitsch, C. (2018). Muscle Fiber Hypertrophy and Myonuclei Addition: A Systematic Review and Meta-analysis. *Medicine & Science in Sports & Exercise*, *50*(7), 1385–1393. https://doi.org/10.1249/MSS.0000000000001593

Conforti, L., Gilley, J., & Coleman, M. P. (2014). Wallerian degeneration: An emerging axon death pathway linking injury and disease. *Nature Reviews Neuroscience*, *15*(6), 394–409. https://doi.org/10.1038/nrn3680

Cossins, J., Webster, R., Maxwell, S., Rodríguez Cruz, P. M., Knight, R., Llewelyn, J. G., Shin, J.-Y., Palace, J., & Beeson, D. (2020). Congenital myasthenic syndrome due to a TOR1AIP1 mutation: A new disease pathway for impaired synaptic transmission. *Brain Communications*, *2*(2), fcaa174. https://doi.org/10.1093/braincomms/fcaa174

Cristea, A., Qaisar, R., Edlund, P. K., Lindblad, J., Bengtsson, E., & Larsson, L. (2010). Effects of aging and gender on the spatial organization of nuclei in single human skeletal muscle

cells. *Aging Cell*, *9*(5), 685–697. https://doi.org/10.1111/j.1474-9726.2010.00594.x

Croxen, R., Young, C., Slater, C., Haslam, S., Brydson, M., Vincent, A., & Beeson, D. (2001). *End-plate γ- and ε-subunit mRNA levels in AChR deficiency syndrome due to ε-subunit null mutations*.

D'Angelo, M. A. (2018). Nuclear pore complexes as hubs for gene regulation. *Nucleus*, *9*(1), 142–148. https://doi.org/10.1080/19491034.2017.1395542

D'Angelo, M. A., Raices, M., Panowski, S. H., & Hetzer, M. W. (2009). Age-Dependent Deterioration of Nuclear Pore Complexes Causes a Loss of Nuclear Integrity in Postmitotic Cells. *Cell*, *136*(2), 284–295. https://doi.org/10.1016/j.cell.2008.11.037

De Leeuw, R., Gruenbaum, Y., & Medalia, O. (2018). Nuclear Lamins: Thin Filaments with Major Functions. *Trends in Cell Biology*, *28*(1), 34–45. https://doi.org/10.1016/j.tcb.2017.08.004

Dechat, T., Pfleghaar, K., Sengupta, K., Shimi, T., Shumaker, D. K., Solimando, L., & Goldman, R. D. (2008). Nuclear lamins: Major factors in the structural organization and function of the nucleus and chromatin. *Genes & Development*, *22*(7), 832–853. https://doi.org/10.1101/gad.1652708

Deepa, S. S., Van Remmen, H., Brooks, S. V., Faulkner, J. A., Larkin, L., McArdle, A., Jackson, M. J., Vasilaki, A., & Richardson, A. (2019). Accelerated sarcopenia in Cu/Zn superoxide dismutase knockout mice. *Free Radical Biology and Medicine*, *132*, 19–23. https://doi.org/10.1016/j.freeradbiomed.2018.06.032

Delbono, O., Rodrigues, A. C. Z., Bonilla, H. J., & Messi, M. L. (2021). The emerging role of the sympathetic nervous system in skeletal muscle motor innervation and sarcopenia. *Ageing Research Reviews*, *67*, 101305. https://doi.org/10.1016/j.arr.2021.101305

Deschenes, M. R., Flannery, R., Hawbaker, A., Patek, L., & Mifsud, M. (2022). Adaptive Remodeling of the Neuromuscular Junction with Aging. *Cells*, *11*(7), 1150. https://doi.org/10.3390/cells11071150

Doherty, T. J., Vandervoort, A. A., Taylor, A. W., & Brown, W. F. (1993). Effects of motor unit losses on strength in older men and women. *Journal of Applied Physiology*, *74*(2), 868–874. https://doi.org/10.1152/jappl.1993.74.2.868

Donnaloja, F., Carnevali, F., Jacchetti, E., & Raimondi, M. T. (2020). Lamin A/C Mechanotransduction in Laminopathies. *Cells*, *9*(5), 1306. https://doi.org/10.3390/cells9051306

Dos Santos, M., Backer, S., Saintpierre, B., Izac, B., Andrieu, M., Letourneur, F., Relaix, F., Sotiropoulos, A., & Maire, P. (2020). Single-nucleus RNA-seq and FISH identify coordinated transcriptional activity in mammalian myofibers. *Nature Communications*,

11(1), 5102. https://doi.org/10.1038/s41467-020-18789-8

Duchen, L. W., & Strich, S. J. (1968). THE EFFECTS OF BOTULINUM TOXIN ON THE PATTERN OF INNERVATION OF SKELETAL MUSCLE IN THE MOUSE. *Quarterly Journal of Experimental Physiology and Cognate Medical Sciences*, *53*(1), 84–89. https://doi.org/10.1113/expphysiol.1968.sp001948

Duong, N. T., Morris, G. E., Lam, L. T., Zhang, Q., Sewry, C. A., Shanahan, C. M., & Holt, I. (2014). Nesprins: Tissue-Specific Expression of Epsilon and Other Short Isoforms. *PLoS ONE*, *9*(4), e94380. https://doi.org/10.1371/journal.pone.0094380

Eiber, N., Fröb, F., Schowalter, M., Thiel, C., Clemen, C. S., Schröder, R., & Hashemolhosseini, S. (2020). Lack of Desmin in Mice Causes Structural and Functional Disorders of Neuromuscular Junctions. *Frontiers in Molecular Neuroscience*, *13*, 567084. https://doi.org/10.3389/fnmol.2020.567084

Farrar, M. J., Bernstein, I. M., Schlafer, D. H., Cleland, T. A., Fetcho, J. R., & Schaffer, C. B. (2012). Chronic in vivo imaging in the mouse spinal cord using an implanted chamber. *Nature Methods*, *9*(3), 297–302. https://doi.org/10.1038/nmeth.1856

Ferraioli, S., Sarigol, F., Prakash, C., Filipczak, D., Foisner, R., & Naetar, N. (2024). LAP2alpha facilitates myogenic gene expression by preventing nucleoplasmic lamin A/C from spreading to active chromatin regions. *Nucleic Acids Research*, gkae752. https://doi.org/10.1093/nar/gkae752

Ferraro, E., Molinari, F., & Berghella, L. (2012). Molecular control of neuromuscular junction development. *Journal of Cachexia, Sarcopenia and Muscle*, *3*(1), 13–23. https://doi.org/10.1007/s13539-011-0041-7

Folker, E. S., & Baylies, M. K. (2013). Nuclear positioning in muscle development and disease. *Frontiers in Physiology*, *4*. https://doi.org/10.3389/fphys.2013.00363

Frock, R. L., Kudlow, B. A., Evans, A. M., Jameson, S. A., Hauschka, S. D., & Kennedy, B. K. (2006). Lamin A/C and emerin are critical for skeletal muscle satellite cell differentiation. *Genes & Development*, *20*(4), 486–500. https://doi.org/10.1101/gad.1364906

Frontera, W. R., & Ochala, J. (2015a). Skeletal Muscle: A Brief Review of Structure and Function. *Calcified Tissue International*, *96*(3), 183–195. https://doi.org/10.1007/s00223-014-9915-y

Frontera, W. R., & Ochala, J. (2015b). Skeletal Muscle: A Brief Review of Structure and Function. *Calcified Tissue International*, *96*(3), 183–195. https://doi.org/10.1007/s00223-014-9915-y

Fry, C.S., Noehren, B., Mula, J., Ubele, M.F., Westgate, P.M., Kern, P.A. and Peterson, C.A. (2014), Fibre type-specific satellite cell response to aerobic training in sedentary adults. J

Physiol, 592: 2625-2635. https://doi.org/10.1113/jphysiol.2014.271288

Fucile, S., Renzi, M., Lax, P., & Eusebi, F. (2003). Fractional Ca2+ current through human neuronal α7 nicotinic acetylcholine receptors. *Cell Calcium*, *34*(2), 205-209.

Fucile, S., Sucapane, A., Grassi, F., Eusebi, F., & Engel, A. G. (2006). The human adult subtype ACH receptor channel has high ca2+ permeability and predisposes to endplate ca2+ overloading. *The Journal of Physiology*, *573*(1), 35–43. https://doi.org/10.1113/jphysiol.2006.108092

Fukuoka, T., Engel, A. G., Lang, B., Newsom-Davis, J., Prior, C., & W.-Wray, D. (1987). Lambert-Eaton myasthenic syndrome: I. Early morphological effects of IgG on the presynaptic membrane active zones. *Annals of Neurology*, *22*(2), 193–199. https://doi.org/10.1002/ana.410220203

Gao, N., Zhao, K., Cao, Y., Ren, X., Jing, H., Xing, G., Xiong, W.-C., & Mei, L. (2020). A Role of Lamin A/C in Preventing Neuromuscular Junction Decline in Mice. *The Journal of Neuroscience*, *40*(38), 7203–7215. https://doi.org/10.1523/JNEUROSCI.0443-20.2020

Gessler L, Huraskin D, Jian Y, Eiber N, Hu Z, Proszynski TJ, Hashemolhosseini S (2024c) The YAP1/TAZ-TEAD transcriptional network regulates gene expression at neuromuscular junctions in skeletal muscle fibers. Nucleic Acids Res 52:600–624.

Gonzalez-Suarez, I., Redwood, A. B., Perkins, S. M., Vermolen, B., Lichtensztejin, D., Grotsky, D. A., Morgado-Palacin, L., Gapud, E. J., Sleckman, B. P., Sullivan, T., Sage, J., Stewart, C. L., Mai, S., & Gonzalo, S. (2009). Novel roles for A-type lamins in telomere biology and the DNA damage response pathway. *The EMBO Journal*, *28*(16), 2414–2427. https://doi.org/10.1038/emboj.2009.196

Grady, R. M., Starr, D. A., Ackerman, G. L., Sanes, J. R., & Han, M. (2005). Syne proteins anchor muscle nuclei at the neuromuscular junction. *Proceedings of the National Academy of Sciences*, *102*(12), 4359–4364. https://doi.org/10.1073/pnas.0500711102

Grönholdt-Klein, M., Altun, M., Becklén, M., Dickman Kahm, E., Fahlström, A., Rullman, E., & Ulfhake, B. (2019). Muscle atrophy and regeneration associated with behavioural loss and recovery of function after sciatic nerve crush. *Acta Physiologica*, *227*(3), e13335. https://doi.org/10.1111/apha.13335

Hachiya, N., Sochocka, M., Brzecka, A., Shimizu, T., Gąsiorowski, K., Szczechowiak, K., & Leszek, J. (2021). Nuclear Envelope and Nuclear Pore Complexes in Neurodegenerative Diseases—New Perspectives for Therapeutic Interventions. *Molecular Neurobiology*, *58*(3), 983–995. https://doi.org/10.1007/s12035-020-02168-x

Haddix, S. G., Lee, Y. I., Kornegay, J. N., & Thompson, W. J. (2018). Cycles of myofiber degeneration and regeneration lead to remodeling of the neuromuscular junction in two mammalian models of Duchenne muscular dystrophy. *PLOS ONE*, *13*(10), e0205926.

https://doi.org/10.1371/journal.pone.0205926

Ham, A. S., Lin, S., Tse, A., Thürkauf, M., Oliveri, F., & Rüegg, M. A. (2024). *Single-nuclei sequencing of skeletal muscle reveals subsynaptic-specific transcripts involved in neuromuscular junction maintenance*. https://doi.org/10.1101/2024.05.15.594276

Hashizume, K., Kanda, K., & Burke, R. E. (1988). Medial gastrocnemius motor nucleus in the rat: Age-related changes in the number and size of motoneurons. *Journal of Comparative Neurology*, *269*(3), 425–430. https://doi.org/10.1002/cne.902690309

Hesselmans, L. F. G. M., Jennekens, F. G. I., Van Den Oord, C. J. M., Veldman, H., & Vincent, A. (1993). Development of innervation of skeletal muscle fibers in man: Relation to acetylcholine receptors. *The Anatomical Record*, *236*(3), 553–562. https://doi.org/10.1002/ar.1092360315

Holt, I., Fuller, H. R., Lam, L. T., Sewry, C. A., Shirran, S. L., Zhang, Q., Shanahan, C. M., & Morris, G. E. (2019). Nesprin-1-alpha2 associates with kinesin at myotube outer nuclear membranes, but is restricted to neuromuscular junction nuclei in adult muscle. *Scientific Reports*, *9*(1), 14202. https://doi.org/10.1038/s41598-019-50728-6

Ito, N., Takatsu, A., Ito, H., Koike, Y., Yoshioka, K., Kamei, Y., & Imai, S. (2022). Slc12a8 in the lateral hypothalamus maintains energy metabolism and skeletal muscle functions during aging. *Cell Reports*, *40*(4), 111131. https://doi.org/10.1016/j.celrep.2022.111131

Ivannikov, M. V., & Van Remmen, H. (2015). Sod1 gene ablation in adult mice leads to physiological changes at the neuromuscular junction similar to changes that occur in old wild-type mice. *Free Radical Biology and Medicine*, *84*, 254–262. https://doi.org/10.1016/j.freeradbiomed.2015.03.021

Iyer, S. R., Folker, E. S., & Lovering, R. M. (2021). The Nucleoskeleton: Crossroad of Mechanotransduction in Skeletal Muscle. *Frontiers in Physiology*, *12*, 724010. https://doi.org/10.3389/fphys.2021.724010

Jang, Y. C., Liu, Y., Hayworth, C. R., Bhattacharya, A., Lustgarten, M. S., Muller, F. L., Chaudhuri, A., Qi, W., Li, Y., Huang, J., Verdin, E., Richardson, A., & Van Remmen, H. (2012). Dietary restriction attenuates age-associated muscle atrophy by lowering oxidative stress in mice even in complete absence of CuZnSOD. *Aging Cell*, *11*(5), 770–782. https://doi.org/10.1111/j.1474-9726.2012.00843.x

Jang, Y. C., & Van Remmen, H. (2011). Age-associated alterations of the neuromuscular junction. *Experimental Gerontology*, *46*(2–3), 193–198. https://doi.org/10.1016/j.exger.2010.08.029

Kadi, F., Schjerling, P., Andersen, L. L., Charifi, N., Madsen, J. L., Christensen, L. R., & Andersen, J. L. (2004). The effects of heavy resistance training and detraining on satellite cells in human skeletal muscles. *The Journal of Physiology*, *558*(3), 1005–1012.

https://doi.org/10.1113/jphysiol.2004.065904

Kerschensteiner, M., Schwab, M. E., Lichtman, J. W., & Misgeld, T. (2005). In vivo imaging of axonal degeneration and regeneration in the injured spinal cord. *Nature Medicine*, *11*(5), 572–577. https://doi.org/10.1038/nm1229

Kim, M., Franke, V., Brandt, B., Lowenstein, E. D., Schöwel, V., Spuler, S., Akalin, A., & Birchmeier, C. (2020). Single-nucleus transcriptomics reveals functional compartmentalization in syncytial skeletal muscle cells. *Nature Communications*, *11*(1), 6375. https://doi.org/10.1038/s41467-020-20064-9

Kim, S., Park, S. H., Myung, K., & Lee, K. (2024). Lamin A/C facilitates DNA damage response by modulating ATM signaling and homologous recombination pathways. *Animal Cells and Systems*, *28*(1), 401–416. https://doi.org/10.1080/19768354.2024.2393820

Kim, T. N., & Choi, K. M. (2013). Sarcopenia: Definition, Epidemiology, and Pathophysiology. *Journal of Bone Metabolism*, *20*(1), 1. https://doi.org/10.11005/jbm.2013.20.1.1

Kosco, E. D., Jing, H., Chen, P., Xiong, W.-C., Samuels, I. S., & Mei, L. (2023). DOK7 Promotes NMJ Regeneration After Nerve Injury. *Molecular Neurobiology*, *60*(3), 1453–1464. https://doi.org/10.1007/s12035-022-03143-4

Koster, A., Ding, J., Stenholm, S., Caserotti, P., Houston, D. K., Nicklas, B. J., You, T., Lee, J. S., Visser, M., Newman, A. B., Schwartz, A. V., Cauley, J. A., Tylavsky, F. A., Goodpaster, B. H., Kritchevsky, S. B., Harris, T. B., & for the Health ABC study. (2011). Does the Amount of Fat Mass Predict Age-Related Loss of Lean Mass, Muscle Strength, and Muscle Quality in Older Adults? *The Journals of Gerontology Series A: Biological Sciences and Medical Sciences*, *66A*(8), 888–895. https://doi.org/10.1093/gerona/glr070

Kovacs, M. T., Vallette, M., Wiertsema, P., Dingli, F., Loew, D., Nader, G. P. D. F., Piel, M., & Ceccaldi, R. (2023). DNA damage induces nuclear envelope rupture through ATR-mediated phosphorylation of lamin A/C. *Molecular Cell*, *83*(20), 3659-3668.e10. https://doi.org/10.1016/j.molcel.2023.09.023

Kume, K., Cantwell, H., Burrell, A., & Nurse, P. (2019). Nuclear membrane protein Lem2 regulates nuclear size through membrane flow. *Nature Communications*, *10*(1), 1871. https://doi.org/10.1038/s41467-019-09623-x

Kummer, T. T., Misgeld, T., & Sanes, J. R. (2006). Assembly of the postsynaptic membrane at the neuromuscular junction: Paradigm lost. *Current Opinion in Neurobiology*, *16*(1), 74–82. https://doi.org/10.1016/j.conb.2005.12.003

Lammerding, J., Fong, L. G., Ji, J. Y., Reue, K., Stewart, C. L., Young, S. G., & Lee, R. T. (2006). Lamins A and C but Not Lamin B1 Regulate Nuclear Mechanics. *Journal of Biological Chemistry*, *281*(35), 25768–25780. https://doi.org/10.1074/jbc.M513511200

Lammerding, J., Schulze, P. C., Takahashi, T., Kozlov, S., Sullivan, T., Kamm, R. D., Stewart, C. L., & Lee, R. T. (2004). Lamin A/C deficiency causes defective nuclear mechanics and mechanotransduction. *Journal of Clinical Investigation*, *113*(3), 370–378. https://doi.org/10.1172/JCI200419670

Larouche, J. A., Mohiuddin, M., Choi, J. J., Ulintz, P. J., Fraczek, P., Sabin, K., Pitchiaya, S., Kurpiers, S. J., Castor-Macias, J., Liu, W., Hastings, R. L., Brown, L. A., Markworth, J. F., De Silva, K., Levi, B., Merajver, S. D., Valdez, G., Chakkalakal, J. V., Jang, Y. C., … Aguilar, C. A. (2021). Murine muscle stem cell response to perturbations of the neuromuscular junction are attenuated with aging. *eLife*, *10*, e66749. https://doi.org/10.7554/eLife.66749

Lee, J. S. H., Hale, C. M., Panorchan, P., Khatau, S. B., George, J. P., Tseng, Y., Stewart, C. L., Hodzic, D., & Wirtz, D. (2007). Nuclear Lamin A/C Deficiency Induces Defects in Cell Mechanics, Polarization, and Migration. *Biophysical Journal*, *93*(7), 2542–2552. https://doi.org/10.1529/biophysj.106.102426

Lexell, J., Taylor, C. C., & Sj, M. (n.d.). *What is the cause of the ageing atrophy? Total number, size and proportion of different fiber types studied in whole vastus lateralis muscle from 15- to 83-year-old men*.

Li, L., Xiong, W.-C., & Mei, L. (2018). Neuromuscular Junction Formation, Aging, and Disorders. *Annual Review of Physiology*, *80*(1), 159–188. https://doi.org/10.1146/annurev-physiol-022516-034255

Li, Y., Lee, Y. I., & Thompson, W. J. (2011). Changes in Aging Mouse Neuromuscular Junctions Are Explained by Degeneration and Regeneration of Muscle Fiber Segments at the Synapse. *The Journal of Neuroscience*, *31*(42), 14910–14919. https://doi.org/10.1523/JNEUROSCI.3590-11.2011

Lin, H., Ma, X., Sun, Y., Peng, H., Wang, Y., Thomas, S. S., & Hu, Z. (2022). Decoding the transcriptome of denervated muscle at single-nucleus resolution. *Journal of Cachexia, Sarcopenia and Muscle*, *13*(4), 2102–2117. https://doi.org/10.1002/jcsm.13023

Liu, J., Huang, Z.-P., Nie, M., Wang, G., Silva, W. J., Yang, Q., Freire, P. P., Hu, X., Chen, H., Deng, Z., Pu, W. T., & Wang, D.-Z. (2020). Regulation of myonuclear positioning and muscle function by the skeletal muscle-specific CIP protein. *Proceedings of the National Academy of Sciences*, *117*(32), 19254–19265. https://doi.org/10.1073/pnas.1922911117

Liu, W., Klose, A., Forman, S., Paris, N. D., Wei-LaPierre, L., Cortés-Lopéz, M., Tan, A., Flaherty, M., Miura, P., Dirksen, R. T., & Chakkalakal, J. V. (2017). Loss of adult skeletal muscle stem cells drives age-related neuromuscular junction degeneration. *eLife*, *6*, e26464. https://doi.org/10.7554/eLife.26464

Liu, W., Wei-LaPierre, L., Klose, A., Dirksen, R. T., & Chakkalakal, J. V. (2015). Inducible depletion of adult skeletal muscle stem cells impairs the regeneration of neuromuscular

junctions. *eLife*, *4*, e09221. https://doi.org/10.7554/eLife.09221

López-Otín, C., Blasco, M. A., Partridge, L., Serrano, M., & Kroemer, G. (2013). The Hallmarks of Aging. *Cell*, *153*(6), 1194–1217. https://doi.org/10.1016/j.cell.2013.05.039

Martinez-Pena Y Valenzuela, I., & Akaaboune, M. (2021). The Metabolic Stability of the Nicotinic Acetylcholine Receptor at the Neuromuscular Junction. *Cells*, *10*(2), 358. https://doi.org/10.3390/cells10020358

Maynard, S., Keijzers, G., Akbari, M., Ezra, M. B., Hall, A., Morevati, M., Scheibye-Knudsen, M., Gonzalo, S., Bartek, J., & Bohr, V. A. (2019). Lamin A/C promotes DNA base excision repair. *Nucleic Acids Research*, gkz912. https://doi.org/10.1093/nar/gkz912

McCormick, R., & Vasilaki, A. (2018). Age-related changes in skeletal muscle: Changes to life-style as a therapy. *Biogerontology*, *19*(6), 519–536. https://doi.org/10.1007/s10522-018-9775-3

Méjat, A., Decostre, V., Li, J., Renou, L., Kesari, A., Hantaï, D., Stewart, C. L., Xiao, X., Hoffman, E., Bonne, G., & Misteli, T. (2009). Lamin A/C–mediated neuromuscular junction defects in Emery-Dreifuss muscular dystrophy. *The Journal of Cell Biology*, *184*(1), 31–44. https://doi.org/10.1083/jcb.200811035

Missias, A. C., Chu, G. C., Klocke, B. J., Sanes, J. R., & Merlie, J. P. (1996). *Maturation of the Acetylcholine Receptor in Skeletal Muscle: Regulation of the AChR g-to-e Switch*.

Muller, F. L., Song, W., Jang, Y. C., Liu, Y., Sabia, M., Richardson, A., Remmen, H. V. (2007). Denervation-induced skeletal muscle atrophy is associated with increased mitochondrial ros production. American Journal of Physiology-Regulatory, Integrative and Comparative Physiology, 293(3), R1159-R1168. https://doi.org/10.1152/ajpregu.00767.2006

Murach, K. A., Englund, D. A., Dupont-Versteegden, E. E., McCarthy, J. J., & Peterson, C. A. (2018). Myonuclear Domain Flexibility Challenges Rigid Assumptions on Satellite Cell Contribution to Skeletal Muscle Fiber Hypertrophy. *Frontiers in Physiology*, *9*, 635. https://doi.org/10.3389/fphys.2018.00635

Naetar, N., Ferraioli, S., & Foisner, R. (2017). Lamins in the nuclear interior − life outside the lamina. *Journal of Cell Science*, *130*(13), 2087–2096. https://doi.org/10.1242/jcs.203430

Nayak, T. K., Bruhova, I., Chakraborty, S., Gupta, S., Zheng, W., & Auerbach, A. (2014). Functional differences between neurotransmitter binding sites of muscle acetylcholine receptors. *Proceedings of the National Academy of Sciences*, *111*(49), 17660–17665. https://doi.org/10.1073/pnas.1414378111

Nayak, T. K., Chakraborty, S., Zheng, W., & Auerbach, A. (2016). Structural correlates of affinity in fetal versus adult endplate nicotinic receptors. *Nature Communications*, *7*(1), 11352. https://doi.org/10.1038/ncomms11352

Oyston, L. J., Lin, Y. Q., Khuong, T. M., Wang, Q.-P., Lau, M. T., Clark, T., & Neely, G. G. (2018). Neuronal Lamin regulates motor circuit integrity and controls motor function and lifespan. *Cell Stress*, *2*(9), 225–232. https://doi.org/10.15698/cst2018.09.152

Packard, M., Jokhi, V., Ding, B., Ruiz-Cañada, C., Ashley, J., & Budnik, V. (2015). Nucleus to Synapse Nesprin1 Railroad Tracks Direct Synapse Maturation through RNA Localization. *Neuron*, *86*(4), 1015–1028. https://doi.org/10.1016/j.neuron.2015.04.006

Pathak, R. U., Soujanya, M., & Mishra, R. K. (2021). Deterioration of nuclear morphology and architecture: A hallmark of senescence and aging. *Ageing Research Reviews*, *67*, 101264. https://doi.org/10.1016/j.arr.2021.101264

Pavlath, G. K., Rich, K., Webster, S. G., & Blau, H. M. (1989). Localization of muscle gene products in nuclear domains. *Nature*, *337*(6207), 570–573. https://doi.org/10.1038/337570a0

Pestronk, A., Drachman, D. B., & Self, S. G. (1985). Measurement of junctional acetylcholine receptors in myasthenia gravis: Clinical correlates. *Muscle & Nerve*, *8*(3), 245–251. https://doi.org/10.1002/mus.880080311

Petrany, M. J., Swoboda, C. O., Sun, C., Chetal, K., Chen, X., Weirauch, M. T., Salomonis, N., & Millay, D. P. (2020). Single-nucleus RNA-seq identifies transcriptional heterogeneity in multinucleated skeletal myofibers. *Nature Communications*, *11*(1), 6374. https://doi.org/10.1038/s41467-020-20063-w

Petrella, J. K., Kim, J., Cross, J. M., Kosek, D. J., & Bamman, M. M. (2006). Efficacy of myonuclear addition may explain differential myofiber growth among resistance-trained young and older men and women. *American Journal of Physiology-Endocrinology and Metabolism*, *291*(5), E937–E946. https://doi.org/10.1152/ajpendo.00190.2006

Pho, M., Berrada, Y., Gunda, A., & Stephens, A. D. (n.d.). Nuclear shape is affected differentially by loss of lamin A, lamin C, or both lamin A and C. *Open Access*.

Purves, D., & Sakmann, B. (1974a). Membrane properties underlying spontaneous activity of denervated muscle fibres. *The Journal of Physiology*, *239*(1), 125–153. https://doi.org/10.1113/jphysiol.1974.sp010559

Purves, D., & Sakmann, B. (1974b). The effect of contractile activity on fibrillation and extrajunctional acetylcholine-sensitivity in rat muscle maintained in organ culture. *The Journal of Physiology*, *237*(1), 157–182. https://doi.org/10.1113/jphysiol.1974.sp010475

Ray, P. D., Huang, B.-W., & Tsuji, Y. (2012). Reactive oxygen species (ROS) homeostasis and redox regulation in cellular signaling. *Cellular Signalling*, *24*(5), 981–990. https://doi.org/10.1016/j.cellsig.2012.01.008

Ribchester, R. R., & Taxt, T. (1984). Repression of inactive motor nerve terminals in partially denervated rat muscle after regeneration of active motor axons. *The Journal of*

Physiology, *347*(1), 497–511. https://doi.org/10.1113/jphysiol.1984.sp015078

Rogozhin, A. A., Pang, K. K., Bukharaeva, E., Young, C., & Slater, C. R. (2008). Recovery of mouse neuromuscular junctions from single and repeated injections of botulinum neurotoxin A. *The Journal of Physiology*, *586*(13), 3163–3182. https://doi.org/10.1113/jphysiol.2008.153569

Rosenheimer, J. L., & Smith, D. O. (1985). Differential changes in the end-plate architecture of functionally diverse muscles during aging. *Journal of Neurophysiology*, *53*(6), 1567–1581. https://doi.org/10.1152/jn.1985.53.6.1567

Ruegg, M. A. (2005). Organization of synaptic myonuclei by Syne proteins and their role during the formation of the nerve–muscle synapse. *Proceedings of the National Academy of Sciences*, *102*(16), 5643–5644. https://doi.org/10.1073/pnas.0501516102

Ruiz, L. P., Macpherson, P. C., & Brooks, S. V. (2023). Maintenance of subsynaptic myonuclei number is not driven by neural input. *Frontiers in Physiology*, *14*, 1266950. https://doi.org/10.3389/fphys.2023.1266950

Saini, J., Faroni, A., Reid, A. J., Mouly, V., Butler-Browne, G., Lightfoot, A. P., McPhee, J. S., Degens, H., & Al-Shanti, N. (2021). Cross-talk between motor neurons and myotubes via endogenously secreted neural and muscular growth factors. *Physiological Reports*, *9*(8). https://doi.org/10.14814/phy2.14791

Sanes, J. R. (n.d.). *DEVELOPMENT OF THE VERTEBRATE NEUROMUSCULAR JUNCTION*.

Sanes, J. R., & Lichtman, J. W. (2001). Induction, assembly, maturation and maintenance of a postsynaptic apparatus. *Nature Reviews Neuroscience*, *2*(11), 791–805. https://doi.org/10.1038/35097557

Scaffidi, P., & Misteli, T. (2006). Lamin A-Dependent Nuclear Defects in Human Aging. *Science*, *312*(5776), 1059–1063. https://doi.org/10.1126/science.1127168

Schaeffer, L., De Kerchove d'Exaerde, A., & Changeux, J.-P. (2001). Targeting Transcription to the Neuromuscular Synapse. *Neuron*, *31*(1), 15–22. https://doi.org/10.1016/S0896-6273(01)00353-1

Scialò, F., Fernández-Ayala, D. J., & Sanz, A. (2017). Role of Mitochondrial Reverse Electron Transport in ROS Signaling: Potential Roles in Health and Disease. *Frontiers in Physiology*, *8*, 428. https://doi.org/10.3389/fphys.2017.00428

Shen JX, Yakel J (2009) Nicotinic acetylcholine receptor-mediated calcium signaling in the nervous system. Acta Pharmacol Sin 30:673–680. https://doi.org/10.1038/aps.2009.64

Shi, L., Fu, A. K. Y., & Ip, N. Y. (2012). Molecular mechanisms underlying maturation and maintenance of the vertebrate neuromuscular junction. *Trends in Neurosciences*, *35*(7),

441–453. https://doi.org/10.1016/j.tins.2012.04.005

Sinha-Hikim, I., Roth, S. M., Lee, M. I., & Bhasin, S. (2003). Testosterone-induced muscle hypertrophy is associated with an increase in satellite cell number in healthy, young men. *American Journal of Physiology-Endocrinology and Metabolism*, *285*(1), E197–E205. https://doi.org/10.1152/ajpendo.00370.2002

Slater, C. R. (2020). 'Fragmentation' of NMJs: A sign of degeneration or regeneration? A long journey with many junctions. *Neuroscience*, *439*, 28–40. https://doi.org/10.1016/j.neuroscience.2019.05.017

Sonjak, V., Jacob, K., Morais, J. A., Rivera-Zengotita, M., Spendiff, S., Spake, C., Taivassalo, T., Chevalier, S., & Hepple, R. T. (2019). Fidelity of muscle fibre reinnervation modulates ageing muscle impact in elderly women. *The Journal of Physiology*, *597*(19), 5009–5023. https://doi.org/10.1113/JP278261

Strambio-De-Castillia, C., Niepel, M., & Rout, M. P. (2010). The nuclear pore complex: Bridging nuclear transport and gene regulation. *Nature Reviews Molecular Cell Biology*, *11*(7), 490–501. https://doi.org/10.1038/nrm2928

Sullivan, T., Escalante-Alcalde, D., Bhatt, H., Anver, M., Bhat, N., Nagashima, K., Stewart, C. L., & Burke, B. (1999). Loss of a-Type Lamin Expression Compromises Nuclear Envelope Integrity Leading to Muscular Dystrophy. *The Journal of Cell Biology*, *147*(5), 913–920. https://doi.org/10.1083/jcb.147.5.913

Sun, J., Yang, H., Yang, X., Chen, X., Xu, H., Shen, Y., Ding, F., Gu, X., Zhu, J., & Sun, H. (2021). Global alternative splicing landscape of skeletal muscle atrophy induced by hindlimb unloading. *Annals of translational medicine*, *9*(8), 643. https://doi.org/10.21037/atm-20-5388

Tajik, A., Zhang, Y., Wei, F., Sun, J., Jia, Q., Zhou, W., Singh, R., Khanna, N., Belmont, A. S., & Wang, N. (2016). Transcription upregulation via force-induced direct stretching of chromatin. *Nature Materials*, *15*(12), 1287–1296. https://doi.org/10.1038/nmat4729

Teixeira, C. E., & Duarte, J. A. (2011). Myonuclear domain in skeletal muscle fibers. A critical review. *Archives of Exercise in Health and Disease*, *2*(2), 92–101. https://doi.org/10.5628/aehd.v2i2.24

Tintignac, L. A., Brenner, H.-R., & Rüegg, M. A. (2015). Mechanisms Regulating Neuromuscular Junction Development and Function and Causes of Muscle Wasting. *Physiological Reviews*, *95*(3), 809–852. https://doi.org/10.1152/physrev.00033.2014

Urzi, A., Lahmann, I., Nguyen, L. V. N., Rost, B. R., García-Pérez, A., Lelievre, N., Merritt-Garza, M. E., Phan, H. C., Bassell, G. J., Rossoll, W., Diecke, S., Kunz, S., Schmitz, D., & Gouti, M. (2023). Efficient generation of a self-organizing neuromuscular junction model from human pluripotent stem cells. *Nature Communications*, *14*(1), 8043.

https://doi.org/10.1038/s41467-023-43781-3

Valdez, G., Tapia, J. C., Kang, H., Clemenson, G. D., Gage, F. H., Lichtman, J. W., & Sanes, J. R. (2010). Attenuation of age-related changes in mouse neuromuscular synapses by caloric restriction and exercise. *Proceedings of the National Academy of Sciences*, *107*(33), 14863–14868. https://doi.org/10.1073/pnas.1002220107

Vannucci, B., Santosa, K. B., Keane, A. M., Jablonka-Shariff, A., Lu, C., Yan, Y., MacEwan, M., & Snyder-Warwick, A. K. (2019). What is Normal? Neuromuscular junction reinnervation after nerve injury. *Muscle & Nerve*, *60*(5), 604–612. https://doi.org/10.1002/mus.26654

Verma, S., Khurana, S., Vats, A., Sahu, B., Ganguly, N. K., Chakraborti, P., Gourie-Devi, M., & Taneja, V. (2022). Neuromuscular Junction Dysfunction in Amyotrophic Lateral Sclerosis. *Molecular Neurobiology*, *59*(3), 1502–1527. https://doi.org/10.1007/s12035-021-02658-6

Villarroel, A., & Sakmann, B. (1996). Calcium permeability increase of endplate channels in rat muscle during postnatal development. *The Journal of Physiology*, *496*(2), 331–338. https://doi.org/10.1113/jphysiol.1996.sp021688

Von Saucken, V. E., Windner, S. E., & Baylies, M. K. (2024). *Postsynaptic BMP signaling regulates myonuclear properties in* Drosophila *larval muscles*. https://doi.org/10.1101/2024.04.10.588944

Wang, A. S., Kozlov, S. V., Stewart, C. L., & Horn, H. F. (2015). Tissue specific loss of A-type lamins in the gastrointestinal epithelium can enhance polyp size. *Differentiation, 89*(1–2), 11–21. https://doi.org/10.1016/j.diff.2014.12.002

Willadt, S., Nash, M., & Slater, C. R. (2016). Age-related fragmentation of the motor endplate is not associated with impaired neuromuscular transmission in the mouse diaphragm. *Scientific Reports*, *6*(1), 24849. https://doi.org/10.1038/srep24849

Wu, H., Xiong, W. C., & Mei, L. (2010). To build a synapse: Signaling pathways in neuromuscular junction assembly. *Development*, *137*(7), 1017–1033. https://doi.org/10.1242/dev.038711

Yoo, S.-Z., No, M.-H., Heo, J.-W., Park, D.-H., Kang, J.-H., Kim, S. H., & Kwak, H.-B. (2018). Role of exercise in age-related sarcopenia. *Journal of Exercise Rehabilitation*, *14*(4), 551–558. https://doi.org/10.12965/jer.1836268.134

York, A. L., & Zheng, J. Q. (2017). Super-Resolution Microscopy Reveals a Nanoscale Organization of Acetylcholine Receptors for Trans-Synaptic Alignment at Neuromuscular Synapses. *Eneuro*, *4*(4), ENEURO.0232-17.2017. https://doi.org/10.1523/ENEURO.0232-17.2017

Yoshida, N., Endo, J., Kinouchi, K., Kitakata, H., Moriyama, H., Kataoka, M., Yamamoto, T., Shirakawa, K., Morimoto, S., Nishiyama, A., Hashiguchi, A., Higuchi, I., Fukuda, K., Ichihara, A., & Sano, M. (2019). (Pro)renin receptor accelerates development of sarcopenia *via* activation of Wnt/YAP signaling axis. *Aging Cell*, *18*(5), e12991. https://doi.org/10.1111/acel.12991

Zhang, B., Yang, Y., Keyimu, R., Hao, J., Zhao, Z., & Ye, R. (2019). The role of lamin A/C in mesenchymal stem cell differentiation. *Journal of Physiology and Biochemistry*, *75*(1), 11–18. https://doi.org/10.1007/s13105-019-00661-z

Zou, Y., Zhang, J., Liu, J., Xu, J., Fu, L., Ma, X., Xu, Y., Xu, S., Wang, X., & Guo, J. (2022). SIRT6 Negatively Regulates Schwann Cells Dedifferentiation via Targeting c-Jun During Wallerian Degeneration After Peripheral Nerve Injury. *Molecular Neurobiology*, *59*(1), 429–444. https://doi.org/10.1007/s12035-021-02607-3